ANALYTICAL METHODS FOR SOLVING COMPLEX PROBLEMS IN FOOD AND ENVIRONMENTAL SCIENCE

By

JAMIE LYNN YORK

DISSERTATION

Submitted in partial fulfillment of the requirements for the degree of Doctor of Philosophy in Chemistry at The University of Texas at Arlington

August, 2019

Arlington, Texas

Supervising Committee:

Kevin A. Schug, Supervising Professor

Kwangho Nam

Krishnan Rajeshwar

Saiful Chowdhury

ACKNOWLEDGEMENTS

First and foremost I would like to thank my advisor, Dr. Kevin A. Schug. Without him I would absolutely not be where I am today. His faith in me has led me to become the Analytical Chemist I am today and I am so grateful to him for providing me this opportunity. I would also like to thank everyone in Schug group. We have a very unique environment and I truly consider you guys as family. Your help and support has been instrumental in my learning and success and I've looked forward to coming into work every day to see you guys. I'd also like to thank Ty Kahler for his wonderful advice. He is a wealth of knowledge and I was very fortunate to get his input on a lot of my projects. I'd also like to thank Restek for their funding and for allowing me to visit for an internship that helped me decide what I want to do for my future career. Also, thanks to Apache for funding some of my research. I would also like to give my appreciation for my committee members Dr. Krishnan Rajeshwar, Dr. Kwangho Nam, and Dr. Saiful Chowdhury for their valuable input and advice.

I have to thank my husband, Nick York, for his unwavering support throughout my entire graduate career. He is my rock and I honestly couldn't have done this without him. I'd also like to thank my parents, Joel and Janet Schenk, and my brother, Justin Schenk for their encouragement throughout my academic journey.

ABSTRACT: Analytical methods for solving complex problems in food and environmental science

Jamie Lynn York, PhD

The University of Texas at Arlington, 2019

Supervising Professor: Kevin A. Schug

Complex samples can be challenging for analysis in a number of different ways. Food and environmental samples can be particularly difficult due to their non-uniformity from sample to sample, possible unknown contents, and complexity in terms of their number of constituents and range of abundances of different species. To overcome challenges faced with the analysis of complex samples, intricate sample handling and processing techniques need to be tailored in order to build optimal methods. These procedures can include sample preparation techniques, on-line sample clean-up, and/or tools that the instrument has to offer. Each complex sample needs to be assessed for possible interferences with target analytes to determine the optimal way to proceed and if the interferences can be removed.

These studies focused on a combination of food and environmental samples where the focus and methods were customized to mitigate matrix interferences. Methods of analysis, such as LC-MS or GC-MS, and sample introduction techniques, such as headspace, were very instrumental in the success of each method. In the first study, coeluting isomers of dimethylnaphthalene were quantitatively deconvoluted into their respective concentrations using gas chromatography- vacuum ultraviolet (GC-VUV) and qualitatively detected in samples of diesel and jet fuel with the use of spectral filters. It was found that all the coeluting pairs of dimethylnaphthalene isomers could be accurately deconvoluted at ratios

with a disparity of nearly two orders of magnitude in relative abundance (1:99). In the next project, a hydraulic fracturing additive used in unconventional oil and gas extraction, proppants, were examined to determine their propensity to leach formaldehyde at lab-simulated downhole conditions by the use of three different instruments: LC-UV, headspace GC-MS, and headspace GC-VUV, to determine the best method of analysis. It was found that under the lab-simulated subsurface conditions the proppant leached less formaldehyde, likely due to competing reactions in the matrix. The next complex sample included another hydraulic fracturing additive, friction reducers. These were qualitatively tested by matrix-assisted laser desorption/ionization for their ethoxylated alcohol content and their behavior at lab-simulated downhole conditions. It was found that upon heating and subjection to shale core and produced water, the ethoxylated alcohol content tended to polymerize or stay relatively the same average weight distribution, indicating that it is likely not breaking down once below the surface.

Carbohydrates were the next study, which were investigated by GC-VUV and samples that coeluted were deconvoluted. Pharmaceutical samples were then analyzed for their carbohydrate content using this previously developed method. Mixtures of carbohydrates that coeluted were deconvoluted to determine concentration of each compound. Finally, a method was developed to simultaneously determine hormones, mycotoxins, and fat-soluble vitamins in eggs. This was performed using an LC-MS/MS coupled with a RAM column for on-line sample removal of large biomolecule interferences. It was found that the hens diet had a great effect on the fat-soluble vitamin and mycotoxin content. Throughout all

of these complex samples, various analytical methods, including multifarious sample preparation techniques, were used to retrieve reliable, accurate, and reproducible data.

Abbreviations

Liquid chromatography- mass spectrometry (LC-MS), gas chromatography- mass spectrometry (GC-MS), gas chromatography- vacuum ultraviolet (GC-VUV), liquid chromatography- ultraviolet (LC-UV), restricted access media (RAM), phenol-formaldehyde (PU), polyurethane (PU), high performance- liquid chromatography ultraviolet (HPLC-UV), gas chromatography (GC), liquid chromatography (LC), dimethylnaphthalene (DMN), headspace gas chromatography- vacuum ultraviolet (HS-GC-VUV), headspace gas chromatography- mass spectrometry (HS-GC-MS), matrix assisted laser desorption/ionization (MALDI), 2,5-dihydroxybenzoic acid (2,5-DHB), 2,4-dihydroxybenzoic acid + 2,2,2-trifluoroethanol (2,5-DHB+E), produced water inorganic (PWI), produced water (PW), oximation/pertrimethylsilylation (O/TMS), trimethylsilyl oxime (TMSO), limit of detection (LOD), limit of quantitation (LOQ), matrix-assisted laser desorption/ionization time of flight mass spectrometry (MALDI-TOF-MS), α-Cyano-4-hydroxycinnamic acid (CHCA), friction reducer (FR), solid phase extraction (SPE), liquid-liquid extraction (LLE), multiple reaction monitoring (MRM), nonsteroidal anti-inflammatory drugs (NSAIDs), Solid phase microextraction (SPME), quick, easy, cheap, effective, rugged, safe (QuEChERS), dispersive solid phase extraction (dSPE), salting-out assisted LLE (SALLE), continuous stirred tank reactor (CSTR), gas chromatography – Fourier transform infrared (GC-FTIR), polycyclic aromatic hydrocarbons (PAHs), two-dimensional gas chromatography (GCxGC), polyethylene naphthalate (PEN), trimethylnaphthalene (TMN), dichloromethane (DCM), time dependent density functional theory (TDDFT), sum of square of residuals (SSR), percent relative standard deviation (%RSD), supplementary information (SI), high performance liquid

chromatography (HPLC), hydraulic fracturing (HF), hydraulic fracturing fluid (HFF), resin coated proppant (RCP), ceramic coated proppant (CCP), 2,4-dinitrophenylhydrazine (2,4-DNPH), United States Environmental Protection Agency (EPA), nano-ESI-high resolution/accurate mass (HRAM), O-2,3,4,5,6-(pentafluorobenzyl) hydroxylamine hydrochloride (PFBHA), single ion monitoring mode (SIM), electron ionization (EI), naturally occurring radioactive materials (NORM), hydrophilic interaction chromatography (HILIC), acetonitrile (ACN), material safety data sheets (MSDS), standard deviation (STDEV), room temperature (RT), none detected (ND), dimethyl sulfoxide (DMSO), Nuclear magnetic resonance (NMR), charge-coupled device (CCD), paraffins, isoparaffins, olefins, naphthenes, and aromatics (PIONA), hexamethyldisilazane (HMDS), United States Department of Agriculture (USDA), cholecalciderol (D3), ergocalciferol (D2), electrospray ionization (ESI), secondary amine (PSA), and graphitized carbon black (GCB).

Table of Contents

LIST OF FIGURES

LIST OF TABLES

CHAPTER ONE: Introduction to Dissertation

1.1 Introduction

Food and environmental samples can be some particularly challenging complex matrices with which to deal. Complex matrices can cause problems with instrument integrity, data reliability, and matrix effects when handled improperly. To overcome these challenges, skillful methods of sample preparation, clean-up, and analysis need to be implemented. In the following research topics, a methodology was tailored for each complex matrix to achieve optimal results for accurate, reliable, and reproducible methods for qualitative and quantitative analysis of target analytes.

1.2 Complex Environmental Samples

The oil and gas industry is in full swing and, as such, methods need to be developed to monitor chemical additives and their behaviors at the subsurface conditions over time for the use of fingerprinting spills, monitoring possible contamination of nearby groundwater sources, and when surveying greener technologies. Environmental samples can be especially challenging due to their non-uniformity. Methods must be optimized to retrieve as much consistency between sample sets, in as efficient means, as possible. Once the methods are developed, they must be put through rigorous method validation and overall proof of concept must be shown.

One class of compounds contained in fuels that have been particularly challenging to separate previously are isomers of dimethylnaphthalenes (DMNs).[1,2,3] New developments in detectors have been an instrumental tool in the deconvolution of coeluting DMNs.[4] Typical methods of analysis for these compounds include gas

chromatography-mass spectrometry, but is dependent on separating these isomers chromatographically. If chromatographic separation falls short, the resulting mass spectra can oftentimes be too similar to differentiate. The vacuum ultraviolet (VUV) detector can measure absorption in a 120-240 nm range where virtually all compounds absorb light and give a unique compound specific absorbance spectra.[4] This allows for coeluting compounds, as in the case of DMNs, to be deconvoluted using Beer's law and their reference spectra from the VUV Library.[5] Spectral filters are another tool unique to the VUV detector and can allow for analysis of very complex samples, such as jet and diesel fuel, to hone in on specific classes of compounds to show the naphthalene contents of this otherwise signal-rich and convoluted chromatogram.[5]

Sometimes a comparison of various techniques can highlight best methods of analysis for a complex matrix, especially when testing matrices that have not been previously analyzed. Proppants are a sand-like material used in hydraulic fracturing fluid to help hold fissures in the shale open during the resource extraction procedure to allow for maximum oil and gas to be extracted. To improve mechanical strength and prevent the sand from crushing into small particles called "fines," which can clog the fissure, a coating can be applied to the proppant.[6] As the oil and gas Industry moves towards "greener methods" of hydraulic fracturing, consideration is taken as to which type of coating can be applied to the sand to give the best performance with the least amount of environmental impact. In these experiments, two types of resin-coated proppants, were investigated for their proclivity to leach chemicals from the resin-coating into the surrounding areas.[7] These types of analyses have not been

studied previously for proppants so there was great advantage in conducting a comparative study of instrumentational performance. Two types of resin-coating, polyurethane and phenol-formaldehyde were soaked in water, a produced water surrogate, produced water, and produced water with added shale core over various amounts of time. Produced water surrogate was made in house with various types of salts to match the ionic concentration of produced water without having all of the other organic and otherwise chemical interferences found in the produced water. It was used as a middle-of-the-road matrix, more complex than water but less complex than produced water. The proppants were found to leach formaldehyde into the surrounding leachate, especially in the case of water.[7] Three different methods of analysis were surveyed for their ability to measure derivatized formaldehyde including headspace gas chromatography- vacuum ultraviolet (HS-GC-VUV), high performance liquid chromatography (HPLC), and headspace gas chromatography-mass spectrometry (HS-GC-MS).[7] HS-GC-MS was found to be the best method for analysis, due to its ability to reach lower limits of detection and its ability to analyze the complex matrices, like produced water with added shale core, without any sample clean-up.[7] It was found that overall higher concentrations of formaldehyde were leached from the phenol-formaldehyde resin-coated proppant. When the proppants were soaked in water, higher concentrations of formaldehyde were detected than in the more complex matrices. The samples that were tested in produced water inorganic and produced water had very similar concentrations, while the samples tested in the produced water with added shale core returned much lower values of formaldehyde, likely due to competing reactions with derivatization.[7]

Friction reducers are another complex matrix that are used in hydraulic fracturing as an additive to the fluid to reduce backpressure at high pumping flow rates. These can be composed of a number of different things that include non-ionic surfactants, such as ethoxylated alcohols.[8] These analytes are typically analyzed by derivatizing and subsequent analysis on LC-MS or by the use of 2D liquid chromatography.[9] The issue with analysis of these friction reducers by this method is the need for sample clean-up in order to be viable for LC-MS analysis. The ethoxylated alcohol content was able to be characterized by matrix-assisted laser desorption/ionization time of flight mass spectrometry (MALDI-TOF-MS) without any clean-up, even in complex matrices such as produced water with added shale core.[10] A survey of different types of matrices to co-crystalize with the media was performed in order to ensure the best method of ionization for the ethoxylated alcohols. α-Cyano-4-hydroxycinnamic acid (CHCA) and 2,4-dihydroxybenzoic (2,4-DHB) with and without the addition of 2,2,2-trifluoroethanol (E) were tested and it was found that 2,4-DHB + E was the best matrix to facilitate ionization in the MALDI-TOF-MS for the ethoxylated alcohol content.[10] The carbon chain lengths of two different polymers contained in the friction reducers were found to be 12 and 14 with varying degrees of polymerization.[10] The matrix was further complicated by soaking the FR in a solvent that they would be subjected to at downhole conditions for 4 or 24 hours at room temperature or 100 °C to determine the behavior of these FR at downhole conditions. The solvents chosen were water, produced water surrogate, produced water, and produced water with added shale. It was found that as the matrix became more complex with the addition of the produced water, etc., the

ethoxylated alcohols tended to not polymerize as much as it did in water, likely due to competing reactions occurring within the matrix.[10]

1.3 Complex Food Samples

Food analysis can be a particularly challenging matrix to work with and requires extensive clean up depending on the target analytes to remove lipids, fats, or any other matrix interreferences. Carbohydrate analysis can be taxing, due to their structural complexity including the alpha/beta anomers at the axial and equatorial positions for hydroxyl groups and flexible ring structures. When these are analyzed by GC-MS their corresponding mass spectra can be easily misinterpreted due the similarity in fragmentation patterns. Multiple carbohydrates were investigated including mono-, di-, and tri- saccharides comparing two different types of derivatization, permethylation and oximation/pertrimethylsilylation, by gas chromatography- vacuum ultraviolet spectroscopic detection.[11] A sample of multiple carbohydrates were mixed together and deconvolutions were performed for coeluting analytes post-run to determine the concentration of each compound.[11] The developed methods were then applied to pharmaceutical products including Tri-Sprintec, Theraflu, and Chloraseptic Max Lozenges to evaluate their carbohydrate content.[11]

One of the more challenging food matrices is arguably eggs. Eggs contain diverse classes of compounds including plasma, lipids, proteins, carbohydrates, fat-soluble vitamins, water-soluble vitamins, minerals, inorganic compounds, carotenoids, and amino acids. In these experiments, classes of compounds suitable for reverse phase chromatography were selected which included fat-soluble

vitamins, naturally occurring hormones, and mycotoxins. Due to its complexity, the sample needed to be extensively cleaned before introduction into the instrument to mitigate some of the large biomolecule interferences. To do this, precipitation of proteins was paired with on-line sample concentration and clean-up with the use of a restricted access media (RAM) column. Different types of eggs were surveyed from hens that were from caged, cage-free, free-range, pasture raised, and home raised conditions for their fat-soluble vitamin, hormone, and mycotoxin content. The use of the on-line sample preparation method using the RAM column proved to be imperative to the method for analysis of the small molecules and allowed automation of sample preparation. The use of unique MRMs on the LC-MS/MS also allowed for analytes that coelute in the chromatogram to be differentiated and quantitated. Two interesting discoveries were found in the egg analysis. Vitamin K1 is produced in leafy green plants and was only detected in some of the eggs from free-range, some from pasture-raised and all of the home-raised eggs tested. This is direct evidence that relates how these hens live based on the contents of their eggs. The second interesting find was the discovery of mycotoxins in thirteen of the fourteen eggs tested. In these experiments, the use of skillful sample preparation, instrumentation automation for on-line clean up, and instrumental tools of using MRMs were all implemented to retrieve quality data.

1.4 Conclusions

Environmental and food samples can be extremely diverse. Each one of the complex samples called for different methods of sample preparation, analysis, and data handling. In the case of DMN samples, the VUV instrument's abilities were the

key to deconvoluting coeluting isomers and detecting DMNs in complex samples. While the VUV instrument's abilities of deconvolution were also used on the carbohydrates, derivatization was also necessary to make the samples amenable for GC analysis. The analysis of proppants was best performed by derivatization to make the formaldehyde less reactive and by sampling the headspace, which allowed for extremely complex samples, like proppants in produced water with added shale core, to be analyzed without any additional clean-up. Another additive used during the hydraulic fracturing process, friction reducers, were also able to be analyzed without any additional clean-up by the use of MALDI-TOF-MS. Finally, eggs only needed precipitation for sample preparation and most of the sample cleaning was performed on-line with the use of a RAM column. In all, each of these methods required different sample preparation techniques, handling, and the use of different and advantageous instrumental capabilities.

1.5 References

1. R. Alexander, R.I. Kagi, P.N. Sheppard, Relative abundance of dimethylnaphthalene isomers in crude oils, *J. Chromatogr*. *A* 267 (1983) 367-372.
2. T. Tesarik, J. Frycka, S. Ghyczy, Gas chromatography separation of naphthalene and biphenyl homologues on capillary columns, *J. Chromatogr. A* 148 (1978) 223-228.
3. A.R.J. Andrews, Z. Wu, A. Zlatkis, The GC separation of C2-Naphthalene isomers using cyclodextrins and crown ethers, *Chromatographia* 34 (1992) 163-165.
4. K.A. Schug, I. Sawicki, D.D. Carlton, H. Fan, H.M. McNair, J.P. Nimmo, P. Kroll, J. Smuts, P. Walsh, D. Harrison, Vacuum ultraviolet detector for gas chromatography, *Anal. Chem*. 86 (2015) 8329-8335.
5. J. Schenk, J. X. Mao, J. Smuts, P. Walsh, P. Kroll, K. A. Schug. Analysis and deconvolution of dimethylnaphthalene isomers using gas chromatography vacuum ultraviolet spectroscopy and theoretical computations. *Anal. Chim. Acta* 945 (2016) 1-8.
6. K. D. Pangilinan, A. C. C. de Leon and R. C. Advincula, Polymers for proppants used in hydraulic fracturing, *J. Pet. Sci. Eng.*, 2016, 145, 154–160.

7. J. Schenk, D. D. Carlton, J. Smuts, J. Cochran, L. Shear, T. Hanna, D. Durham, C. Cooper, K. A. Schug. Lab-simulated downhole leaching of formaldehyde from proppants by high performance liquid chromatography (HPLC), headspace gas chromatography- vacuum ultraviolet (HS-GC-VUV) spectroscopy, and headspace gas chromatography- mass spectrometry (HS-GC-MS). *Environ. Sci: Processes Impacts* 21 (2019) 214-223.
8. D. Durham. Hydraulic fracturing chemicals overview, Proceedings of the 251st American Chemical Society National Meeting and Exposition, San Diego, CA, 2016.
9. V. Elsner, O. J. Schmitz, V. Wulf, E. Naegele. Separation of homologous series of technical detergents with the Agilent 1290 infinity 2D-LC solution coupled with evaporative light scattering detector. Agilent application note, 2014. https://www.agilent.com/cs/library/applications/5991-2775EN.pdf. Accessed August 1, 2018.
10. J. L. York, R. H. Magnuson, D. Camdzic, K. A. Schug. Characterization of ethoxylated alcohols in frictions reducers using matrix-assisted laser desorption/ionization- time-of-flight- mass spectrometry. *Rapid Commun. Mass Spectrom.* 33 (2019) 1286-1292.
11. J. Schenk, G. Nagy, N. L. B. Pohl, A. Leghissa, J. Smuts, K. A. Schug. Indentification and deconvolution of carbohydrates with gas chromatography-vacuum ultraviolet spectroscopy. *J. Chromatogr. A* 1513 (2017) 210-221.

CHAPTER TWO: Methods and considerations for handling complex samples

Jamie L. York,[1] Kevin A. Schug[1]

[1]Department of Chemistry & Biochemistry, The University of Texas at Arlington, Arlington, TX 76019, United States

2.1 Introduction

There are many challenges faced with complex sample matrices that analytical chemists have to overcome. These challenges can be met by skillful sample preparation, on-line sample clean-up/pre-treatment, and/or the use of instrumental tools. Sample preparation is a good place to start and includes such methods as solid phase extraction (SPE), liquid-liquid extraction (LLE), salting-out, derivatization, filtration, centrifugation, and many others. Multiple approaches can also be combined, but this can quickly become cumbersome for large sample sets. On-line sample clean-up can be a welcomed alternative to relieve some of the manual steps and allow automation from the instrument of choice, but is not always a viable option. Lastly, the instrument's abilities should not be undervalued. Multiple reaction monitoring (MRM) transitions can be very useful when using a triple quadrupole mass spectrometer but can sometimes fall short when analyzing similar compounds that don't produce unique MRMs. Instrument tools that allow deconvolutions are also possible when chromatography falls short, as in the case of vacuum ultraviolet spectroscopic detection for gas chromatography. In addition to this, things like spectral filters are a great tool to highlight certain classes of compounds in a convoluted complex matrix when analyzing by gas chromatography- vacuum ultraviolet spectroscopy. All of these options for sample preparation, clean-up, and analysis should be taken into consideration when dealing with complex sample matrices in order to retrieve meaningful, reliable, and reproduceable data for the determination of target analytes.

2.2 Considering your sample

Before deciding on a technique to move forward with method development, it is important to consider what is in your sample and what could be a possible interference. Consideration needs to be given to the analytes' ability to be analyzed by GC and if not in native form, if they can be derivatized to be made GC-amenable. Derivatization can be a useful technique, but unless it can be automated, it is best to be avoided if the sample set is large – to save time and sanity. GC should not be written off too quickly though, especially when dealing with complex samples. Headspace sampling can be a terrific technique paired with GC to save time on the front-end during sample preparation and, in many cases, no other sample clean-up is necessary. The measurement of ethanol content in blood samples is a great example of this technique and requires no clean-up of the matrix prior to injection.[1] There are very few volatile substances that can be in a blood sample that will interfere with the measurement of ethanol, and if an appropriate column chemistry is used in conjunction with headspace sampling, no matrix clean-up is required.

LC is imperative for samples with higher molecular weight, those that require extensive derivatization, or those that are otherwise non-volatile and/or thermally-labile, which makes them not amenable for GC analysis. Special attention needs to be given to clean-up of the sample matrix to ensure that the LC column is not ruined, the lines do not get clogged, and/or the system is not dirtied by the complex sample. Precipitation is also a concern for LC, so compatibility between the mobile phase solvents, mobile phase additives, and samples should be taken into consideration.

Food, environmental, and biological samples are some examples of matrices that can be especially tricky. In the case of food analysis, the USDA Food Composition Databases are a great tool to use when evaluating possible interferences.[2] This will give a general idea of what is expected to be in a sample, as far as components with different physicochemical properties, such as fats, carbohydrates, and proteins. Environmental samples can be challenging because of their non-uniformity and will need tailored methods to mitigate any interferences, while still getting as much consistency between sample sets as possible. Biological samples, and in some cases food samples, are plagued with large biomolecules and proteins that can greatly hinder analysis and make instrumentation dirty. In order to move forward, it is best to get a handle on what analytes to target and how to exclude or work around interferences.

2.3 Matrix interferences and the effect they can have on analysis

Interferences can occur within the sample matrix and effect the sample analysis in a number of different ways. Sample signal can be of concern and matrix effects can mask, suppress, augment, or increase measured analyte signal. This can occur chromatographically as in the case of coelution, or during ionization, in the case of mass spectrometric detection, and result in highly variable or unreliable data. To correct for matrix effects encountered during electrospray ionization, the use of stable isotopically labelled internal standards are recommended. This is so that the internal standard nearly perfectly coelutes with the analyte of interest, experiences the same ionization suppression or enhancement as the analyte, and thus, can be more effectively used to correct analyte response. An example of this can be seen in

previous research where estrogens were detected in phosphate-buffered saline-bovine serum albumin, gelded horse serum, and mouse serum.[3] Internal standards were used to compensate for any fluctuation during the sample preparation procedure and ionization, but since deuterated internal standards were used, a deuterium isotope effect was observed resulting in slightly different retention times between the internal standard and target analytes.[3]

It is worth noting, when choosing an internal standard it is important to find an internal standard that is structurally unique, not present in the samples, and coelutes with your analyte but has unique MS transitions. Carbon-13 and nitrogen-15 labeled internal standards are oftentimes preferred over deuterated standards, to eliminate any deuterium isotope effects.[4] Deuterium isotope effects, in terms of altered chromatographic retention, will be exacerbated the longer the analyte and its deuterated internal standard are retained in the column, especially in reversed phase LC mode.

One concern of sample interferences can also be reactivity, especially in the case of reactive analytes. This can happen when the contents of the sample react with target analytes, and is oftentimes not reproducible and can hurt precision. The best way to alleviate this would be to remove the interference that is reacting, but this can be problematic since it is not always clear what is reacting, especially in extremely complex or unknown samples. A specific case of this can be seen in the detection of formaldehyde, an extremely reactive analyte, in a sample of shale core and produced water. The formaldehyde was originating from a resin-coating applied to a proppant, a hydraulic fracturing additive used in unconventional oil and gas

extraction.[5] The leaching of formaldehyde from the resin-coating on the proppants was tested at lab-simulated subsurface conditions by heating to subsurface temperatures and with the addition of the shale core and produced water, two components that these additives are likely to contact during hydraulic fracturing. When the shale core and produced water were added to the sample matrix, the concentration and sometimes precision in measuring the formaldehyde was diminished, likely due to competing reactions taking place from the matrix.[5] An example of the results for these experiments can be seen in Figure 2.1.

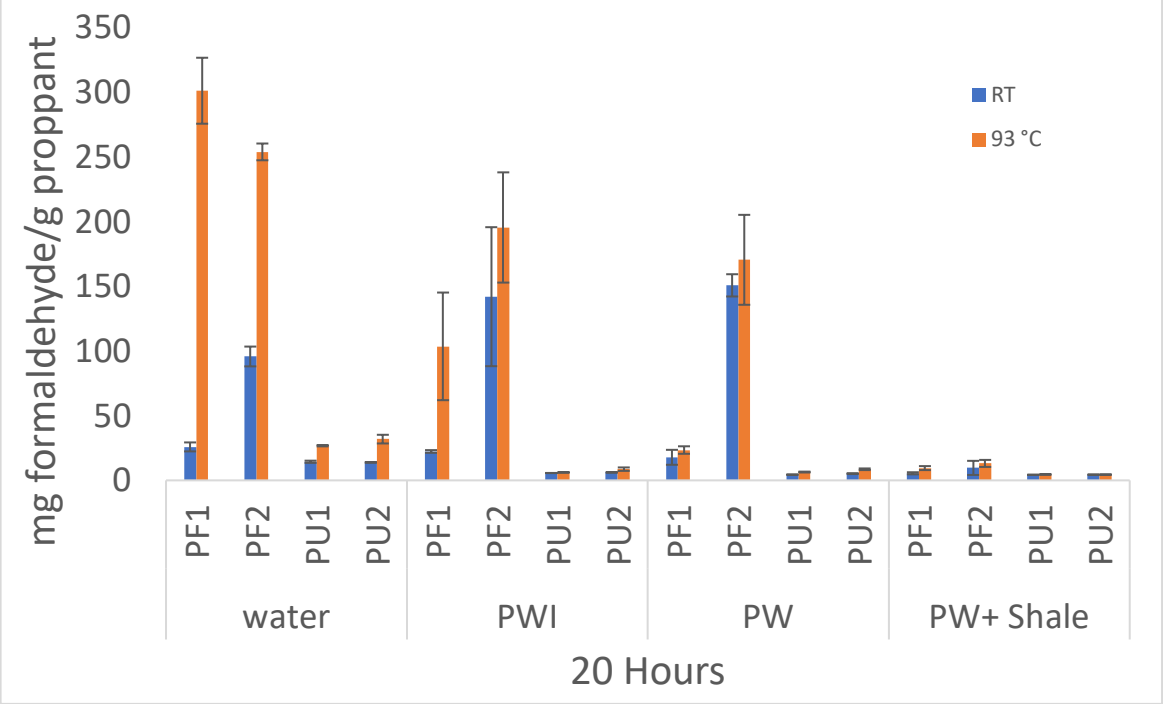

Figure 2.1. Four different resin-coated proppants (2 phenol-formaldehyde (PF1 and PF2) and 2 polyurethane (PU1 and PU2)) tested for derivatized formaldehyde leaching after 20 hours of soaking in water, produced water inorganic, produced water, or produced water with added shale core. Each were tested either at room temperature or heated to 200 °F (93 °C). The produced water with added shale core matrix returned lower quantities of the derivatized formaldehyde leaching from the proppants, likely due to competing reactions in the matrix with the derivatization of the fomaldehyde.[5]

2.4 Sample Preparation

Sample preparation should be ideally kept to a minimum to streamline sample throughput, but that is not always a viable option when handling complex samples. There are numerous techniques to choose from that can be implemented; the choices depend on the nature of your sample matrix and analyte.

Solid phase extraction (SPE) is a sample preparation technique that can be of use in preconcentrating samples, removing interferences, or desalinating samples. This can be especially useful in aqueous environmental matrices, like in the case of detecting nonsteroidal anti-inflammatory drugs (NSAIDs) from drinking water, surface water, and wastewater, where the analytes are present in low concentrations.[6] The set up usually consists of a manifold and cartridges that are used to trap and elute analytes. Large volumes of an aqueous sample can be loaded onto a cartridge, and eluted in a smaller volume, to preconcentrate the analyte. The system can use positive or negative pressure and a variety of sorbets are available from which to choose.

Solid phase microextraction (SPME) can be used to extract volatiles and non-volatiles from a liquid or gas matrix. SPME consists of a fiber coated with a stationary phase, liquid polymer, or both on the end of a plunger of a syringe or needle.[7] SPME can be used to sample from liquid by direct emersion or gas by headspace sampling. This method of sampling is ideal for off-site sample collection because it is easily transported to and from the site and back to the lab for analysis. Both SPE and SPME techniques require special apparatuses including cartridges, manifolds, and fibers that are available from manufactures and can be somewhat

costly. However, the selective extraction attainable through the use of these techniques can be very effective for eliminating unwanted matrix interferences prior to analysis.

Salting-out can also be a useful technique for sample preparation. The addition of salts can help reduce the hydration of target analytes and make them more amenable for extraction. Salting-out can be used to remove solid particles, fats, waxes, and even DNA from a sample. It can be used in combination with headspace or liquid phase extraction techniques. Salting-out is an integral part of the popular method referred to as QuEChERS (quick, easy, cheap, effective, rugged, safe), which also often includes dispersive solid phase extraction (dSPE).[8]

Salting-out can also be useful during sampling when using the headspace technique coupled to gas chromatography to facilitate analytes into the gas phase and can be used with the addition of traditional salts or ionic liquids. Liquid-Liquid extraction (LLE) can also use salting-out, called salting-out assisted LLE (SALLE), and is similar to QuEChERS. In one example from previous research, SALLE was implemented to extract oxytocin in plasma samples.[9] These analytes are oftentimes difficult due to their extremely low concentrations and interferences present in the plasma. By using SALLE the methods were able to overcome these challenges and obtain lower limits of detection.[9] Dispersive solid phase extraction is another sample preparation clean-up technique if water, polar, non-polar, and/or pigmentations need to be removed from the matrix. As the name implies, in dSPE, solid phase extraction particles are dispersed in the sample (rather than their use in a column format); they are then centrifuged to remove them. In previous work using QuEChERs and dSPE

as a sample clean-up technique, nicotine and its metabolites were detected in catfish, tuna, salmon, and tilapia.[10] It was found that the different types of fish required different dSPE components to optimize the method but with the optimized methods minimal or no matrix effects were present.[10] The use of salts can be a simple and economical alternative to purchasing additional sample preparation materials.

Various other simple and cost-effective sample preparation techniques can also be performed in the lab. Liquid-liquid extraction (LLE) is typically performed with two immiscible solvents and can be used to extract certain analytes based on their relative solubilities in the two solvents. This can be challenging when performing a multi-class compound analysis due to the differing degrees of solubility of the analyte classes.

Filtering and centrifugation are very important steps in the sample preparation process, especially for LC analysis. Centrifugation can help remove solids or small particulates from a sample and ensure that your autosampler and system do not become compromised. When trying to remove proteins, precipitation is a quick and easy tool to use. Typically, a chilled organic solvent such as acetonitrile or acetone can facilitate the precipitation of proteins due to their limited solubility in these solvents. Finally, when targeting trace analytes from a complex matrix, concentration by dehydration can be used by drying down the sample with a stream of N_2 and regenerating with a solvent and has the ability to also be automated. These methods require materials that most labs are likely to already have (centrifuge, filters, glassware, gases, solvents) so can be cost-effective.

Derivatizing the sample is sometimes a necessity. Derivatization is not just a GC technique. It can also be performed for LC to make a small molecule (>100 *m/z*) larger and more amendable for MS, or give the molecule a UV or fluorescence-active moiety.[11,12] In previous research, dansyl chloride was used to derivatize estrone, 17α-estradiol, 17β-estradiol, and estriol for their determination in human cerebrospinal fluid.[12] By this method, no offline extraction or cleanup was necessary and levels in the pg/mL were able to be detected using LC-MS/MS.[12] Three examples of common methods of derivatization techniques can be seen in Figure 2.2. When choosing which sample preparation technique is best for your complex matrix, it is important to consider your specific target analytes and the interferences you want to rid your sample of in addition to how much time you want to spend handling each sample.

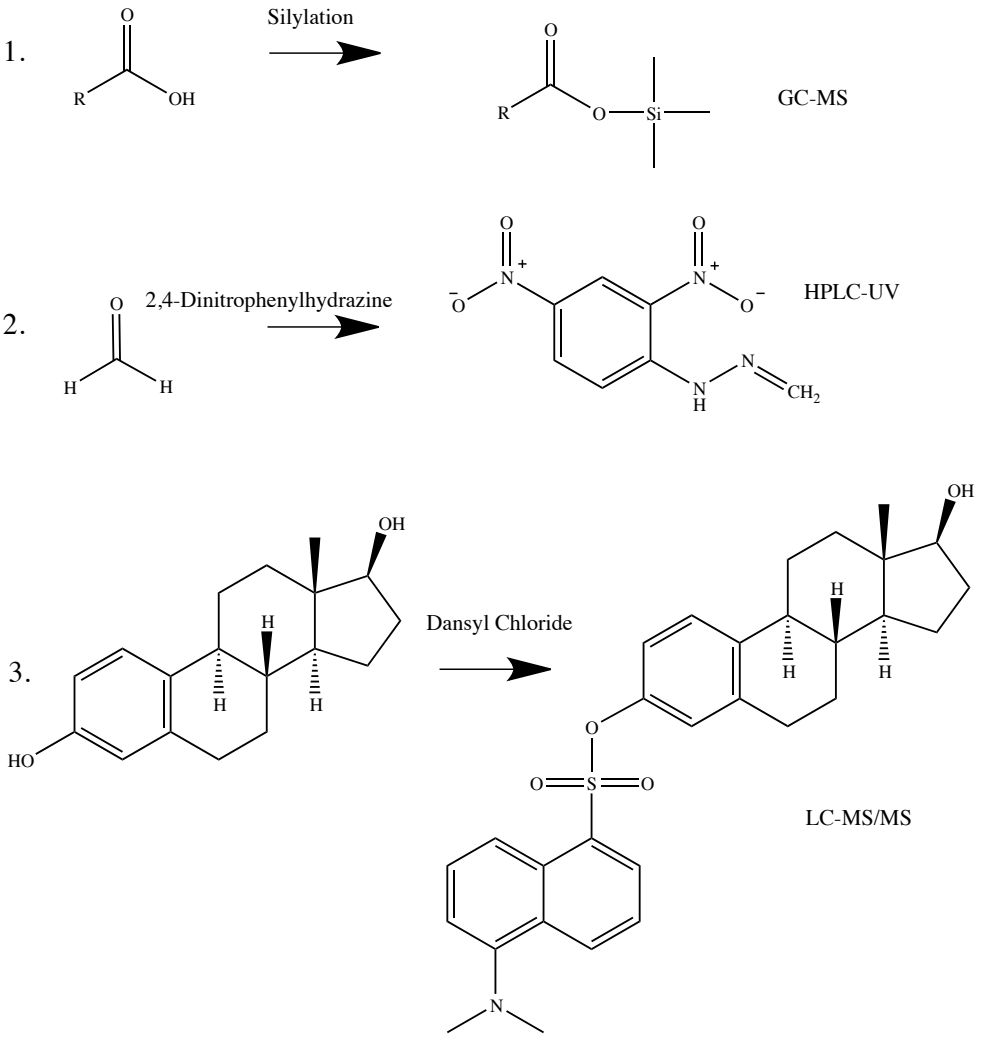

Figure 2.2. Examples of common methods of derivatization for different methods of analysis. 1. Silylation performed on a carboxyl group to make less polar and more volatile for analysis on GC-MS. 2. Derivatization performed on formaldehyde by reacting it with 2,4-dinitrophenylhydrazine to add a chromophore to the molecule before subsequent analysis by HPLC-UV. 3. Dansyl chloride derivatization on estradiol for analysis by LC-MS/MS.[6,12,13]

2.5 On-line sample treatment

There are various other techniques that can be implemented on-line. Moving sample preparation and sample treatment on-line can be advantageous because it requires less manual sample handling, increased recovery, improved limits of detection, less human error, and reduced exposure of compounds to the

environment, which can be useful for analytes that are photosensitive or reactive to oxygen. One common method of on-line sample treatment includes on-line SPE, which can be implemented to clean and preconcentrate target analytes in an automated fashion.[6] Other forms of sample preparation that can be automated include the use of a continuous stirred tank reactor (CSTR) for on-line sample dilution. A CSTR contains a reservoir that allows fluid to travel through the apparatus. This device can be used to continuously dilute a sample injected into it. In previous research, a CSTR was used in the study of native carbohydrates to study the electrospray response factors by LC-MS/MS.[14] By using the CSTR apparatus, analyte response data for a large range of analyte concentrations were able to be obtained with only one injection.

Restricted access media (RAM) can be particularly useful when dealing with complex matrices, especially when targeting small molecules and trying to rid the sample of large biomolecule interferences prior to LC analysis.[15,16,17,18] RAM columns work on a similar principle to size exclusion chromatography. The outer surface of the stationary phase has a non-retentive and size-restrictive layer, while the inner pores of the support material have a bonded group, like C4, C8, C18, and so on. Only the small molecules can access and interact with the inner-pore phase to be retained on the column, while the large molecules are unretained and washed to waste. This can be especially useful when looking at small molecules in complex matrices such as whole blood or plasma where there is an abundance of protein interferences. This is a technique that can be put in-line, in the flow path before the analytical column, so that the extraction process is completely automated. This can

provide a welcomed alternative to extensive sample preparation and sample handling.

An example of this methodology was used in the quantification of lipid mediators in skeletal muscles using the RAM column coupled to LC-MS/MS.[19] This technique requires the use of one or two high-pressure valves in the column oven and some extensive LC programming for loading, eluting, and washing parameters. An example of LC settings and the valve setup can be seen in Figure 2.3.[20]

LC Time Program					
Time (min)	**A + B mL/min**	**C + D mL/min**	**% B**	**%D**	**Valve position**
0.00	0.05	0.05	60	0	1,0
1.00	G	0.10	60	0	1,0
1.50	0.22	1.00	60	0	1,0
5.00	0.22	1.00	60	0	1,0
5.50	0.22	0.22	60	0	1,0
6.00	0.22	0.22	60	0	0,0
7.00	G	0.00	G	0	0,0
9.00	G	0.00	G	0	1,0
9.50	0.35	0.30	G	100	1,0
13.00	0.35	0.30	G	100	1,0
14.00	0.35	0.10	78	100	0,1
14.01	0.35	0.10	5	100	0,1
19.00	0.35	0.20	5	100	0,1
19.01	0.05	0.20	5	0	0,1
20.50	0.10	0.20	5	0	1,0
20.51	0.10	0.60	5	0	1,0
22.00	0.10	0.60	5	0	1,0

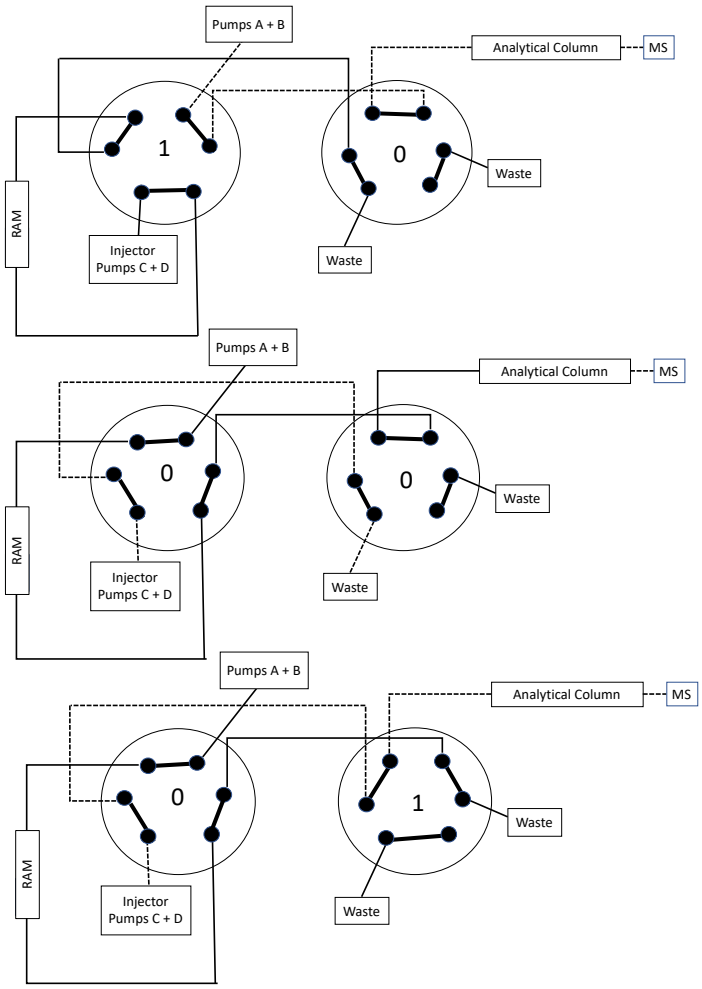

Figure 2.3. LC settings for mobile phase concentration, flow rate, valve positions, and valve diagrams. From 0-6 min the sample is being loaded by pumps C + D onto the RAM column, while the analytical column is being equilibrated with pumps A + B. The analytes are back eluted from the RAM column by pumps A + B from 6-9 min and sent to the analytical column. The valves switch and pumps A + B perform the analytical separation from 9-14 min, while pumps C + D wash the RAM column. Finally, at 20.5 min the valves are switched to their starting position and the RAM and analytical columns are equilibrated for the next injection.[20]

When dealing with trace analysis on complex samples, the RAM column can be loaded with large sample injections without effecting the peak shape. In addition to large sample volumes, the RAM can also be loaded with multiple injections to allow for ultra-trace analysis to be performed. In previous research, bisphenol A was

able to be detected in human saliva samples by using a RAM column in combination with LC-MS/MS.[21] Parts per trillion levels of bisphenol A were detectable by performing multiple injections on the RAM column to concentrate the analyte and remove unwanted large biomolecules.[21]

2.6 Instrumental tools

Many instrumental tools can be very valuable and can save time and effort in sample preparation/method development. Instrument tools can include things like multiple reaction monitoring (MRM), spectral filters, and programs that allow for deconvolution of coeluting signals. In the case of mass spectrometry, MRMs allow for high sensitivity and specificity from complex matrices, as long as unique transitions can be acquired. Although useful for the differentiation of unlike compounds, this is not always an option when analyzing isomeric compounds. In previous work on cannabinoids, a number of isomers were analyzed and it was found that some of the compounds had common fragmentation pathways when using MRMs on the GC-MS/MS.[13] In order to differentiate analytes with common fragmentation pathways, the compounds had to be chromatographically separated. This was partially achieved by silylating the cannabinoids; however, some potential interferences still existed. It was still necessary to monitor less sensitive secondary and tertiary precursor-to-product ion transitions to provide adequate specificity.[13]

In complex matrices, there is likely to be a case where the target analytes are isomeric, are not resolved chromatographically, and do not produce unique MRM transitions when analyzed by the mass spectrometer. These can still be accurately quantified using instrumental tools with the right detector. The vacuum ultraviolet

(VUV) detector measures in the 120- 240 nm range, where virtually all compounds have a unique, compound specific absorbance spectra.[22,23] Since Beer's law is additive, the overlapping VUV absorption signals arising from coelution can be easily deconvoluted.[22,23] A straightforward least squares approach can be used to discern individual component contributions to the overlapping signals.[23] An example of deconvolution can be seen in Figure 2.4, where coeluting isomers of dimethylnaphthalenes have been separated into their respective contributions to the coeluted peak.[23] In order to use this tool, the analytes have to first be amendable to GC, which can complicate things if the analytes are not volatile or thermally stable. The similarity of spectra between the coeluting compounds is a governing factor of how accurately the compounds can be deconvoluted. The more distinct the absorbance spectra, the easier the compounds are to deconvolute over a wider dynamic range of concentrations and the more similar the spectra are the more difficult they are to differentiate.

Spectral filters can also be a great tool in conjunction with VUV for complex samples when certain classes of compounds are of interest. Spectral filters can be applied to samples that are too complex to perform deconvolutions on because what compounds are coeluting with target analytes may not be known. In the VUV range certain classes of compounds absorb strongly in different ranges. Saturated compounds absorb in the 125-160 nm range, unsaturated compounds absorb in the 170- 240 nm range.[23] This information can be used to build and apply a spectral filter to apply to a chromatogram post-run. In the same set of experiments performed for coeluting isomers of dimethylnapthalenes, spectral filters were used on samples of

diesel fuel and jet fuel, which are extremely complex, to show where naphthalene, methylnaphthalenes, dimethylnaphthalenes, and trimethylnaphthalenes elute.[23] This was done by experimentally determining where naphthalene class compounds absorb strongly (210-220 nm) and applying a filter in that range to selectively identify where the naphthalenes elute without performing deconvolutions.[23]

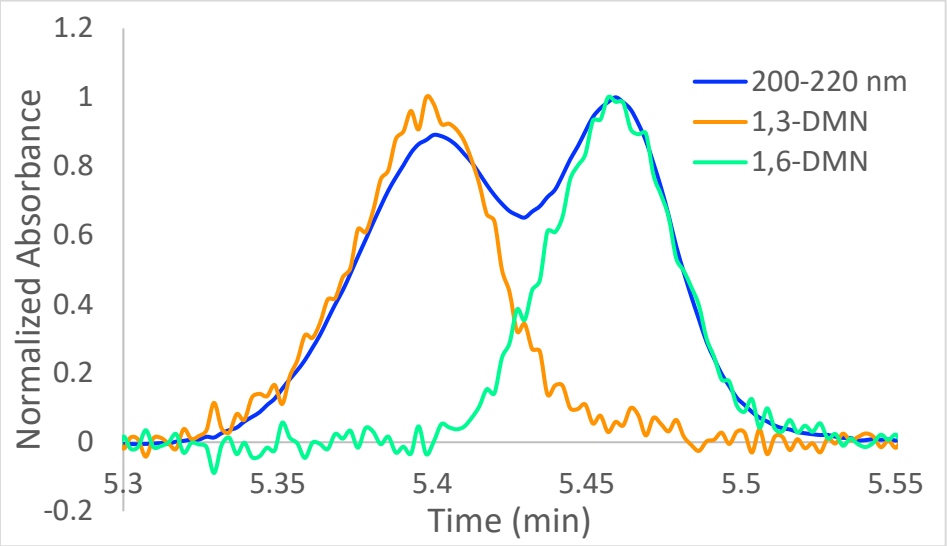

Figure 2.4. Example of coeluting isomers of dimethylnapthalene measured at the 200-220 nm range (blue). Deconvolutions were performed into the respective concentrations for each isomer (green and orange) using manufacturer software.[23]

2.7 How to evaluate which is the best option to use for your analysis

A good place to start when deciding what is best to try for method development in complex samples is to first take into account what you are targeting and what you want to remove. Knowing your sample and the possible interferences can facilitate at least an educated guess on what types of sample handling should be implemented first and can save a lot of guess work, time, and money. Excessive fats, waxes, and proteins can dirty instruments, so special attention needs to be given to remove these from the matrix. Next, decide on how removal of problematic

compounds can be performed. Does it need extensive clean-up on the front-end to remove matrix interferences or can the use of an instrument tool/on-line sample treatment mitigate unsavory effects on sample analysis?

A flow-chart of the topics covered in this article for sample preparation, on-line sample treatment, and instrumental tools discussed in this article can be seen summarized in Figure 2.5. When starting with a complex sample the first consideration is which method to choose, LC or GC. Once LC or GC is determined there are a number of different sample preparation and automated sample handling choices that are amenable for each technique. Finally, depending on the detector chosen, available tools may aid in the analysis of the complex sample and offer additional tools that can help with complex sample analysis. This flow-chart is by no means an exhaustive list, but can be a good starting point when considering the available options.

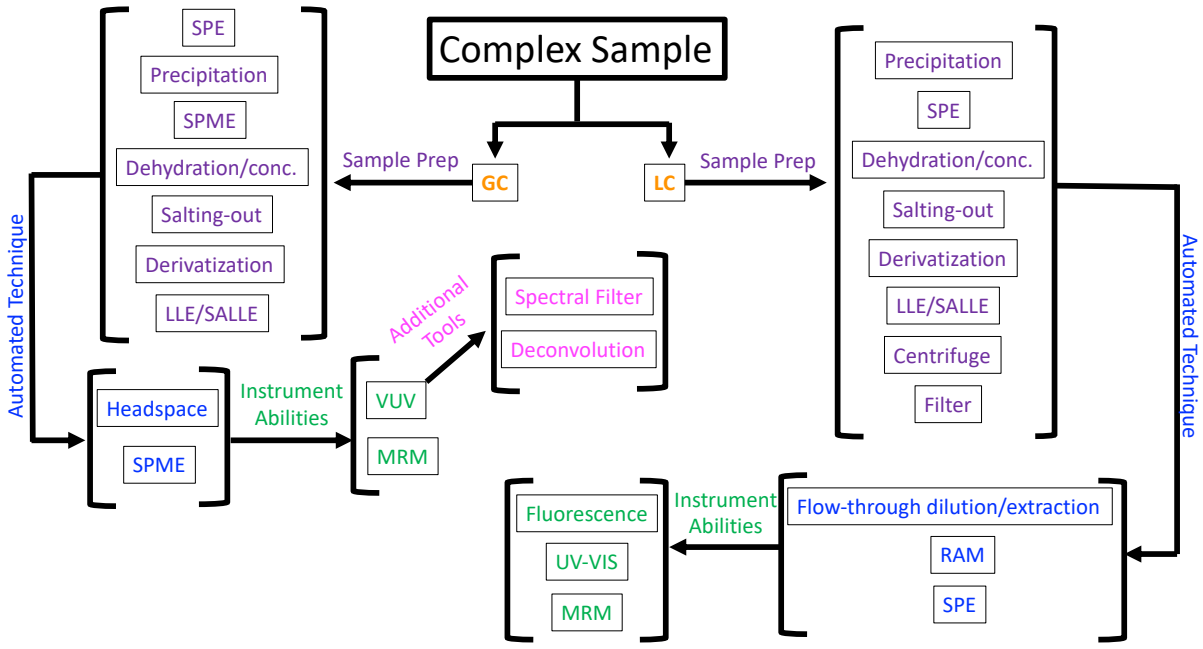

Figure 2.5. Flow chart of a selection of common available options on how to treat complex samples highlighted in this article. The process begins by deciding whether the target analytes are more amenable to GC or LC analysis.

2.8 Conclusion

When starting a new project, it can be overwhelming to try to anticipate problems your newly assigned complex matrix may give you, but there are many solutions that can be implemented to save time and money. After the sample matrix is evaluated and a method of analysis is chosen (GC or LC), it will help determine what type of sample clean-up is appropriate for the matrix. If the analytes are going to be analyzed via GC, headspace is a great option due to the limited need for sample clean-up; SPME sampling in solution or in the headspace might be the next best choice to consider. If using LC and excessive proteins are of concern, a simple dilute, filter or centrifuge, and shoot with the right solvent might just do the trick. Ultra-trace analyte analysis in a complex matrix can be accomplished with the use of

a RAM column and multiple injections. The most important thing when trying to develop a method for a complex matrix is to start with literature and make the best educated guess you can, and to not be afraid to try something new. In the end, the proof of performance and method validation is key in acquiring reliable, reproducible, and accurate data.

2.9 References

1. Zamengo, L.; Tedeschi, G.; Frison, G.; Griffoni, C.; Ponzin, D.; Jones, A. W. Inter-laboratory proficiency results of blood alcohol determinations at clinical and forensic laboratories in Italy. *Forensic Sci. Int.* 295, **2019**, 213-218.
2. USDA Food Composition Databases. United States Department of Agriculture Research Service, 2019. https://ndb.nal.usda.gov/ndb/search/list (accessed June 27, 2019).
3. Nguyen, H.P.; Li, L.; Nethrapalli, I.S.; Guo, N.; Toran-Allerand, D.; Harrison, D.E.; Astle, C.M.; Schug, K.A.* Evaluation of Matrix Effects in Analysis of Estrogen using Liquid Chromatography – Tandem Mass Spectrometry. *J. Sep. Sci. 34,* **2011**, 1781-1787.
4. Grant, R. Everything you wanted to know about internal standards but were too afraid to ask. 2019. https://glc2.workcast.com/clusterSVCFS1/NAS/OnDemand/10994/1775713496937128/Media/10994_20190530100329002_edit1.mp4?mc_cid=0a08c656b8&mc_eid=64db5d8f3e (accessed June 27, 2019).
5. Schenk, J.; Carlton, D.D.; Smuts, J.; Cochran, J.; Shear, L.; Hanna, T.; Durham, D.; Cooper, C.; Schug, K.A. Lab-simulated downhole leaching of formaldehyde from proppants by high performance liquid chromatography (HPLC), headspace gas chromatography- vacuum ultraviolet (HS-GC-VUV), and headspace gas chromatography- mass spectrometry (HS-GC-MS). *Environ. Sci.: Processes Impacts*, 21, **2019**, 214-223.
6. Marta, Z.; Bobaly, B.; Fekete, J.; Magda, B.; Imre, T.; Szabo, P. T. Simultaneous determination of ten nonsteroidal anti-inflammatory drugs from drinking water, surface water, and wastewater using micro UHPLC-MS/MS with on-line SPE system. *J. Pharm. Biomed. Anal.* 160, **2018**, 99-108.
7. Spietelun, A.; Pilarcyzyk, M.; Kloskowski, A.; Namiesnik, J. Current trends in solid-phase microextraction (SPME) fibre coatings. *Chem. Soc. Rev.,* 39, **2010,** 4524-4537.
8. Anastassiades, M.; Lehotay, S. J.; Stajnbaher, D.; Schenck, F. J. Fast and Easy Multiresidue Method Rmploying Acetonitrile Extraction/partitioning and "Dispersive Solid-Phase Extraction" for the Determination of Pesticide Residues in Produce. *J. AOAC Int.* 86, **2003**, 412-431.

9. Liu, D.; Han, X.; Liu, X.; Cheng, M.; He, M.; Rainer, G.; Gao, H.; Zhang, X. Measurement of ultra-trace level of intact oxytocin in plasma using SALLE combined with nano-LC-MS. *J. Pharm. Biomed. Anal.*173, **2019**, 62-67.
10. Chang, Y.-W.; Nguyen, H.P.; Chang, M.; Burket, S.R.; Brooks, B.W.; Schug, K.A.* Determination of nicotine and its metabolites accumulated in fish tissue using QuEChERS and hydrophilic interaction liquid chromatography coupled with tandem mass spectrometry. J. Sep. Sci. 38, **2015**, 2414-2422.
11. Baghdady, Y.; Schug, K.A.* A Review of In Situ Derivatization Techniques for Enhanced Bioanalysis using Liquid Chromatography – Mass Spectrometry. *J. Sep. Sci.* 39, **2016**,102-114.
12. Fan, H.; Papouskova, B.; Lemr, K.; Wigginton, J.G.; Schug, K.A.* Bulk Derivatization and Direct Injection of Human Cerebrospinal Fluid for Trace Level Quantification of Endogenous Estrogens Using Trap-and-Elute LC-MS/MS. *J. Sep. Sci*. 37, **2014**, 2010-2017.
13. Leghissa, A.; Hildenbrand, Z.L.; Foss Jr., F.W.; Schug, K.A. Determination of cannabinoids from a surrogate hops matrix using multiple reaction monitoring gas chromatography – triple quadrupole – mass spectrometry. *J. Sep. Sci*. *41,* **2018**, 459-468.
14. Thacker, J.; Schug, K. A. Use of a continuous stirred tank reactor for the determination of electrospray response factors and its application to underivatized sugars under various solvent parameters. J. Am. Soc. Mass Spectrom. 30, **2019**, 439-447.
15. Yang, S.H.; Fan, H.; Classon, R.J.; Schug, K.A. Restricted Access Media as a Streamlined Approach towards On-line Sample Preparation: Recent Advancements and Applications. *J. Sep. Sci.* 36*,* **2013**, 2922-2938.
16. Papouskova, B.; Fan, H.; Lemr, K.; Schug, K.A. Aspects of Trapping Efficiency And Matrix Effects in Development of a Restricted Access Media-Based Trap-and-Elute Liquid Chromatography-Mass Spectrometry Method. *J. Sep. Sci*. 37*,* **2014**, 2192-2199.
17. Baghdady, Y.Z.; Schug, K.A. Evaluation of Efficiency and Trapping Capacity of Restricted Access Media Trap Columns for Online Trapping of Small Molecules. *J. Sep. Sci. 39*, **2016**, 4183-4191.
18. Dipe de Faria, H.; Abrao, L.; Santos, M.; Barbosa, A.; Figueiredo, E. New advances in restricted access materials for sample preparation: A review. *Anal. Chim. Acta.* 959, **2017**, 43-65.
19. Wang, Z.; Bian, L.; Mo, C.; Kukula, M.; Schug, K. A.; Brotto, M. Targeted quantification of lipid mediators in skeletal muscles using restricted access media-based trap-and-elute liquid chromatography-mass spectrometry. *Anal. Chim. Acta.* 984, **2017**, 151-161.
20. Fan, H.; Papouskova, B.; Lemr, K.; Wigginton, J.G.; Schug, K.A. Bulk Derivatization and Direct Injection of Human Cerebrospinal Fluid for Trace Level Quantification of Endogenous Estrogens Using Trap-and-Elute LC-MS/MS. *J. Sep. Sci*. *37*, **2014**, 2010-2017.
21. Yang, S.H.; Morgan, A.A.; Nguyen, H.P.; Moore, H.; Figard, B.J.; Schug, K.A.* Quantitative Determination of Bisphenol A from Human Saliva using Bulk

Derivatization and Trap-and-Elute HPLC-Electrospray Ionization – Mass Spectrometry. *Environ. Toxicol. Chem*. 30, **2011**,1243-1251.
22. Schug, K. A.; Sawicki, I.; Carlton, D. D.; Fan, H.; McNair, H. M.; Nimmo, J. P.; Kroll, P.; Smuts, J. Walsh, P.; Harrison, D. Vacuum ultraviolet detector for gas chromatography. *Anal. Chem.* 85, **2015**, 8329-8335.
23. Schenk, J.; Mao, J. X.; Smuts, J.; Walsh, P.; Kroll, P.; Schug, K. A. Analysis and deconvolution of dimethylnaphthalene isomers using gas chromatography vacuum ultraviolet spectroscopy and theoretical computations. *Anal. Chim. Acta.* 945, **2016**, 1-8.

CHAPTER THREE: Analysis and deconvolution of dimethylnaphthalene isomers using gas chromatography vacuum ultraviolet spectroscopy and theoretical computations

Jamie Schenk,[1] James X. Mao,[1] Jonathan Smuts,[2] Phillip Walsh,[2] Peter Kroll,[1] Kevin A. Schug[1*]

[1] Department of Chemistry & Biochemistry, The University of Texas at Arlington, Arlington, TX 76019, United States

[2] VUV Analytics, Inc., Cedar Park, TX 78613, United States

3.1 Abstract

An issue with most gas chromatographic detectors is their inability to deconvolve coeluting isomers. Dimethylnaphthalenes are a class of compounds that can be particularly difficult to speciate by gas chromatography – mass spectrometry analysis, because of their significant coelution and similar mass spectra. As an alternative, a vacuum ultraviolet spectroscopic detector paired with gas chromatography was used to study the systematic deconvolution of mixtures of coeluting isomers of dimethylnaphthalenes. Various ratio combinations of 75:25; 50:50; 25:75; 20:80; 10:90; 5:95; and 1:99 were prepared to test the accuracy, precision, and sensitivity of the detector for distinguishing overlapping isomers that had distinct, but very similar absorption spectra. It was found that, under reasonable injection conditions, all of the pairwise overlapping isomers tested could be deconvoluted up to nearly two orders of magnitude (up to 99:1) in relative abundance. These experimental deconvolution values were in agreement with theoretical covariance calculations performed for two of the dimethylnaphthalene isomers. Covariance calculations estimated high picogram detection limits for a minor isomer coeluting with low to mid-nanogram quantity of a more abundant

isomer. Further characterization of the analytes was performed using density functional theory computations to compare theory with experimental measurements. Additionally, gas chromatography – vacuum ultraviolet spectroscopy was shown to be able to speciate dimethylnaphthalenes in jet and diesel fuel samples.

Keywords: Polyaromatic hydrocarbons, Coelution, Covariance analysis, Diesel fuel, Jet fuel, Electronic absorption spectra, Density functional theory

3.2 Introduction

Hydrocarbons are a type of organic compound found naturally in sedimentary rock deposits of shale formations and tar pits. They have received considerable attention in research because of their use in a wide range of fields from oil and gas to plastics, electricity generation, and pharmaceuticals. Some of the techniques for evaluating hydrocarbons in crude oil include gas chromatography – mass spectrometry (GC-MS), liquid chromatography – mass spectrometry (LC-MS), and gas chromatography – Fourier transform infrared (GC-FTIR) spectroscopy.[1] Gas chromatography is an essential tool in analyzing crude oil and associated refinery products, because they can contain thousands of different volatile and semi-volatile hydrocarbon compounds, including parent and alkylated polycyclic aromatic hydrocarbons (PAHs). GC readily separates some of these components; whereas others, specifically some isomeric substituted PAHs, present greater difficulties for definitive speciation.[2]

One disadvantage of GC is its general inability to decipher between compounds that coelute. GC works by separating compounds based on their differential partition coefficient into a stationary phase. When compounds have common physicochemical properties, such as vapor pressure and polarity, they may

be unresolved by GC. When using GC-electron ionization-MS, the presence of coeluting analytes leads to highly complex mass spectra that may be difficult to deconvolute. If the coeluting compounds are isomeric and isobaric, the observed fragmentation patterns may be misinterpreted and lead to incorrect identifications.[3]

An alternate solution to separating coeluting peaks could be to use comprehensive two-dimensional gas chromatography (GCxGC). In GCxGC, two sequential separations are performed on two different columns that provide complementary selectivity.[4] While GCxGC may have an order of magnitude or more greater peak capacity than GC, this method requires additional hardware and coupling with a fast detector in order to accommodate the time scale of second dimension chromatographic separations. Ultra-fast-scan quadrupole or time-of-flight mass spectrometer systems have generally been needed to gather ample and useable information.[5] Other typical GC detectors that have a high response rate and can keep up with GCxGC separations do not generally provide any qualitative information.

Dimethylnaphthalenes (DMN) are a class of substituted PAHs that are commonly found in crude oils and associated products.[6] It is important to be able to identify the DMN isomers from one another because of their different carcinogenicities, industrial uses, and environmental polluting effects. Some DMNs pose no notable threat to the environment (1,4-DMN, 2,7-DMN, 1,5-DMN, 1,6-DMN and 1,8-DMN), while others (1,2-DMN, 1,3-DMN, 2,6-DMN, and 2,3-DMN) are considered toxic to marine life and/or humans. Thus, it is important to be able to speciate isomers in a sample to assess health impact or industrial performance. 2,6-

DMN is arguably the most profitable of all the isomers and is used as a precursor in the synthesis of high performance plastic and liquid crystal polymer products, such as polyethylene naphthalate (PEN).[7,8]

Structurally speaking, DMN can be found in ten different isomers, some of which have very similar polarities and boiling points. It is possible to separate DMN isomers that coelute under various different conditions but finding one method with the ability to differentiate between all isomers that coelute has been a significant challenge.[6] Further, assignment of separated (or coeluted) DMNs has been hampered by lack of detection specificity.

In some of the earliest attempts to separate DMN isomers, Tesarik et al. (1978) experimented with capillary and packed column GC and reported that complete separation of all DMNs was not obtained.[9] In 1983, under the conditions described in Alexander et al. and using an OV-1 column, all of the isomers were resolved, except 1,5- and 2,3-DMN, which coeluted. They further experimented with a OV-1701 phase to resolve the issue, but this resolved all of the isomers, except 2,6- and 2,7-DMN.[6] Successful attempts were later made in 1992 using a cyclodextrin stationary phase although the 2,6/2,7 isomers were only partially separated.[10] Further use of this stationary phase was used in 1993 to separate nine of the ten isomers using cyclodextrin-modified micellar electrokinetic chromatography in association with a sodium dodecyl sulfate mobile phase modifier.[11] This method featured a mode of capillary electrophoresis using the basis of differential partitioning of an analyte between an ionic micelle and the surrounding aqueous phase. Later, Shinbo et al. (1998) reported the use of a cyclophane CP44-

bonded silica gel stationary phase for HPLC separation of various naphthalene derivatives. Their results yielded better separation for DMNs at low temperatures (0 °C) than a comparative ODS phase, which gave little to no separation even at low temperatures.[12] The use of a liquid-crystalline stationary phase has also been reported to separate some of the more challenging DMN isomers.[13] The separation of coeluting isomers of 2,6- and 2,7-DMN have been said to be the most challenging by GC and thus, additional methods such as extractive crystallization, solvent extraction using various zeolites, and dissolution of a 2,6- and 2,7-DMN mixture in supercritical CO_2 have been explored.[14,15,16]

Recently, a new vacuum ultraviolet (VUV) absorption spectroscopy detector for GC has been introduced.[17] Until now, spectroscopic measurements in the VUV wavelength range (100–185 nm), where virtually all chemical compounds absorb photons, have largely been relegated to bright-source synchrotron facilities.[17] A new bench-top VUV detector captures full absorption spectra from 120 to 240 nm.[17,18,19] In the gas phase, absorption spectra for different compounds, including isomeric and isobaric species, are unique and this property can be used to enhance detection specificity.[17,18] Due to the general additivity of absorption processes, spectra can also be easily deconvoluted if multiple compounds coelute. Analytes exiting the GC column are carried by an inert make-up gas through a heated transfer line and into the detector flow cell (80 µL volume). A deuterium lamp is used as the light source and absorption is measured using a charge-coupled detector with a maximum sampling rate of 100 Hz.

The aim of this study was to test the accuracy, precision, and sensitivity of the GC-VUV detector to distinguish between various combinations and concentrations of DMN isomers that overlap on a chromatogram. The DMN isomers represented a challenging case for deconvolution of closely-related coeluting compounds, and thus, some limits in terms of performance of this capability by the VUV detector could be established. Different ratios of coeluting isomers were mixed together in combinations of 75:25, 50:50, 25:75, 10:90, 5:95, and 1:99, and then analyzed. Covariance calculations were performed to find the theoretical dynamic detection limit for the overlapping isomers. The results for covariance calculations were then compared to the experimental values, and good agreement was observed. Further, the dimethylnaphthalene analyte set was used to investigate the correlation between theoretically computed (using density functional theory) and experimentally measured spectra. The experimental VUV spectra and theoretical computed spectra matched each other well with minor exceptions. The potential for deconvolving theoretical mixture spectra was also evaluated.

3.3 Material and methods

3.3.1 Materials

Eight DMN standards were purchased from different vendors (the 1,7- and 1,8-DMN isomers were not acquired and evaluated in this study). 2,6-, 2,7-, and 1,3-DMN were purchased from Tokyo Chemical Industry Co., Ltd. (Tokyo, Japan) at >98%, >98%, and >95% purity, respectively. 1,4-, 1,5-, and 1,2-DMN were purchased from Sigma-Aldrich (St. Louis, MO) with 95% purity for all. 2,3-DMN was purchased from Alfa Aesar (Ward Hill, MA) in 97% purity and 1,6-DMN was

purchased from Matrix Scientific (Columbia, SC) with 95% purity. Two trimethylnaphthalene (TMN) standards were also purchased. 2,3,5-TMN was purchased from TCI America (Portland, OR) and 1,4,5-TMN was purchased from VWR (Radnor, PA), both in 95% purity. All standards were initially prepared to 1000 ppm concentration in a dichloromethane (DCM) solvent. GC-MS grade DCM was purchased from Fischer Scientific (Fair Lawn, NJ). Diesel and jet fuel samples were acquired commercially from an anonymous source and diluted 1:3 parts with DCM solvent prior to analysis.

3.3.2 Instrumentation

A Shimadzu GC-2010 gas chromatograph (Shimadzu Scientific Instruments, Inc., Columbia, MD) was coupled with a VGA-100 VUV detector (VUV Analytics, Inc., Cedar Park, TX) and used to collect chromatograms and spectra from DMN standards, diesel, and jet fuel. The data acquisition rate was set to 10 Hz and the transfer and flow cell temperatures were set to 300 °C. Nitrogen was used as the makeup gas and was set to 0.25 psi to minimize band broadening in the flow cell. The GC was equipped with an Rtx-1 column (30 m × 0.25 mm x 0.25 μm) obtained from Restek Corporation (Bellefonte, PA) and was used at a constant velocity of 30 cm/s with a helium carrier gas. The injection port was set to 270 °C with a 10:1 split ratio and a 0.3 μL injection volume. The GC oven profile for DMN standards analysis was isothermal at 150 °C; this condition ensured coelution of critical pairs of DMN isomers. The GC oven profile for diesel and jet fuel samples used temperature programming. The oven was set to 50 °C for 2 min, followed by a 5 °C/min ramp to 270 °C, and held for 20 min.

3.3.3 Sample preparation and data analysis

Each of the coeluting pairs of isomer standards (1,4- and 2,3-DMN; 1,3- and 1,6-DMN; 2,6- and 2,7-DMN) were mixed in ratios of 25:75, 50:50, 75:25, 80:20, 90:10, 95:5, and 99:1, and analyzed in triplicate. The chromatographic data comprising time-dependent absorbance spectra were imported into the VUV Model & Analyze software (VUV Analytics, Inc.) to perform deconvolutions of the coeluting peaks. The deconvolutions were carried out in this case using the 200–220 nm wavelength range, but in principle any wavelength range where significant differential absorption is observed could be chosen. A covariance analysis was performed to theoretically predict detection limits and compare with experimental results. The details of the covariance analysis are given in the Electronic Supplementary Information and an associated reference.[20]

Further, a mixture of the eight DMN standards in equal quantities were spiked into the diesel and jet fuel samples. A spectral filter was assigned and applied in order to illuminate the DMN content in these complex samples with and without spiking. Injections of trimethylnapthalene standards were used to confirm and assign the region of elution for that compound class.

3.3.4 Computational details

All geometries were optimized at MP2[21] /aug-cc-pvdz[25] level and the absorption spectra were then computed using time dependent density functional theory (TDDFT) using a PBE0 functional[22,23,24] and a aug-cc-pvdz basis set. All calculations were carried out using the Gaussian 09 program.[26]

3.4 Results and discussion

3.4.1 Empirical deconvolution

In this study, we investigated the limits of some of the most difficult systems to deconvolve, those based on coeluting DMNs, to better understand the limits of VUV deconvolution capabilities. Conveniently, VUV spectroscopy follows the Beer-Lambert Law. As in UV–Vis spectroscopy, absorption features for two or more non-interacting species are additive. In the gas phase, absorption spectra are highly featured. Considering these capabilities, coeluting species in a chromatogram detected by VUV spectroscopy can be deconvolved.[18,19]

In order to perform a deconvolution, two requirements have to be met. The first is that the compounds that are coeluting must be known and their pure spectra must be present in the VUV software library. Figure 3.1 shows the pure absorbance spectra for all DMNs tested in this experiment, as well as that for naphthalene for comparison. The naphthalenes all have the same general peak shape, but spectral features for each are unique and compound specific. Substitution on the naphthalene ring generally shifts absorption maxima to longer wavelengths. The second requirement is that spectra for coeluting compounds must be sufficiently distinct. The VUV software is able to perform deconvolutions on coeluting compounds by fitting the spectrum at each data point of the coeluting peak with a linear combination of the pure spectra for the coeluting compounds following Equation (1):

Equation (1) $A_{coelution} = f_1A_1 + f_2A_2$

where $A_{coelution}$ is the total absorbance for the coeluting compounds, A_1 and A_2 are the pure absorbance spectra for each of the compounds, and f_1 and f_2 are scaling factors for each of the compounds. The values of the scaling factors are optimized by a fitting procedure, such as general linear least squares optimization[20], with f_1 and f_2 as fit coefficients.

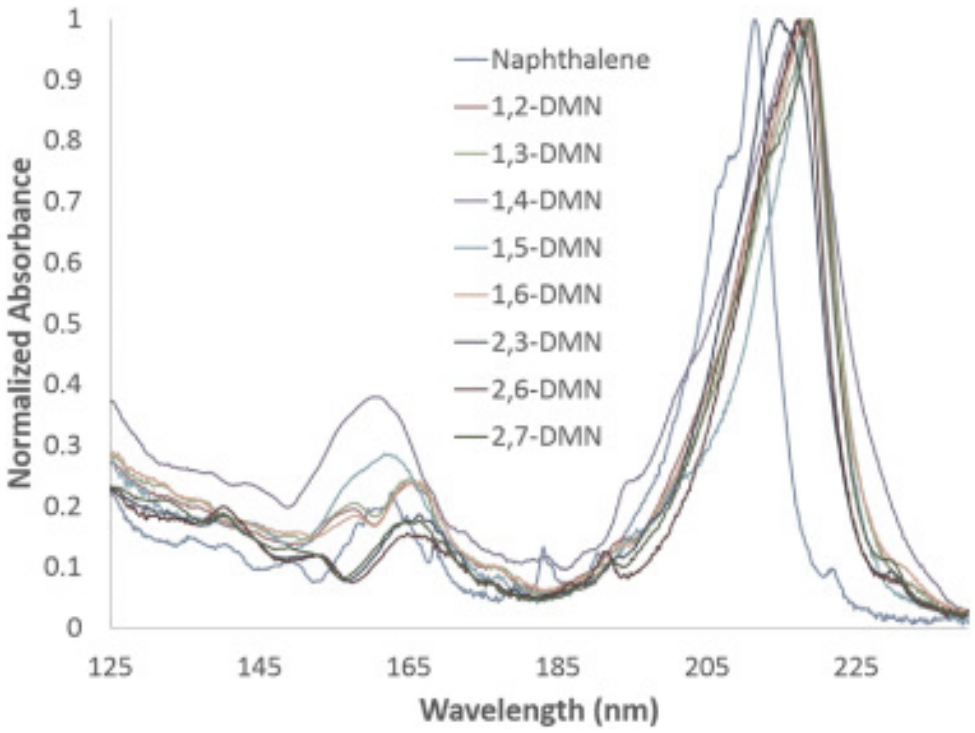

Figure 3.1 Measured normalized absorbance spectra for dimethylnaphthalene isomers and naphthalene obtained using GC-VUV.

The fit coefficients f_1 and f_2 plotted over the time region of a coelution event represent chromatographic signals for each of the coeluting compounds. Measured VUV absorbance spectra are often converted into chromatographic signals using spectral filters. For example, a chromatographic signal can be constructed by averaging the 125–240 nm absorbance from each scan and plotting the results versus time (spectral filters are described in more detail in Section 3.2.4). If a

spectral filter is applied to each of the pure absorbance spectra in Equation (1), and each fit coefficient is multiplied by the corresponding spectral filter result, the resulting chromatographic signals represent the contribution from each compound to the original combined signal that was generated using the same filter. In this case, the deconvoluted chromatographic signals can be summed to recover the original combined signal. The similarity for two absorbance spectra is evaluated by calculating the sum of square of residuals (SSR) between them. This was performed pair-wise for the eight isomers tested and can be seen in Table 3.1. In the extreme case where the spectrum of a DMN isomer is compared to itself using an SSR, we get a residual of zero, which essentially means that this isomer cannot be deconvolved from itself. When comparing coeluting isomers 1,6- and 1,3-DMN, a very small residual was determined (1.17). These will be the most challenging of the isomers tested to deconvolve based on VUV absorbance. A comparison of isomers 1,4- and 2,3-DMN returns the highest residual (38.8), indicating that these will be the least challenging of the isomers to deconvolute based on their VUV absorption profiles. For reference, the SSR between 1,4-DMN and naphthalene is 121.3. In many cases of GC analysis, co-eluting compounds may not be closely related isomers and will have very distinct spectra.[19,19,27,28] This makes them very easy to deconvolve over a wide dynamic range of concentrations, in comparison to the dimethylnaphthalenes considered here.

Table 3.1 Spectral similarity between DMN isomers, as measured by sum squared residuals in pairwise comparison of spectral signatures for different isomers. (Isomers that coelute are highlighted in like colors).

DMN	1,2-	1,3-	1,4-	1,5-	1,6-	2,3-	2,6-	2,7-
1,2-	0.00	0.820	16.0	7.00	0.600	11.8	9.04	3.31
1,3-	0.820	0.00	17.6	4.26	1.17	15.5	9.99	3.29
1,4-	16.0	17.6	0.00	26.8	17.0	38.8	42.7	30.7
1,5-	6.97	4.26	26.8	0.00	6.48	21.1	11.7	7.73
1,6-	0.600	1.17	17.0	6.48	0.00	9.80	7.25	3.04
2,3-	11.8	15.5	38.8	21.1	9.80	0.00	4.55	9.45
2,6-	9.04	9.99	42.7	11.7	7.25	4.55	0.00	4.13
2,7-	3.31	3.29	30.7	7.73	3.04	9.45	4.13	0.00

Using GC-VUV for analysis, all of the coeluting DMN isomers investigated could be deconvolved using the same instrument parameters and column. Each isomer was prepared at the target total concentration of 1000 ppm, and the exact concentration prepared for each was recorded. These standards were mixed into various ratios with a coeluting isomer. Each sample was analyzed in triplicate using isothermal conditions to ensure coelution was achieved and the average deconvolution result and standard deviation were computed. The measured ratio was compared to the prepared ratio as seen in Table 3.2. Figure 3.2 shows the chromatograms for different coeluting ratios of 1,4- and 2,3-DMN. While Table 3.2 shows that a 99:1 ratio can be reasonably deconvolved for all of the mixtures tested, Figure 3.2A shows that the minor component in this extreme ratio is certainly near, if not at or below the detection limit. At these relative amounts, the lesser component can be barely discerned from the baseline, but it is difficult to judge visually from this scale. Figs. 3S1 and 3S2 in the Electronic Supplementary Information document show additional examples of deconvolved chromatograms for the other DMN isomer

pairs at the different ratios tested. The results are consistent for all isomer pairs tested.

Table 3.2 Experimental deconvolution results for different prepared and determined ratios of DMN isomer mixtures (n = 3 for each).

Total 1000 ppm	Prepared ratio	Average deconvolved ratio	Standard deviation
1,4-DMN: 2,3-DMN	75.9: 24.1	75.7: 24.3	0.25
	51.2: 48.8	47.5: 52.5	2.6
	25.9: 74.1	24.6: 75.4	0.12
	20.8: 79.2	20.1: 79.9	0.55
	10.4: 89.6	10.1: 89.9	0.14
	5.2: 94.8	5.1: 94.9	0.62
	1.1: 98.9	1.3: 98.7	0.47
1,3-DMN: 1,6-DMN	75.3: 24.7	74.9: 25.1	1.1
	50.4: 49.6	48.6: 51.4	1.6
	25.3: 74.7	22.8: 77.2	1.6
	20.2: 79.8	16.9: 83.1	1.5
	10.1: 89.9	6.1: 93.9	0.38
	5.1: 94.9	4.4: 95.6	3.5
	1.0: 99.0	1.3: 98.7	0.47
2,6-DMN: 2,7-DMN	74.9: 25.1	74.5: 25.5	0.53
	49.8: 50.2	48.5: 51.5	1.2
	24.9: 75.1	24.5: 75.5	1.8
	19.9: 80.1	19.0: 81.0	1.5
	9.9: 90.1	10.9: 89.1	0.76
	5.0: 95.0	4.6: 95.4	1.3
	1.1: 98.9	1.9: 98.1	1.2

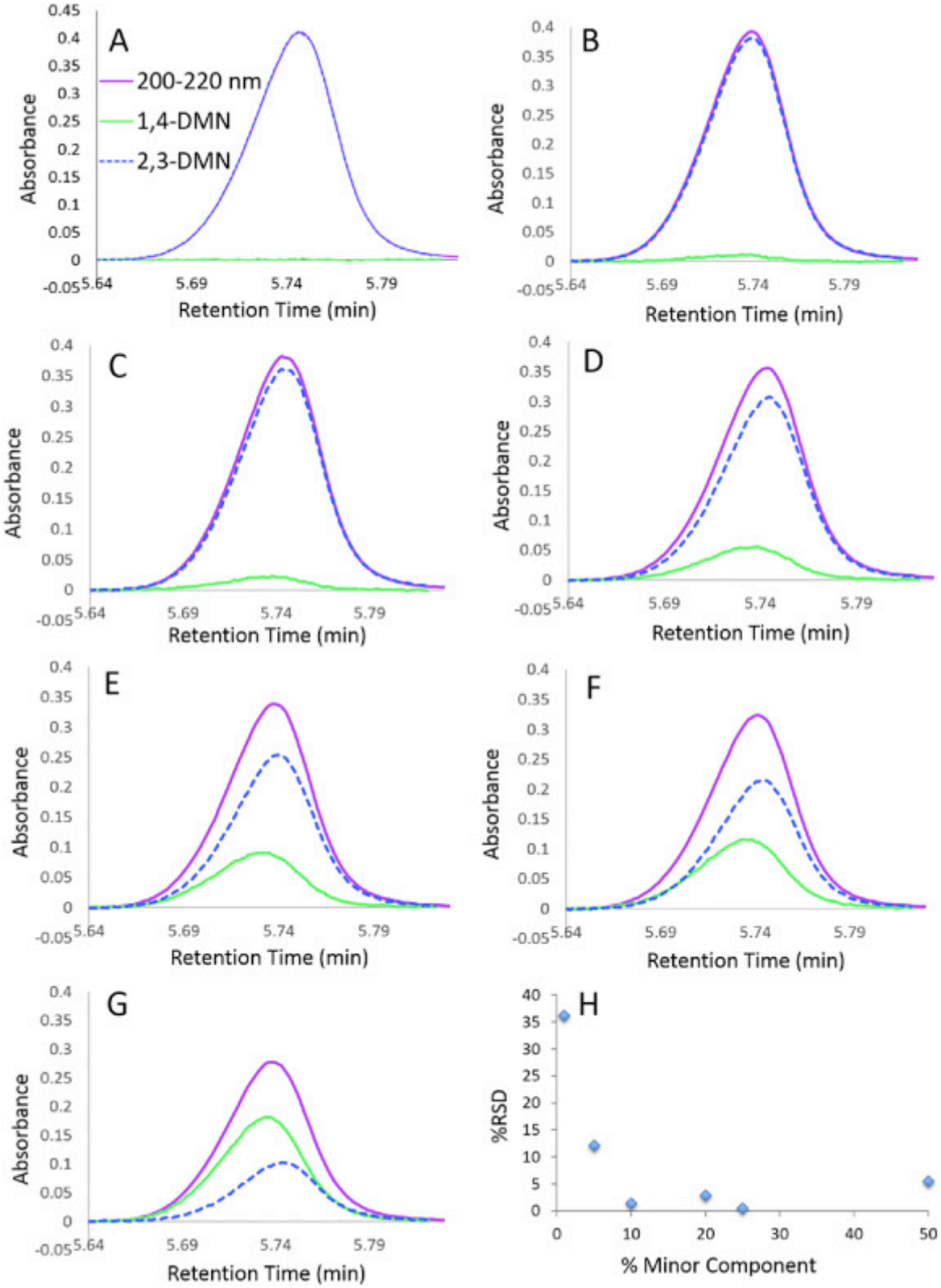

Figure 3.2 Deconvolution of A) 1:99, B) 5:95, C) 10:90, D) 20:80, E) 25:75, F) 50:50, and G) 75:25 1,4-DMN:2,3-DMN mixtures. H) Precision (% RSD) for deconvolution results (n = 3) as a function of % of minor component present in the mixture.

Figure 3.2H shows precision for the deconvolutions of the different ratios for the 1,4- and 2,3-DMN isomers. The graph was constructed by taking the %RSD of the minor component and plotting it versus the target ratio. This graph supports that the limit of deconvolution has been reached when there was approximately 1% of the minor component in the mixture because of the high %RSD. The error decreases dramatically as the relative proportion of DMN analytes becomes less disparate. At ratios greater than 10% of the minor component, less than 6%RSD was observed in the deconvolved measurements. Because this isomer pair was characterized by one of the most distinct pair of spectra (SSR = 38.8), further evaluation to deconvolve 99.5:0.5 and 99.9:0.1 ratio mixtures were attempted. The results (data not shown) only worsened in terms of precision and accuracy of the deconvolution. This further justifies the determined limit of 99:1 (specifically, 990 ppm: 10 ppm) for the deconvolution of this coeluting pair under the experimental conditions tested.

3.4.2 Covariance analysis

Covariance calculations (the procedure for which is detailed in the Electronic Supplementary Information for this article) make use of measured absorption cross-sections to theoretically determine limits for distinguishing overlapping amounts of absorbing species. Covariance calculations were used to estimate the uncertainties in determining the amounts of 2,6- and 2,7-DMN from a deconvolution procedure and the degree to which the uncertainties are affected by correlation between the two compounds. One of the outputs of the covariance calculation is the standard deviation (σ) of the on-column DMN mass used in the calculation. A threshold was set, equal to ten times the standard deviation, in order to judge the likely success of

a deconvolution procedure for a given case. A signal from a DMN mass greater than 10σ is deemed easily observable above the baseline floor of the deconvoluted signal(s).

As a reference point, a covariance calculation was performed for a system consisting of 13.6 ng of each isomer, representing a 50:50 mix of 2,6- and 2,7-DMN. The resulting 10σ levels were 0.33 ng and 0.31 ng, respectively. Interpreting the 10σ level as an amount of signal that would be clearly observable over the baseline noise of the deconvoluted DMN signals, a deconvolution could reasonably be expected to be successful in this scenario.

A second calculation was performed, but for 0.273 ng 2,6-DMN and 27.0 ng 2,7-DMN, corresponding to a 1:99 mix of the DMN isomers. The 10σ levels were 0.32 ng and 0.31 ng, respectively. Their similarity to the prior case is not very surprising in light of the linear nature of absorbance. However, it is notable that the 10σ threshold for 2,6-DMN is larger than its simulated mass, indicating that the 2,6-DMN deconvoluted signal is becoming harder to distinguish from baseline. From a strict 10σ threshold, this scenario represents an approximate limit for mixing the two isomers and performing a successful deconvolution. Mixing less than 0.273 ng 2,6-DMN with 27.0 ng 2,7-DMN would fair even worse.

The calculated correlation factor (see explanation in Supplementary Information) for the 1:99 DMN case is −0.993, indicating strong anti-correlation (a value of −1 indicates perfect anti-correlation). The strong correlation between the two isomers is expected due to the similarity of the shapes of their absorbance spectra. It was expected that the uncertainties in determining the DMN masses are

affected by this as well, and were significantly larger than the corresponding isolated compound cases (this was confirmed by covariance calculations for the isolated isomers). It is reasonable to expect that compounds having more dissimilar spectra may be mixed in wider ranging ratios. A scenario was constructed in order to illustrate this, using a combination of 2,6-DMN and naphthalene, again in a 1:99 ratio. The 10σ levels were 0.044 ng and 0.053 ng, respectively, nearly a full order of magnitude better than the 2,6- and 2,7-DMN case. Spectral deconvolution of a 1:999 ratio would not be out of the question for this hypothetical mixture. The correlation factor for this case was −0.745, indicating that the two compounds were not strongly correlated.

Relating the covariance calculations to expected uncertainties of measured parameters relies on assumptions about the magnitude and degree of randomness of error in measured absorbance values. Measuring the uncertainty in chromatographic absorbance measurements can be difficult, and most real systems exhibit at least some systematic component to measurement error. Therefore, covariance results should usually be thought of as preliminary estimates of what might be expected rather than hard, theoretical predictions. Nevertheless, the results of the covariance analysis of 2,6- and 2,7-DMN isomers supported the limit of deconvolution estimated from the experimental measurements for the dimethylnaphthalenes presented earlier.

3.4.3 Theoretical computations

The individual absorbance spectra of all DMN isomers in this investigation, as well as naphthalene, were calculated using a TDDFT method and are shown

in Fig. 3.3 In comparison to experimental spectra (Fig. 3.1), one can immediately see that most important features in the experimental spectra are reproduced nicely in the theoretical spectra. Overlaid experimental and theoretical spectra for each isomer are shown in Fig. 3S3. Namely, the theoretical spectra showed the correct order of main peak positions, as well as relative peak strengths. As mentioned above, for deconvolution, one of the requirements is that the individual pure compound's spectrum must exist in the VUV reference library. Certainly there will be cases that some of the compounds' spectra are not available. One attractive idea is directly using theoretical spectra, which can always be acquired conveniently, to deconvolute a measured mixture spectrum. With this in mind, we investigated the potential for deconvolution by replacing actual spectra with theoretical spectra, and the results of this work are shown in Table 3.3. For mixtures where one component's relative abundance was comparable to another component, such as the 75:25, 50:50, and 25:75 ratios, the deconvolution gave reasonable results. However, when the majority of the mixture was only one component, the deconvolution exaggerated the ratio of the lower abundance component significantly. It was concluded that this method was able to evaluate reliably a limit of three-fold excess, which is significantly worse performance than the experimental result.

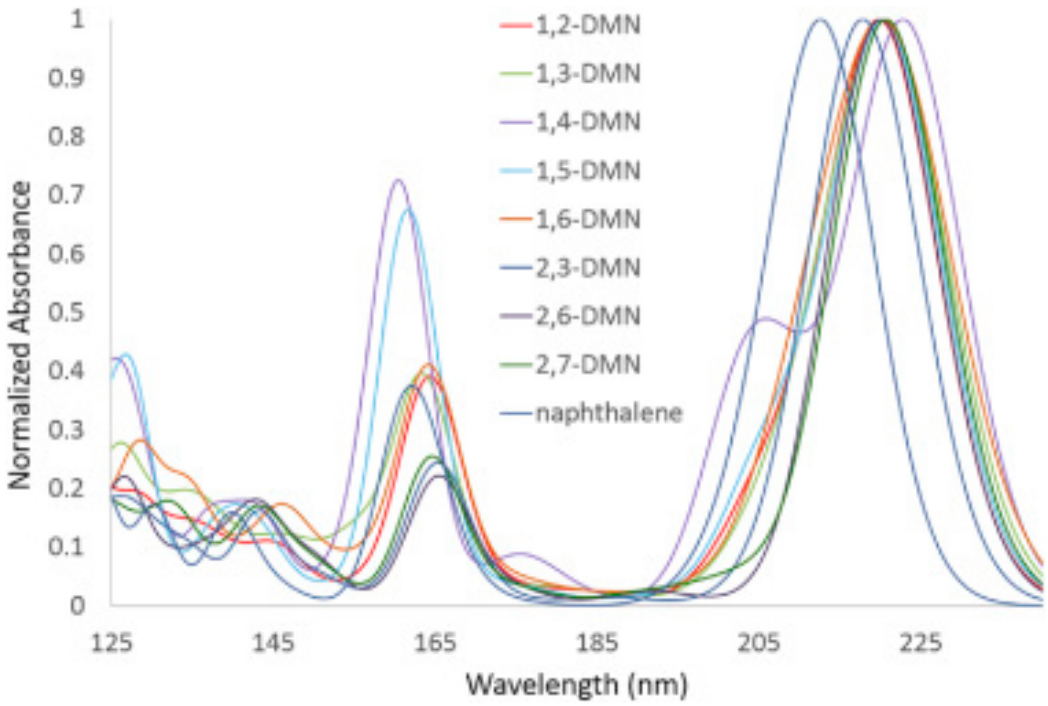

Figure 3.3 Computed normalized absorbance spectra for dimethylnaphthalene isomers and naphthalene obtained using time dependent density functional theory.

Table 3.3 Deconvolution of mixed theoretically computed spectra.

Total 1000 ppm	Prepared ratio	Deconvolved ratio
1,4-DMN: 2,3-DMN	75.1:24.9	67:33
	50.1:49.9	50:50
	25.1:74.9	33:67
1,3-DMN: 1,6-DMN	75.3:24.7	68:32
	50.4:49.6	55:45
	25.3:74.7	39:61
2,6-DMN: 2,7-DMN	72.8:27.2	69:31
	49.5:50.5	46:54
	24.6:75.4	26:74

In this research, the theoretical spectra were simulated by using Gaussian functions with a full width at half maximum of 0.4 eV as broadening functions for calculated line spectra. We believe that with further investigations to include optimization of this parameter, or the direct use of oscillator strengths obtained from computation, a reliable estimation routine for deconvolution, especially for the

samples without available pure experimental spectra in the library, could be possible. More research is needed in this area. Importantly, with the introduction of the VUV detector, experimental data can now be generated more quickly than previously, and this data can be used to help refine computational methods in this arena.

3.4.4 Diesel and jet fuel

Diesel and jet fuel are complex samples containing various different unknown compounds that could coelute with dimethylnaphthalenes during a GC analysis. It is extremely difficult to identify all compounds in such fuel samples and thus, there are limited entries for their pure spectra in the VUV library. Characterization of compound classes in diesel fuel using GC-VUV and GCxGC-VUV has been recently reported.[29,30] However, currently, diesel and jet fuel do not meet the requirements to perform direct deconvolution since we do not have pure spectra of the coeluting compounds. Instead, we were able to selectively identify classes of molecules, such as naphthalene, methylnaphthalenes, dimethylnaphthalenes, and trimethylnaphthalenes by applying spectral filters. Spectral filters are created digitally by the software to project chromatographic signals originating from absorption in specified ranges of wavelengths. The concept is somewhat analogous to ion extraction in GC-MS. Spectral filters can be used to enhance detection limits or distinguish between different classes of compounds.

Pure samples of jet and diesel fuels were analyzed. Analysis was performed using the spectra filters 125–160 nm, where all saturated compounds absorb light, and 170–240 nm, where unsaturated compounds absorb strongly. The absorbance

spectra for various monoaromatics and naphthalenes were investigated and it was found that monoaromatic compounds absorb strongly in the 180–200 nm range while naphthalene compounds absorb strongly in the 210–220 nm range. This is shown in Fig. 3S4 of the Electronic Supplementary Information for this article. A spectral filter was applied to segregate and visualize the signals originating from monoaromatics and naphthalenes, and this filter was applied to the original chromatograms (Fig. 3.4 and 34 for jet and diesel fuels, respectively). We were able to selectively identify where naphthalene, methylnaphthalenes, dimethylnaphthalnes, and trimethylnaphthalenes eluted from jet and diesel fuel without having to perform deconvolution. The jet fuel exhibited significantly fewer interferences for this analysis compared to diesel fuel. The eight standards for DMNs were mixed in equal ratios and analyzed under the same conditions as jet and diesel fuels to confirm their elution time in comparison with the spectral filter. The two standards for TMNs were analyzed individually to confirm elution time in comparison with the spectral filter placed on diesel and jet fuel. The region of jet fuel that had probable TMNs were analyzed using a library search and the top matches identified the signals as TMNs.

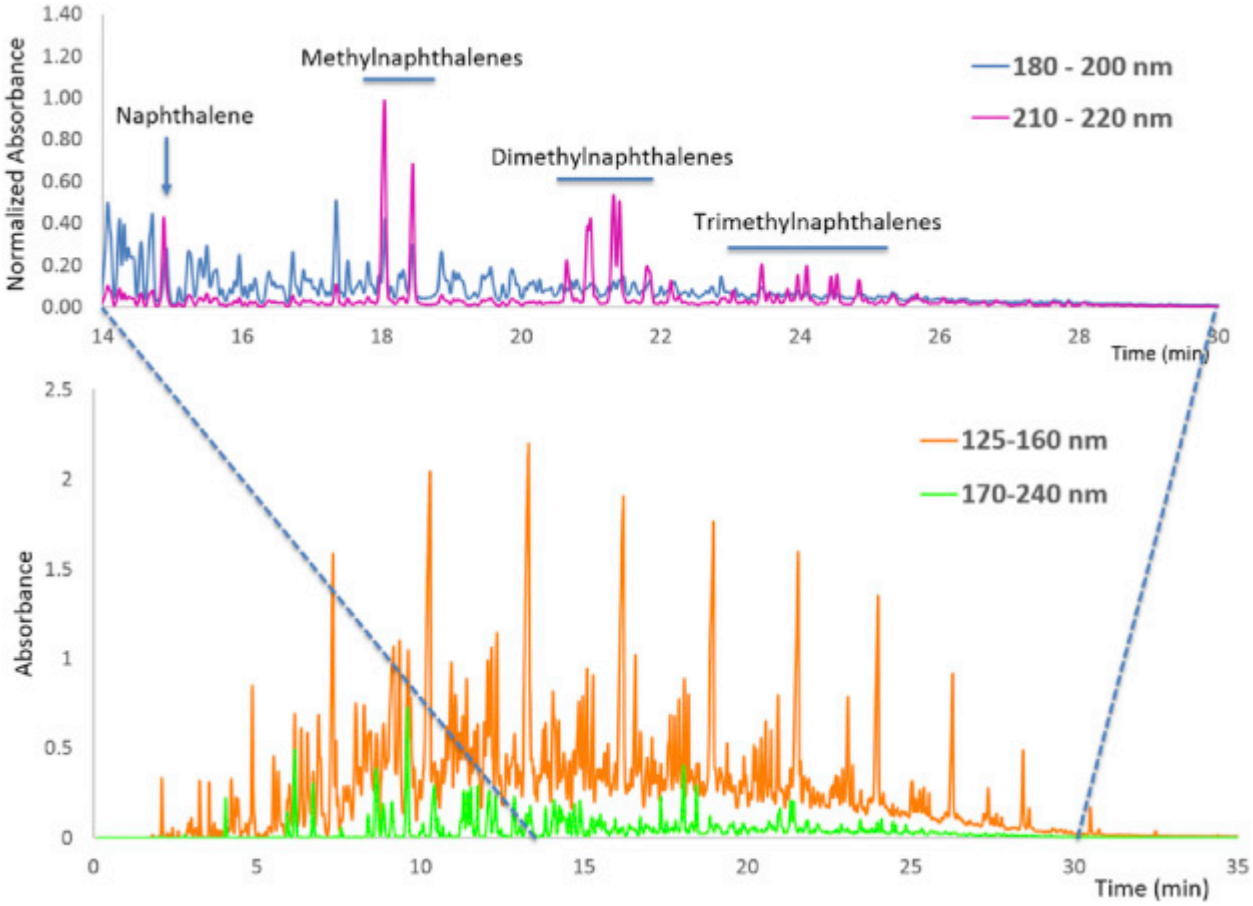

Figure 3.4 Chromatographic analysis of jet fuel using GC-VUV and spectral filters. Bottom: Full analysis with spectral filters to segregate saturated (125–160 nm) from unsaturated (170–240 nm) components. Top: Spectral filters applied to narrowed time domain to accentuate mono-, di-, and trimethylnaphthalenes (maximum absorbance at 210–220 nm).

3.5 Conclusions

The aim of this experiment was to evaluate, experimentally and computationally, the ability to deconvolve mixtures of eight different isomers of DMN based on their overlapping VUV absorption spectra. Analytical standards were analyzed separately to collect reference spectra. In parallel, the theoretical spectra for each isomer were calculated using TDDFT. The limits for deconvolution in terms of relative abundance of overlapping signals was tested for both experimentally and

computationally mixed spectra. It was found that the experimental deconvolutions gave more desirable results than the theoretical deconvolution computations.

In general, the ability to simply deconvolute co-eluting compounds based on the additivity of spectral features is a unique feature of the VUV detector, relative to other gas chromatographic detection techniques. For dissimilar compounds, coelutions of compounds with relative abundances disparate by more than three orders of magnitude could be reasonably expected to be deconvolved. In the case of the DMNs, where spectra for each isomer are quite similar, a practical limit of approximately two orders of magnitude difference in relative abundance has been established, under reasonable injection conditions. It is important to note that from a detection standpoint, the fundamental limit for mixing two of these isomers is not the mixing ratio itself. There is a limit on the amount of compound that can be detected in the presence of another compound. Once the on-column amount for one of the compounds is set, a minimum mixing ratio is determined by the detection limit of the other compound in the presence of the first.

This study should help further define the practical operating limits of the VUV detector. Conditions were established for a relatively fast GC analysis for chromatographic separation of multiple isomers. This methodology was then applied to build a spectral filter to analyze specific content in complex samples of diesel and jet fuel to illuminate DMN elution. The use of GC-VUV has proven to be a complementary technique that can provide good specificity in the analysis of complex hydrocarbon mixtures. Further refinement of computational capabilities could further enhance the experimental capabilities of the instrument in the future.

Conflict of interest

In the interest of full disclosure, the authors wish to note that KAS is a member of the Scientific Advisory Board, while JS and PW are employees, of VUV Analytics, Inc.

Acknowledgements

Support for this research was provided by VUV Analytics, Inc. The authors would like to further thank Shimadzu Scientific Instruments, Inc. for providing the gas chromatograph and Restek Corporation for providing the GC column used in these studies.

3.6 References

1. J.L.P. Pavon, A.G. Pena, C.G. Pinto, B.M. Cordero, Differentiation of types of crude oils in polluted soil samples by headspace-fast gas chromatography-mass spectrometry, J. Chromatogr. A 1137 (2006) 101-109.
2. J.H. Christensen, G. Thomas, Practical aspects of chemometrics for oil spill fingerprinting, J. Chromatogr. A 1169 (2007) 1-22.
3. M. Jalali-Heravi, H. Parastar, Assessment of the Co-elution problem in gas chromatography-mass spectrometry using non-linear techniques, Chem. Intell. Lab. Sys 101 (2010) 1-13.
4. P. Marriott, R. Shellie, Principles and applications of comprehensive two-dimensional gas chromatography, Trends Anal. Chem. 21 (2002) 573-583.
5. G. Christianson, P. Dasgupta, K. Schug, Anal. Chem. (2014) 623-647 seventh ed.
6. R. Alexander, R.I. Kagi, P.N. Sheppard, Relative abundance of dimethylnaphthalene isomers in crude oils, J. Chromatogr. A 267 (1983) 367-372.
7. N. Karaikul, P. Rangsunvigit, S. Kulprathipanja, Unexpected Roles of toluene in the catalytic isomerization of 1,5- to 2,6-Dimenthylnaphthalene, Appl. Catal. A Gen. 312 (2006) 102-107.
8. C. Li, L. Li, W. Wu, D. Wang, A.V. Tokarev, O.V. Kikhtyanin, G.V. Echevskii, Highly selective synthesis of 2,6-Dimethylnaphthalene over alkaline treated ZSM-12 zeolite, Prodedia Eng. 18 (2011) 200-205.
9. T. Tesarik, J. Frycka, S. Ghyczy, Gas chromatography separation of naphthalene and biphenyl homologues on capillary columns, J. Chromatogr. A 148 (1978) 223-228.
10. A.R.J. Andrews, Z. Wu, A. Zlatkis, The GC separation of C_2-Naphthalene isomers using cyclodextrins and crown ethers, Chromatographia 34 (1992) 163-165.
11. S. Terabe, Y. Miyashita, Y. Ishihama, O. Shibata, Cyclodextrin-modified micellar electrokinetic chromatography: separation of hydrophobic and enantiomeric compounds, J. Chromatogr. A 636 (1993) 47-55.

12. T. Shinbo, Y. Sudo, Y. Shimabukuro, T. Kanamori, T. Masuoka, T. Iwatsubo, A. Yamasaki, K. Ogasawara, K. Mizoguchi, Preparation of a cyclophane-bound stationary phase and its application to separation of naphthalene derivatives, J. Chromatogr. A 803 (1998) 95-101.
13. Z. Witkiewicz, J. Oszczudlowski, M. Repelewicz, Liquid-crystalline stationary phases for gas chromatography, J. Chromatogr. A 1062 (2005) 155-174.
14. I.D.G.A. Putrawan, T.H. Soerawidjaja, Separation of dimethylnaphthalene isomers by extractive crystallization, Sep. Purif. Tech. 39 (2004) 79-88.
15. T. Inui, S.B. Pu, Separation of 2,6-Dimethylnaphthalene from a mixture of its isomers using lithium-incorporated zeolite Y synthesized by Rapid crystallization method, Sep. Tech. 5 (1995) 229-237.
16. G.S. Lee, Y. Iwai, S. Abe, Y. Shimoyama, Y. Arai, Effect of ion exchange rate of Y- type zeolite on selective absorption of 2,6- and 2,7-Dimethylnaphthalene isomers in supercritical carbon dioxide, Sci. Tech. Adv. Mater 7 (2006) 672-677.
17. K.A. Schug, I. Sawicki, D.D. Carlton, H. Fan, H.M. McNair, J.P. Nimmo, P. Kroll, J. Smuts, P. Walsh, D. Harrison, Vacuum ultraviolet detector for gas chromatography, Anal. Chem. 86 (2015) 8329-8335.
18. L.Bai,J.Smuts,P.Walsh,H.Fan,Z.Hildenbrand,D.Wong,D.Wetz,K.A.Schug, Permanent gas analysis using gas chromatography with vacuum ultraviolet detection, J. Chromatogr. A 1388 (2015) 244-250.
19. H. Fan, J. Smuts, P. Walsh, D. Harrison, K.A. Schug, Gas chromatography-vacuum ultraviolet spectroscopy for multiclass pesticide identification, J. Chromatogr. A 1389 (2015) 120-127.
20. W.H. Press, B.P. Flannery, S.A. Teukolsky, W.T. Vetterling, J.R. Chipperfield, Numerical Recipes in C: the Art of Scientific Computing, second ed., Cam- bridge University Press, Cambridge, 1992.
21. C. Moller, M.S. Plesset, Note on an approximation treatment for many- electron systems, Phys. Rev. 46 (1934) 618-622.
22. J.P.Perdew,K.Burke,M.Ernzerhof,Generalizedgradientapproximationmade simple, Phys. Rev. Lett. 77 (1996) 3865-3868.
23. J.P. Perdew, K. Burke, M. Ernzerhof, Errata e generalized gradient approxi- mation made simple, Phys. Rev. Lett. 77 (3865) (1996). Phys. Rev. Lett. 1997, 78, 1396.
24. C. Adamo, V. Barone, Toward reliable density functional methods without adjustable parameters: the PBE0 model, J. Chem. Phys. 110 (1999) 6158-6170.
25. T.H. Dunning Jr., Gaussian basis sets for use in correlated molecular calcula- tions. I. The atoms boron through neon and hydrogen, J. Chem. Phys. 90 (1989) 1007-1023.
26. M.J. Frisch, G.W. Trucks, H.B. Schlegel, G.E. Scuseria, M.A. Robb, J.R. Cheeseman, G. Scalmani, V. Barone, B. Mennucci, G.A. Petersson, H. Nakatsuji, M. Caricato, X. Li, H.P. Hratchian, A.F. Izmaylov, J. Bloino, G. Zheng, J.L. Sonnenberg, M. Hada, M. Ehara, K. Toyota, R. Fukuda, J. Hasegawa, M. Ishida, T. Nakajima, Y. Honda, O. Kitao, H. Nakai, T. Vreven, J.A. Montgomery Jr., J.E. Peralta, F. Ogliaro, M. Bearpark, J.J. Heyd, E. Brothers, K.N. Kudin, V.N. Staroverov, R. Kobayashi, J. Normand, K. Raghavachari, A. Rendell, J.C. Burant, S.S. Iyengar, J. Tomasi, M. Cossi, N. Rega, J.M. Millam, M. Klene, J.E.

Knox, J.B. Cross, V. Bakken, C. Adamo, J. Jaramillo, R. Gomperts, R.E. Stratmann, O. Yazyev, A.J. Austin, R. Cammi, C. Pomelli, J.W. Ochterski, R.L. Martin, K. Morokuma, V.G. Zakrzewski, G.A. Voth, P. Salvador, J.J. Dannenberg, S. Dapprich, A.D. Daniels, O€. Farkas, J.B. Foresman, J.V. Ortiz, J. Cioslowski, D.J. Fox, Gaussian 09, Revision E.01, Gaussian, Inc, Wallingford CT, 2009.
27. H. Fan, J. Smuts, L. Bai, P. Walsh, D.W. Armstrong, K.A. Schug, Gas chromatography-vacuum ultraviolet spectroscopy for analysis of fatty acid methyl esters, Food Chem. 194 (2016) 265-271.
28. C.A. Weatherly, Y. Zhang, J. Smuts, H. Fan, C. Xu, K.A. Schug, J.C. Lang, D.W. Armstrong, Analysis of long-chain unsaturated fatty acids by ionic liquid gas chromatography, J. Agric. Food Chem. 64 (2016) 1422-1432.
29. B.M. Weber, P. Walsh, J.J. Harynuk, Determination of hydrocarbon group-type of diesel fuels by gas chromatography with vacuum ultraviolet detection, Anal. Chem. 88 (2016) 5809-5817.
30. T. Groeger, B. Gruber, D. Harrison, M. Saraji-Bozorgzad, M. Mthembu, A. Sutherland, R. Zimmermann, A vacuum ultraviolet absorption array spectrometer as a selective detector for comprehensive two-dimensional gas chromatography: concept and first results, Anal. Chem. 88 (2016) 3031-3039.

3.7 SUPPLEMENTAL INFORMATION

Analysis and Deconvolution of Dimethylnaphthalene Isomers Using Gas Chromatography Vacuum Ultraviolet Spectroscopy and Theoretical Computations

Jamie Schenk[†], Xiaojian Mao[†], Jonathan Smuts[§], Phillip Walsh[§], Peter Kroll[†], Kevin A. Schug*[†]

[†] Department of Chemistry & Biochemistry, The University of Texas at Arlington, Arlington, Texas 76019, United States

[§] VUV Analytics, Inc., Cedar Park, Texas 78613, United States

Abstract

The following describes a general covariance analysis scheme, which was used in this study to understand the limits of deconvolution in gas chromatography – vacuum ultraviolet spectroscopy. Additional examples of chromatograms obtained for various mixtures of different DMN isomer pairs other than that shown in the main document are given in Figure 3S1 – 3S2. Also shown are collective absorption spectra for monoaromatics and napthalenes (Figure 3S3), information for which was used to build selective spectral filters and a supplemental application of spectral filters to a diesel fuel analysis (Figure 3S4).

Covariance Analysis

The combined absorbance for a set of *n* different molecular species is given by

$$A(\lambda) = \frac{1}{\ln(10)} \frac{d}{V} N_A \left(\gamma_1(\lambda) \frac{m_1}{MW_1} + \gamma_2(\lambda) \frac{m_2}{MW_2} + \ldots + \gamma_n(\lambda) \frac{m_n}{MW_n} \right),$$

or

$$A(\lambda) = \frac{1}{\ln(10)} \frac{d}{V} N_A \sum_{i=1}^{n} \gamma_i(\lambda) \frac{m_i}{MW_i}, \qquad \text{eq. 1}$$

where m_i is the amount of mass of molecule i in the flow cell, MW_i is the molar mass of molecule i, $\gamma_i(\lambda)$ is the absorption cross section in cm^2/molecule for molecule i, N_A is Avagadro's number, d is the flow cell length, and V is the flow cell volume.

The wavelength dependence of the absorbance is contained in the individual molecular cross sections. In a practical absorbance measurement, the cross sections actually consist of arrays of discrete points, corresponding to wavelength values at which the cross sections were previously determined. The deconvolution of a chromatographic event is accomplished by a general linear least squares fit of eq. 1 to a measured absorbance spectrum, which would ideally have been sampled at the same wavelength values as the cross sections.

The general linear fit procedure is described in detail in Reference 1. In the application to absorbance fitting the basis functions are

$$X_{i,j} = \frac{1}{\ln(10)} \frac{d}{V} N_A \left(\frac{\gamma_{i,j}}{MW_i} \right) \qquad \text{eq. 2}$$

and the parameters to be fit are the masses, m_i. The additional subscript j in eq. 2 accounts for the wavelength dependence of the basis functions: there is a term like this corresponding to each wavelength value being fit. The basis functions form a set of column vectors, one for each molecule. The covariance matrix is calculated from the inverse of the following matrix[1]:

$$\alpha_{kl} = \sum_{j=1}^{p} \frac{X_{k,j} X_{l,j}}{\sigma_j^2} \qquad \text{eq. 3}$$

where *p* is the number of wavelength values and σ_j is an estimate of the uncertainty in the measured absorbance data at the wavelength value corresponding to *j*, expressed in terms of its standard deviation. There is one term like eq. 3 for each combination of pairs of the *n* molecules, resulting in an *n*×*n* matrix. The covariance matrix is[1]

$$C = \alpha^{-1}. \qquad \text{eq. 4}$$

The diagonal elements of the covariance matrix are the variances of the fit parameters (the m_i). From these, estimates of the standard deviation uncertainties can be obtained.

The off-diagonal elements give a measure of the correlation between two different parameters. A correlation factor can be defined by normalizing the off-diagonal elements:

$$r_{kl} = \frac{C_{kl}}{\sqrt{C_{kk} C_{ll}}}. \qquad \text{eq. 5}$$

The value of the correlation factor lies between +/- 1, with 1 corresponding to perfect correlation and -1 to perfect anti-correlation. The closer r_{kl} is to -1, the greater degree to which molecule *k* and *l* can be exchanged and result in indistinguishable absorbance spectra. In the limit of r_{kl} = -1, it is not possible to determine the amounts of both simultaneously. The covariance matrix is symmetric with respect to its diagonal, so $C_{kl} = C_{lk}$ for all of the off-diagonal elements. In order for the computed variances to be meaningful, a reasonable estimate for the measurement uncertainty has to be provided. The σ_j in eq. 3 are estimates of the standard

deviations of a set of measured values about their mean for each measured data point *j*. It is possible to estimate standard deviations on a wavelength-by-wavelength basis from a baseline scan at the beginning of a chromatographic separation. This is reasonable for zero absorbance conditions, but the uncertainties depend on the absorbance magnitude as well, and it is harder to directly measure this during chromatographic absorbance measurements. A given amount of molecule suspended in or streaming through a flow cell might be sufficient, but this scenario was not available during the measurements reported here. However, the standard deviation uncertainties scale roughly with the square root of the transmittance, so the following procedure was adopted in order to estimate the uncertainties for the specific cases studied:

1. Calculate $\sigma_{j,0}$ for all *j* from a set of absorbance scans in a flat region of the baseline at the beginning of a chromatographic run (where the absorbance is zero). 100 scans or so is sufficient. These are the standard deviations for a zero absorbance condition.
2. Calculate the absorbance *A*, and then the transmittance, $T=10^{-A}$, from eq. 1 for the specific set of conditions being considered.
3. Calculate the estimated uncertainty from

$$\sigma_j = \frac{\sigma_{j,0}}{\sqrt{T_j}} \qquad \text{eq. 6}$$

References

1. W.H. Press, S.A. Teukolsky, W.T. Vetterling, and B.P. Flannery, *Numerical Recipes in C: The Art of Scientific Computing, Second Edition*, Cambridge University Press, 1992. See especially section 15.4.

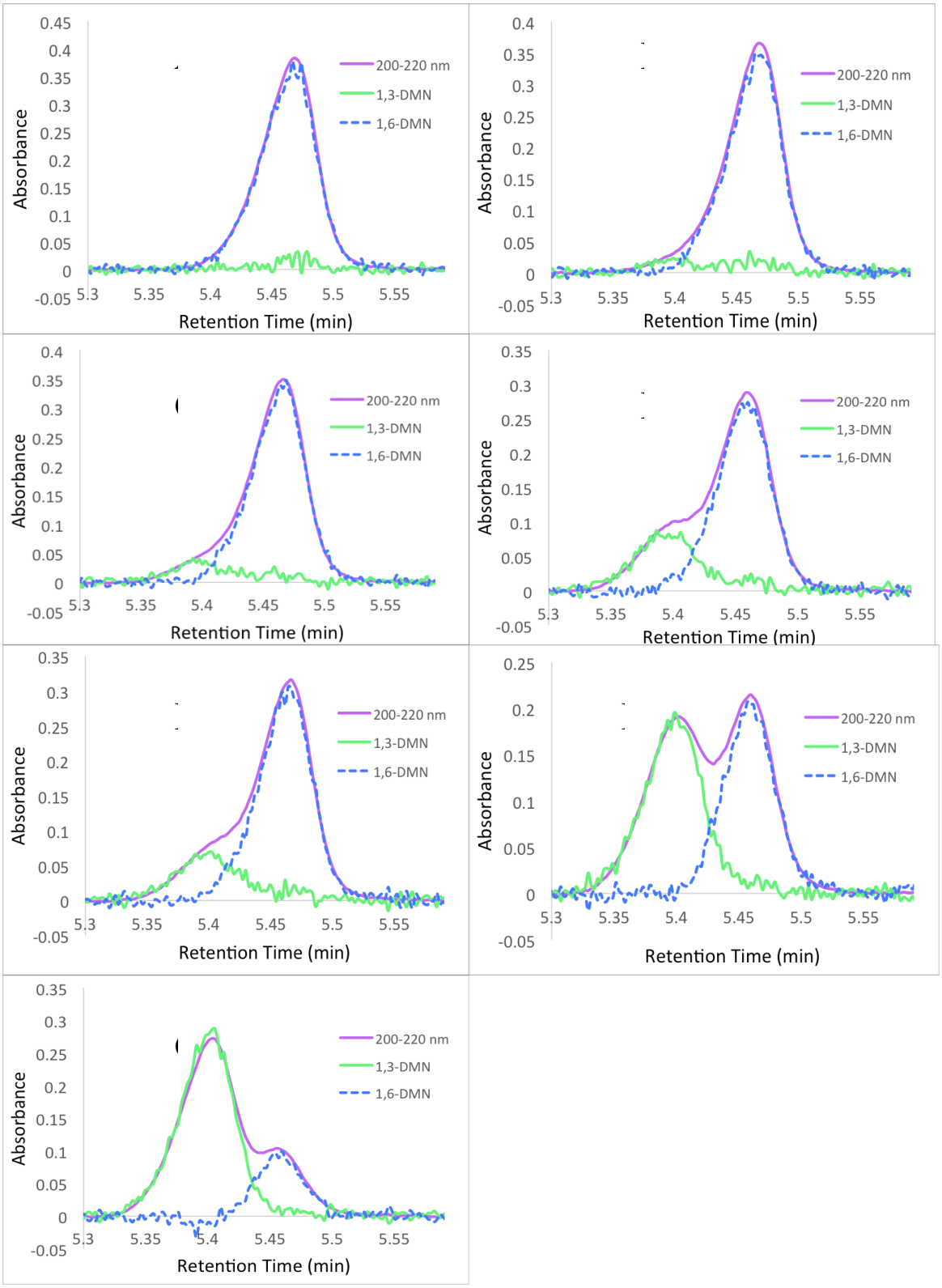

Figure 3S1. Deconvolution of A) 1:99, B) 5:95, C) 10:90, D) 20:80, E) 25:75, F) 50:50, and G) 75:25 1,3-DMN:1,6-DMN mixtures.

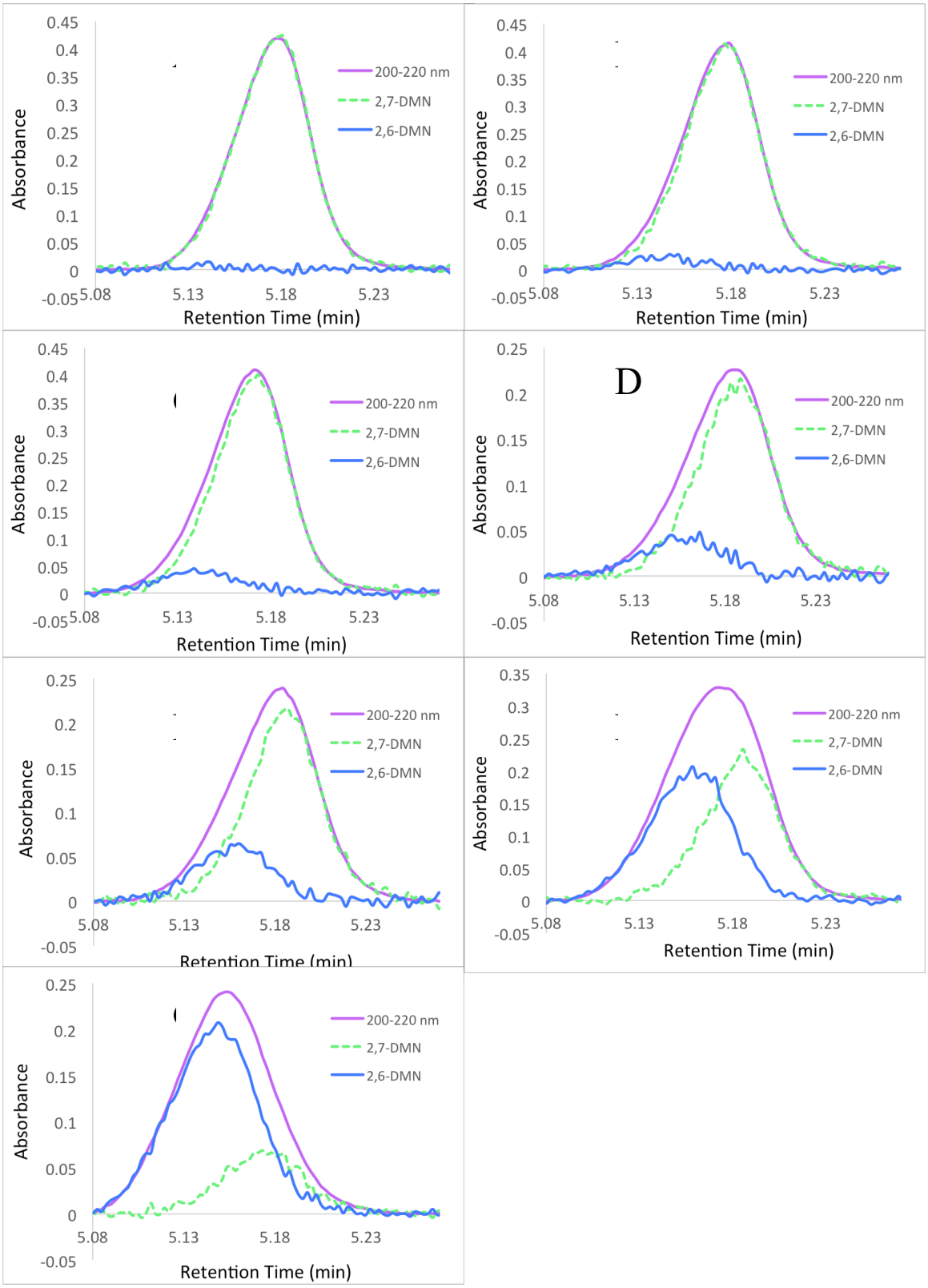

Figure 3S2. Deconvolution of A) 1:99, B) 5:95, C) 10:90, D) 20:80, E) 25:75, F) 50:50, and G) 75:25 2,6-DMN:2,7-DMN mixtures.

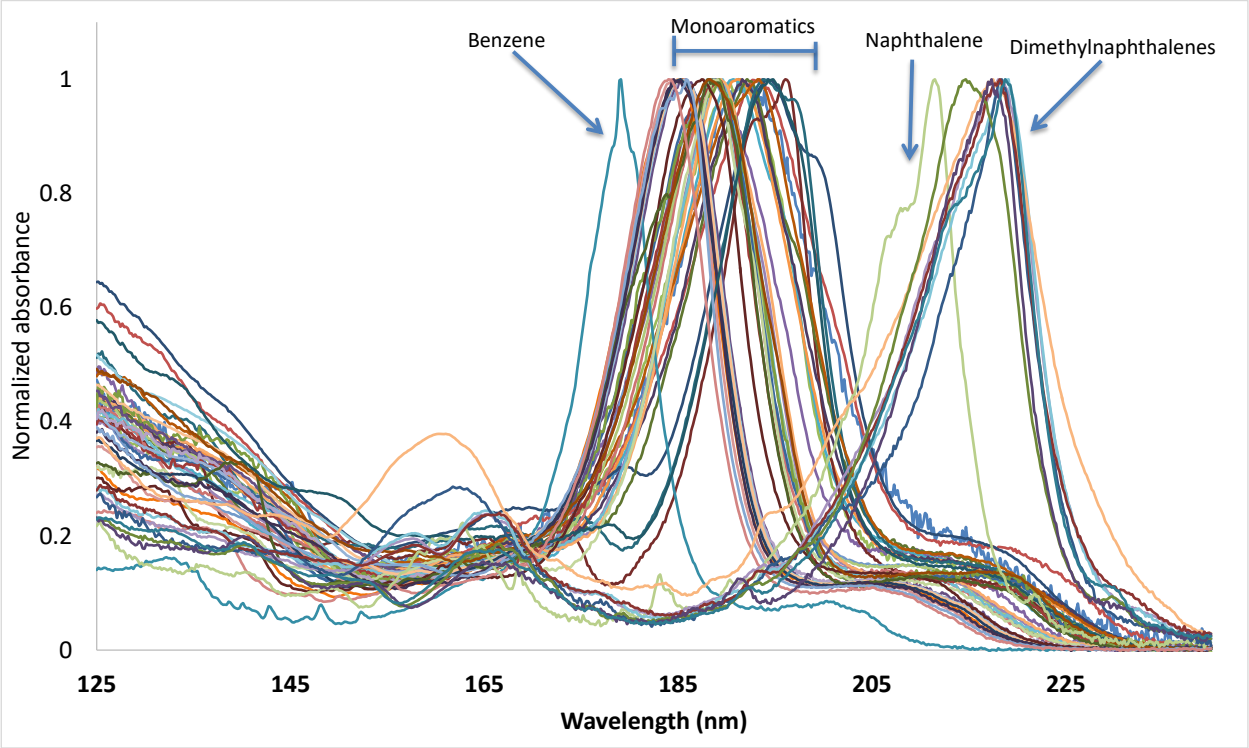

Figure 3S3. Absorbance spectra for monoaromatics and naphthalenes obtained from the VUV library. Monoaromatics absorb strongly in the 180-200nm range and naphthalenes absorb strongly in the 210-220nm range. Using this information we are able to build a spectra filter to apply to complex samples to enhance our detection limits and distinguish between these two classes of compounds.

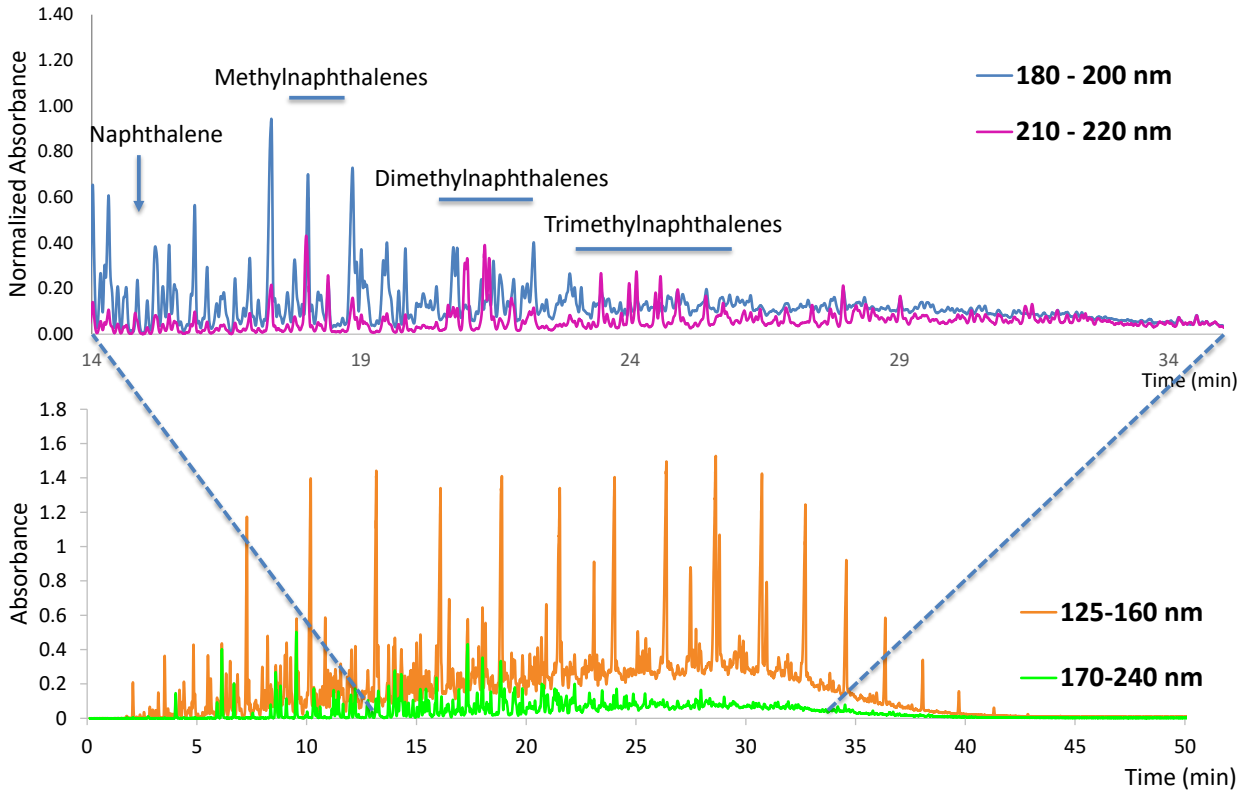

Figure 3S4. Chromatographic analysis of diesel fuel using GC-VUV. Bottom: Full analysis with spectral filters to segregate saturates (125 – 160 nm) from unsaturates (170 – 240 nm). Top: Spectral filters applied to narrowed time domain to accentuate mono-, di-, and trimethylnaphthalenes (maximum absorbance at 210 – 220 nm). The diesel fuel is characterized by more interferences than jet fuel (Figure 3.4 in main article).

CHAPTER FOUR: Lab-simulated downhole leaching of formaldehyde from proppants by high performance liquid chromatography (HPLC), headspace gas chromatography-vacuum ultraviolet (HS-GC-VUV) spectroscopy, and headspace gas chromatography-mass spectrometry (HS-GC-MS)

Jamie Schenk,[a] Doug D. Carlton, Jr,[ab] Jonathan Smuts,[c] Jack Cochran,[c] Lindsey Shear,[c] Ty Hanna,[d] Danny Durham,[d] Cal Cooper[d] and Kevin A. Schug[*ab]

[a]Department of Chemistry and Biochemistry, The University of Texas at Arlington, 700 Planetarium Pl., Box 19065, Arlington, TX 76019-0065, USA.

[b]Affiliate of the Collaborative Laboratories for Environmental Analysis and Remediation (CLEAR), The University of Texas at Arlington, Arlington, TX, USA

[c]VUV Analytics Inc., Cedar Park, TX, USA

[d]Apache Corporation, Houston, TX, USA

4.1 Abstract

The ability of different methods to analyze formaldehyde and other leachates from proppants was investigated under lab-simulated downhole conditions. These methods include high performance liquid chromatography (HPLC), headspace gas chromatography-vacuum ultraviolet spectroscopy (HS-GC- VUV), and headspace gas chromatography-mass spectrometry (HS-GC-MS). Two different types of resin-coated proppants, phenol-formaldehyde- and polyurethane-based, were examined. Each proppant was tested at different time intervals (1, 4, 15, 20, or 25 hours) to determine the timeframe for chemical dissolution. Analyses were performed at room temperature and heated (93 °C) to examine how temperature affected the concentration of leachates. Multiple matrices were examined to mimic conditions in subsurface environment including deionized water, a solution surrogate to mimic the ionic concentration of produced water, and recovered produced water. The complexity of these samples was further enhanced to simulate downhole conditions

by the addition of shale core. The influence of matrix components on the analysis of formaldehyde was greatly correlated to the quantity of formaldehyde measured. Of the three techniques surveyed, HS-GC-MS was found to be better suited for the analysis of formaldehyde leachates in complex samples. It was found that phenol-formaldehyde resin coated proppants leached higher concentrations of formaldehyde than the polyurethane resin coated proppants.

4.2 Introduction

Hydraulic fracturing (HF) is a stimulation technique that has garnered significant attention in shale energy basins, where it is used to increase the productivity of wells in low permeability formations containing natural resources, such as natural gas and oil. Proppants are mixed into the hydraulic fracturing fluid (HFF) and serve to prop open the fissures once the high pressure is relieved. Typical proppants are made of sand and some are treated with a coating to improve mechanical strength.[1,2] Three main types of proppant are available, namely frac sand, resin coated proppants (RCP), and ceramic coated proppants (CCP).[2] The added resin coating on the sand can have several advantages and disadvantages. One advantage is to increase mechanical strength and help reduce the occurrence of proppant "fines".[1,2] Fines are produced when sand is crushed under high pressure and generates small uneven particles, which can pack tightly into the fissure and block the passage of resources.[2] Some disadvantages of using coated sand are the possibility of leaching chemicals from the resin coating, the increased cost relative to uncoated sands, and increased proppant density.[2]

In the work presented here, two different types of RCP, phenol-formaldehyde (PF) and polyurethane (PU), were examined for their propensity to leach chemicals, particularly form- aldehyde, at ambient and lab-simulated downhole conditions. The conditions subsurface, or downhole, can include temperatures ranging from 40–100 °C and pressures ranging from 4000–6000 psi.[3] Phenolic resins have been a popular choice for use during hydraulic stimulation because they have characteristic properties that are more resilient under subsurface conditions.[2] However, phenolic resins are also known to leach carcinogenic compounds, such as formaldehyde and phenols, and as such, many industry operators have moved towards environmentally-friendly alternatives.[4] PU resins are an alternative to phenolic resins, which exhibit comparable properties of resilience.[1] The majority of proppant placed into the formation never leaves, so the possibility of formaldehyde leaching into surrounding waters over time can pose environmental and health risks. This could be particularly troublesome in regions where there are fault lines, which have the capability of connecting the shale layer to groundwater.

The detection and quantitation of formaldehyde is known to be challenging because of the highly reactive nature of formaldehyde. The most common method of analysis involves reaction with an acidic solution of 2,4-dinitrophenylhydrazine (2,4-DNPH) to form the corresponding hydrazone, which is separated and analyzed by LC-UV.[5–7] United States Environmental Protection Agency (EPA) Method 1667 analyzes formaldehyde, iso-butyraldehyde, and furfural using such an approach but is somewhat labor-intensive.[8] Methods based on the EPA 1667 have been reported[5–7] that are more ergonomic and have shown promise. Limitations of using

HPLC (especially with UV detection alone) with complex samples include limited selectivity and specificity, as well as the requirement of additional filtration/centrifugation to clean up the sample prior to HPLC analysis. The limitations of selectivity and specificity have been overcome by detecting the 2,4-DNPH formaldehyde derivative using a nano-ESI-high resolution/accurate mass (HRAM) instrument with data-dependent MS^3 and neutral loss scanning.[9] This method has been reported to attain high attomole LOD, but complex samples require clean-up for direct-injection into this sophisticated instrument.[9]

Pharmaceuticals are a common complex matrix where the presence of formaldehyde is of concern. Methods of derivatizing formaldehyde with O-2,3,4,5,6-(pentafluorobenzyl) hydroxylamine hydrochloride (PFBHA) and successive analysis by static headspace GC-MS have been reported with LODs as low as 0.5 mg L^{-1}.[10,11] Sample preparation for this method is simple and rapid, but the instrumentation requires a chemical ionization source, which some laboratories may not have readily available.[10,11] Formaldehyde content in pharmaceutical samples have also been derivatized to diethoxymethane using an acidic solution of ethanol and analyzed by HS-GC-FID or HS-GC-MS with LODs of 2.44 ppm and 0.05 ppm respectively.[12,13] In order for GC-FID to achieve such LODs, large quantities of salt (2 g NaCl) must be added to the sample matrix to create a salting-out effect.

The aim of this work is to investigate the most widely used method of formaldehyde analysis, based on high performance liquid chromatography (HPLC) and compare its ability to determine formaldehyde leaching from different RCPs to two other analytical methods, one based on headspace gas chromatography-

vacuum ultraviolet spectroscopy (HS-GC-VUV) and the other on headspace gas chromatography-mass spectrometry (HS-GC-MS). It was predicted that headspace sampling will be more appropriate due to its robustness in analyzing complex samples without the need for extensive cleanup. Temperatures were altered to simulate downhole conditions and to observe how temperature affects the release of compounds from the resin coatings in the presence of different solution matrices over time. Further characterization was per- formed using the HS-GC-MS to look at leachates in the presence of more complex matrices including produced water inorganic (PWI) mimic and produced water (PW), with and without shale core.

4.3. Experimental

4.3.1 Materials and instrumentation

Two different samples of phenol-formaldehyde proppants (PF1 and PF2) and two different samples of polyurethane proppants (PU1 and PU2) from undisclosed commercial sources, as well as a sample of shale core, were obtained from Apache Corporation (Houston, TX). Experiments were designed to examine two main factors. The first was to evaluate a timeline of formaldehyde leaching from the proppants under lab-simulated downhole conditions, especially with the variation of temperature. The second was to quantify the amount of formaldehyde leached from RCP prepared using different resin chemistries. The temperature of 93 °C was chosen because this corresponds to 200 °F, which is the upper level temperature stress condition expected downhole. Pressure was not altered.

Formaldehyde, diethoxymethane, and p-toluenesulfonic acid standards were purchased from Sigma-Aldrich (St. Louis, MO). LC-MS grade water, methanol, and

acetonitrile were purchased from Honeywell Burdick & Jackson (Muskegon, MI). 2,4-Dinitrophenylhydrazine and hydrochloric acid were purchased from Spectrum Laboratory Products, Inc. (New Brunswick, NJ). A formaldehyde 2,4-dinitrophenylhydrazine (DNPH) standard was obtained from Restek Corporation (Bellefonte, PA). Ethanol (200 proof) was purchased from Decon Labs, Inc. (Prussia, PA). Produced water (PW) was collected at a commercial salt water disposal well and is a mixture of produced water from surrounding Midland County, TX oil fields. Produced water inorganic (PWI) is a surrogate of the produced water used in regard to ionic strength and inorganic composition, but without the organic content of produced water. The composition of PWI includes $BaCl_2$, $CaCl_2$, $MgCl_2$, $SrCl_2$, Na_2SO_4, $NaHCO_3$, and NaCl with an overall salinity of 12%.

The high-performance liquid chromatography experiments were performed on a Shimadzu Prominence LC (Shimadzu Scientific Instruments, Inc., Columbia, MD) coupled with a Shimadzu SPD-M20A diode array detector. The HPLC was equipped with a Raptor^{TM} ARC-C18 (100 mm, 3.0 mm ID, 2.7 mm d_p) column obtained from Restek Corporation (Bellefonte, PA). 3 mL of sample was injected. The mobile phase consisted of water with a diluent of methanol : acetonitrile (13 :1) mixture, pumped at 0.6 mL min^{-1}. A gradient mobile phase was programmed with 30% organic for 3.5 minutes, then increased linearly to 40% organic at 3.5 minutes, to 70% organic at 6.5 minutes, and then back down to 30% at 6.51 minutes and stopped, after a total run time of 8.51 minutes. These conditions are comparable to conditions prescribed in EPA 1667.[7]

Headspace gas chromatography-vacuum ultraviolet absorbance spectroscopic analysis (HS-GC-VUV) was performed using an Agilent 6890 gas chromatograph (Santa Clara, CA) coupled with a VGA-100 vacuum ultraviolet absorbance detector from VUV Analytics, Inc. (Cedar Park, TX). The GC was equipped with an Rxi-624Sil MS column (30 m, 0.25 mm ID, 1.4 mm d_f) from Restek Corporation. Other columns including a SLB-IL111 (60 m, 0.25 mm ID, 0.2 mm d_f) from Sigma-Aldrich, a RT-Q Bond (30 m, 0.32 mm ID, 10 mm d_f) from Restek, and a RTX- Volatile Amine (60 m, 0.32 mm ID, 0 mm d_f) were tested on the GC-VUV. Carrier gas was a constant flow of 2 mL min^{-1} (helium), and samples were injected using a split ratio of 5 : 1 and an injector temperature of 250 °C. Temperature programming began at 35 °C (held 2 min), was ramped at 10 °C min^{-1} to 150 °C and held for 1 min. Data acquisition rate for the detector was set to 4.5 Hz; detector transfer line and flow cell temperatures were set to 275 °C. A post-column makeup gas flow (nitrogen) of 0.25 psi was used. The Gerstel MPS2 headspace autosampler heated samples for 15 min at 70 °C with agitation and then a 250 mL headspace volume was injected into the HS- GC-VUV instrument.

Headspace gas chromatography-mass spectrometry (HS-GC- MS) was performed using a Shimadzu GCMS-TQ8040 equipped with an AOC-5000 plus Shimadzu autosampler. The headspace autosampler heated samples with agitation for 15 min at 60 °C before injecting 250 mL headspace samples into the GC inlet. The GC was equipped with a Phenomenex ZB-WAXplus column (Torrance, CA) with dimensions of 0.25 mm thickness, 30 m length, and 0.25 mm diameter. A 20 : 1 split ratio was used with constant flow rate of 1.92 mL min^{-1} helium gas; injection port

temperature was 200 °C; and total flow was 43.3 mL min^{-1}. The oven was set to 40 °C for 4.2 min, followed by a 40 °C min^{-1} ramp to 180 °C, and held for 2 min. The mass spectrometer source was set to 230 °C in single ion monitoring mode (SIM), using m/z of 59 (C_3H_7O) and 103 ($C_5H_{11}O_2$) for quantitation.[12]

4.3.2 Sample preparation for liquid chromatography

Proppant was weighed (1.0 g) into a vial and DI water was added (2.00 mL). The vial was capped and left at room temperature, or in an oven at 93 °C, for 1, 4, 15, 20, or 25 hours. Once the time was complete, the liquid contents were decanted to a 1.7 mL Eppendorf tube, leaving behind the proppant, and centrifuged for 10 min at 13,000 RPM. The supernatant (1485 mL) was transferred to LC vials and derivatized. The derivatizing solution was prepared by dissolving 2,4-dinitrophenylhydrazine (2,4-DNPH) in acetonitrile and recrystallizing twice for purification. The solution was vacuum filtered and the solid, recrystallized 2,4-DNPH (20 mg), was dissolved in a 15.0 mL solution of 12 M HCl, water, and acetonitrile 2:5:1 v/v/v ratio. The derivatizing reagent was added (15 mL) to the supernatant, shaken, and left for 1 hour, and analyzed. The derivation reaction can be seen in Scheme 1.[7]

4.3.3 Sample preparation for gas chromatography

Samples were prepared by weighing proppant (approximately 1.0 g) into 10 mL headspace vials. Deionized water (1.00 mL) was added to the vials containing proppant and samples were left at room temperature, or heated to 93 °C, for 1, 4, 15, 20 or 25 hours. The vials were allowed to come to room temperature and ethanol containing 1% p-toluenesulfonic acid (1.00 mL) was added. The derivatization

reaction can be seen in Scheme 2.[12] Analysis was performed on HS-GC-MS and HS-GC-VUV, as previously described.

HS-GC-MS was used to test the ability of the proppants to leach formaldehyde in the presence of produced water inorganic (PWI) and produced water (PW) under the same sample preparation procedures as described above using DIW. In sequentially more complex experiments, shale core and produced water were added to the matrix in the presence of proppant to further mimic downhole conditions. Samples were constructed by weighing proppant (1.0 g) and shale core (1.0 g) into a 20 mL headspace vial. PW (2.00 mL) was added to the sample matrix and left for various amounts of time (1, 4, 15, 20, and 25 hours) either at room temperature or heated to 93 °C. The derivatizing reagent, ethanol containing 1% p-toluenesulfonic acid, was added (2.00 mL) before analysis was performed.

In addition, HS-GC-MS was used to detect other leachates from the proppants in the presence of varying matrices. DIW, PWI, or PW (2.00 mL) were added to 1.0 g of proppant. The samples were either analyzed immediately or heated to 93 °C for 24 hours. Analysis of the solution headspace was performed after heating with agitation to 80 °C for 5 min using a Q3 scan on the Shimadzu GCMS-TQ8040.

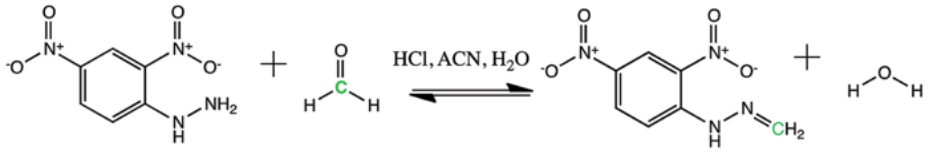

Scheme 1. Reaction of 2,4-dinitrophenylhydrazine with formaldehyde to form the 2,4-DNPH derivative for LC-UV detection.

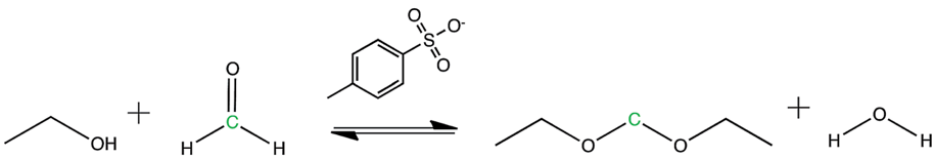

Scheme 2. Reaction of ethanol with formaldehyde in the presence of an acid catalyst to form diethoxymethane for HS-GC-MS and HS-GC-VUV analysis.

4.3.4 Method validation

The methods used in these experiments were validated in terms of linearity, range, limit of detection (LOD), precision, accuracy, and specificity. Linearity was shown by the determination of R^2 coefficient from the responses of different concentrations in triplicate. All standards were immediately analyzed after being prepared to maintain consistency with the analysis of real samples. LOD was calculated as 3s/m, where s was the standard deviation of the signal of a low-level analyte, measured seven times, and m was the slope of the calibration curve. A summary of the method validation experiments can be seen in Table 4.2. Precision was tested for HS-GC-MS and LC-UV at 9, 3, and 0.2 mg L^{-1} for both methods by analyzing each concentration five times. Accuracy was investigated for HS-GC-VUV by performing spiked recovery tests for formaldehyde and formic acid. Specificity was tested by analyzing a blank for comparison to the positive identification of the derivatized products for each method.

4.4 Results and discussion

4.4.1 High performance liquid chromatography

HPLC experiments were based on EPA Method 1667 for analysis of formaldehyde and the results are shown in Fig. 4.1. The LOD was measured to be 0.1 mg L^{-1} and standards at 0.1, 0.5, 1, 5, 10, and 30 mg L^{-1} were analyzed in

triplicate and returned an R^2 value of 0.996. Proppants PF1 and PF2 at ambient temperatures measured from below the detection limit to 7 mg formaldehyde to grams of proppant (mg g^{-1}), with the exception of proppant PF1 at 25 hours, which measured 18±15 mg g^{-1} formaldehyde released. Upon heating to 93 °C, proppants PF1 and PF2 measured around 28 to 50 mg g^{-1}, with PF1 registering slightly higher concentrations than PF2. Proppants PU1 and PU2, were below the limit of detection for room temperature samples and measured as concentrated as 9 mg g^{-1} for the heated samples, with proppant PU2 measuring slightly higher than PU1.

This is the standard and most widely accepted method for detection and quantitation of formaldehyde. However, this method has numerous limitations. One of these limitations is the procedure itself. Though most of the formaldehyde should be in the water as a hydrate, the manipulation of the samples during the derivatization process could allow an opportunity for volatile formaldehyde to be lost. Additionally, this method has complications with complex sample matrices and limited selectivity. To simulate downhole conditions, the analysis of the proppants in PWI, PW, and PW + shale core are important to obtain a well-rounded concept of how these enhanced oil recovery additives might behave in subsurface conditions. The complexity of the addition of PW and other ingredients poses a challenge to clean the samples enough for HPLC injection. Extensive desalination, centrifugation, and/or filtration are needed to prevent salt deposits and clogs in the lines/injector of the instrument. For this reason, two alternate methods were investigated. Each utilized the headspace sampling technique as a means to overcome the challenge of analysis from the complex matrix.

4.4.2 Gas chromatography – vacuum ultraviolet spectroscopy

The VUV measures gas phase absorption from 125–240 nm[14,15] and in this range a compound specific absorbance spectrum can be obtained and searched against a library database for positive identification. This method was originally chosen because of its potential to detect formaldehyde without derivatization. Hard ionization methods, such as EI, are known to overly degrade formaldehyde, making it nearly impossible to detect in its native form using standard mass spectrometry approaches. In the VUV detection range, formaldehyde has a unique absorbance spectrum, which gives this instrument enhanced selectivity, especially compared to the HPLC method. An attempt to detect formaldehyde in its native form proved to be challenging due to the coelution of the formaldehyde and water peaks. This is not typically an issue for VUV, as deconvolving overlapping peaks is a touted capability for the VUV detector.[16–18] However, in this case, the water was in such greater abundance relative to formaldehyde that deconvolution of the two signals could not be performed.

Efforts were made to separate the native formaldehyde peak chromatographically. SLB-IL111 exhibited good selectivity toward formaldehyde but had poor peak shapes (Fig. 4.2A). On the RT-Q Bond, the formaldehyde eluted on the tail of the water peak (Fig. 4.2B). Finally, the RTX-Volatile Amine column was able to separate the formaldehyde and water peaks with good selectivity and efficiency but sporadically, the water peak shifted and coeluted with the formaldehyde peak (Fig. 4.2C). Consequently, we opted for derivatizing the formaldehyde.

4.4.3 Method validation and results

The method to derivatize formaldehyde to form diethoxymethane as a major product was chosen for detection because of its stability and simplicity of procedure. Samples for HS-GC-VUV were prepared by derivatizing formaldehyde with 1% p-toluenesulfonic acid in ethanol, in the presence of water. Standards were analyzed at 20, 50, 100, and 200 mg L^{-1} and had an R^2 value of 0.973. Accuracy was tested for PF1 and PF2 by spiking formaldehyde or formic acid and measuring at different time intervals.

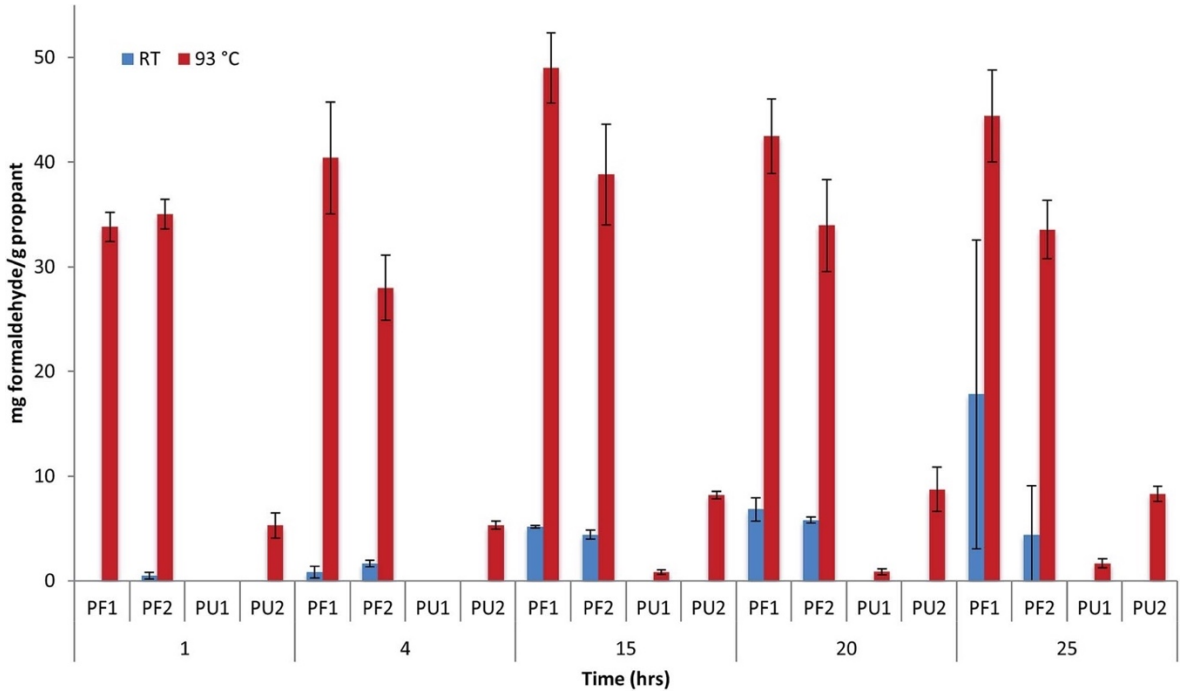

Figure 4.1 Quantitation of formaldehyde from proppants phenol-formaldehyde 1 (PF1), phenol-formaldehyde 2 (PF2), polyurethane 1 (PU1), and polyurethane 2 (PU2) in deionized water analyzed by HPLC with UV detection. PF1 and PF2 leached more formaldehyde than the PU proppants, especially upon heating.

The spiked recovery for formic acid was consistently more accurate than formaldehyde and PF2 had low spiked recovery percent- ages for formaldehyde as

seen in Table 4.1. The LOD for this method was determined to be 20 mg L^{-1}, which was not adequate for our analysis of formaldehyde leaching from proppants. For this reason, room temperature samples, and PU proppants were not analyzed by this method. After one hour of heating, proppants PF1 and PF2 measured 60 ± 10 and 550 ± 500 mg g^{-1}, respectively (Fig. 4.2A). Release of formaldehyde from proppant PF1 continued to increase after 4 hours of heating, and measured 80 ± 20 mg g^{-1}, while proppant PF2 decreased to 350 ± 300 mg g^{-1}. After 15 hours at 93 °C, a leveling of released formaldehyde could be seen for proppant PF1 (average of 80 ± 30 mg g^{-1}), while proppant PF2 decreased to an average of 200 ± 100 mg g^{-1} of formaldehyde released.

Simultaneous formic acid data was also collected by the VUV analysis using the same method of derivatization to form ethyl formate from formic acid. Fig. 4.3B shows the data collected for the formic acid for proppants PF1 and PF2 upon heating and shows a linear increase in leaching as time evolves. The linearity of the increase in formic acid could originate from the formaldehyde being oxidized at a constant rate as the formaldehyde was leaching from the proppants. Such a possibility was discussed by del Barrio et al.; specifically, that the derivatization procedure is reversible when more than 1% of water is in the sample for both formaldehyde and formic acid.[13] If the reversibility of the reaction accounted for the large error bars for the derivatization of formaldehyde, they should additionally be seen in the derivatization of formic acid. The linearity and repeatability of the formic acid data posits that the equal volume of water is not the underlying issue for the poor precision seen for formaldehyde measurements.

More likely, the formaldehyde undergoes competing reactions as it leaches from the proppants. These competing reactions include the derivatization of formaldehyde to diethoxymethane and the oxidation of the formaldehyde to formic acid. A trend can be seen in the comparison of Fig. 4.3A and B, especially for PF2, which shows these competing reactions in play. As the analysis of formaldehyde evolved over 1–15 hours, the concentration measured decreased with each measurement. In contrast to this, the formic acid increased, which suggests that the formaldehyde may be being oxidized to form formic acid. It should also be noted that the formic acid derivative has an order of magnitude stronger absorbance in the VUV detector than its formaldehyde counterpart at the same concentration. This is attributable to the double bond present in ethyl formate, which makes it a stronger chromophore.

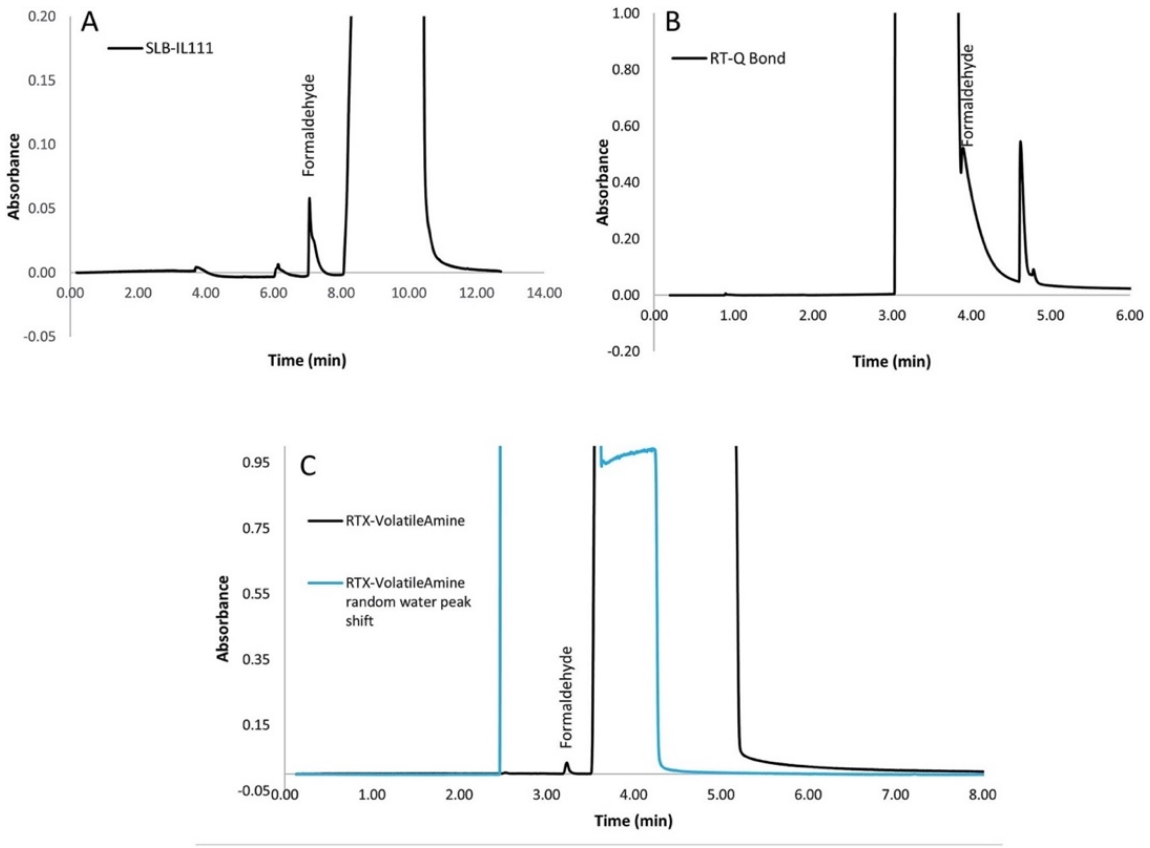

Figure 4.2 (A) Formaldehyde and water separation on SLB-IL111 column with poor peak shape. (B) Formaldehyde tailing on the water peak on the RT- the RTX-Volatile Amine but over time the water peak shifting to coelute with Q› Bond column. (C) Formaldehyde and water peaks separated using formaldehyde.

Table 4.1 Spiked recovery results (%) for proppants PF1 and PF2 at 1, 4, and 15 hours for formic acid and formaldehyde using HS-GC-VUV.

	1 h	4 h	15 h
Formic acid			
PF1	105 ± 10	105 ± 20	110 ± 20
PF2	110 ± 10	110 ± 20	110 ± 20
Formaldehyde			
PF1	80 ± 10	80 ± 20	100 ± 30
PF2	30 ± 30	40 ± 30	60 ± 40

4.5 Headspace gas chromatography-mass spectrometry

HS-GC-MS was investigated as the next analytical tool for detecting formaldehyde leaching by the derivatization of formaldehyde to diethoxymethane. As previously discussed, formaldehyde would degrade and be undetectable using EI without derivatization. The same procedure to derivatize formaldehyde to diethoxymethane used in the VUV experiments was also used in the HS-GC-MS experiments for comparability. The LOD for this method was determined to be 0.1 mg L^{-1}, which is more suited to detect formaldehyde leaching from proppants than the VUV. The MS method should also be significantly more selective than the HPLC, and more amenable for use with complex matrices.

4.5.1 Method validation and results

Calibration standards were prepared and analyzed at 0.1, 0.5, 1, 5, 10, 25, 50, and 500 mg L^{-1} in the matrix of interest. The R^2 values for the derivatized formaldehyde prepared and analyzed in DIW, PWI, PW, and PW plus shale core were 0.994, 0.996, 0.993, and 0.995, respectively. Identification of formaldehyde leaching from the proppants in DIW, PWI, and PW are presented in Fig. 4.4. After resting in the DIW at ambient temperature for one hour, proppant PF1 leached an average of 16 ± 1 mg g^{-1} (n= 3) of formaldehyde while proppant PF2 leached an average of 64 ± 4 mg g^{-1} (Fig. 4.4A). Proppants PU1 and PU2, leached approximately 13 ± 1 mg g^{-1} for all room temperature samples measured. Upon heating, an increase of formaldehyde was observed for PF1, PF2, PU1, and PU2, measuring in at 168 ± 8, 520 ± 30, 32 ± 2, and 35 ± 2 mg g^{-1}, respectively. The largest variability in formaldehyde can be seen in proppants PF1 and PF2 for the

heated samples. After four hours at 93 °C, PF1 and PF2 were measured to release 91 ± 7 and 265 ± 6 mg g^{-1}, respectively.

Although it is not stated what type of PF resin is on proppant PF1, the MSDS sheet for PF2 states that it has a Novolac resin, which are typically produced with a molar excess of formaldehyde,[19] and could account for the higher concentration detected. Novolac resins are manufactured using an acid catalyst, such as sulfuric acid, phosphoric acid, hydrochloric acid, oxalic acid, or p-toluenesulfonic acid.[19] The decrease in formaldehyde from 1 h to 4 h could be attributed to the formaldehyde being oxidized as previously seen in the VUV analysis or the p-toluenesulfonic acid used in the derivatization procedure could be curing the resin. Following 15 h of heating, samples PF1 and PF2 were measured to release 318 ± 6 and 340 ± 20 mg g^{-1} of formaldehyde, respectively. This suggests that after 15 h, formaldehyde is still being leached from the two phenol- formaldehyde proppants into the matrix. The level of formaldehyde starts to hold relatively constant after 15 h, indicating that the leaching of formaldehyde, derivatization to diethoxymethane, oxidation to formic acid, and/or curing has come to equilibrium.

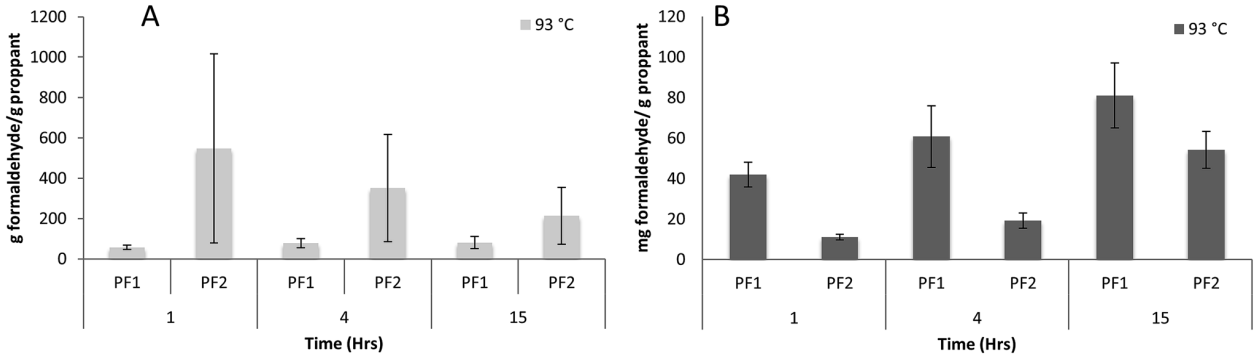

Figure 4.3 Quantitation of phenol-formaldehyde 1 (PF1) and phenol-formaldhyde 2 (PF2) in deionized water matrix analyzed by HS-GC-VUV for (A) formaldehyde and (B) formic acid.

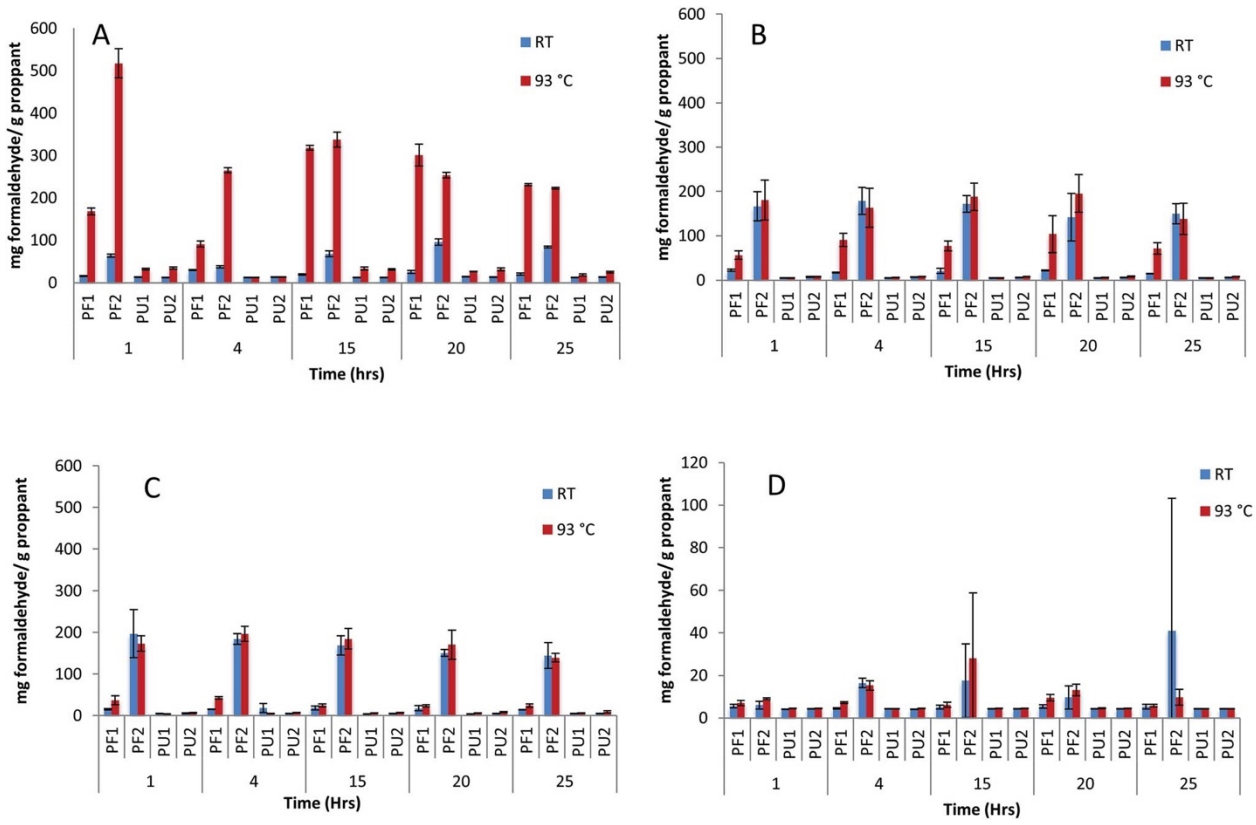

Figure 4.4 Phenol-formaldehyde 1 (PF1), phenol-formaldehyde 2 (PF2), polyurethane 1 (PU1), and polyurethane 2 (PU2) analyzed using HS-GC-MS for formaldehyde leaching in (A) deionized water, (B) produced water inorganic, (C) produced water, and (D) produced water with the addition of shale core.

Table 4.2 Summary of results for proppants in water using the three different analytical testing methods.

Method	LLOD (mg L^{-1})	Linear range (mg L^{-1})	R^2	Limitations
LC-UV	0.1	0.1–30	0.996	Complex matrices, selectivity, derivatization
HS-GC-VUV	20	20–200	0.973	Sensitivity, derivatization
HS-GC-MS	0.1	0.1–500	0.994	Derivatization

4.5.2 Proppant measured in produced water inorganic

Since this method is able to analyze complex matrices without issue, the same sets of experiments were conducted using the surrogate produced water, which was prepared to mimic the ionic concentration of the produced water used in these experiments, but without the hydrocarbon content. The produced water inorganic (PWI) contains various metals, including calcium, barium, magnesium, and

strontium, which can catalyze reactions. These experiments were performed to incrementally increase the complexity of the matrix, to some- where between the complexity of DIW and PW, and to make it possible to gauge any possible differences in the reaction kinetics or optimum detector settings with the presence of select additional constituents.

Fig. 4.4B displays the results for the parallel experiments which were performed with the PWI. The two polyurethane proppants, PU1 and PU2, were shown to release between 4–6 mg g^{-1} of formaldehyde for the ambient and heated samples, with proppant PU2 reporting consistently slightly higher concentrations than for PU1. At one hour, proppant PF1 and PF2 measured in at 232 and 17030mg g^{-1} for the room temperature samples, and 56 ± 9 and 180 ± 50 mg g^{-1} for the heated samples, respectively. When tested at 4 h, PF1 and PF2 returned concentrations of 18 ± 1 and 180 ± 30 mg g^{-1} for ambient samples, and 90 ± 20 and 160 ± 40 mg g^{-1} for samples heated to 93 °C. After 4 h, the measured formaldehyde concentration for the heated samples stayed relatively consistent and measured much lower for the PWI samples than for the DIW samples tested.

This is the opposite trend that would be expected from introducing inorganic salt into an aqueous sample matrix. In theory, high salt concentrations salt-out volatiles, facilitating their transfer to the headspace, as seen for the room temperature samples. Counter-intuitively, the opposite effect is observed, and the slightly lower measured concentrations could be attributed to competing reactions in the matrix. As previously discussed, some of the salts that make up the PWI are $BaCl_2$, $CaCl_2$, $MgCl_2$, $SrCl_2$, Na_2SO_4, $NaHCO_3$, and NaCl. It is questionable to

suggest that the $CaCl_2$, $SrCl_2$, and/or NaCl reacted with the water to form the corresponding hydroxide, which then reacted with the formaldehyde in a Cannizzaro reaction to form formic acid, because the formation of the correlated hydroxides all occur at temperatures much higher than 93 °C. Since formaldehyde is such a strong reducing agent, it is possible that it was still being oxidized in the presence of water by a metal catalyst from the PWI matrix to produce formic acid.[20] This could account for the smaller concentrations observed for formaldehyde upon heating than previously seen with the DI water. It is also possible that the variability between the PF proppants differ because of their degree of being cured. Both PF proppants are partially cured, but if PF2 is more cured than PF1, it would need less of the free formaldehyde to fully cure, thus allowing more formaldehyde to leach.

4.5.3 Proppants measured in produced water

PW was the most complex of the aqueous matrices tested. It is a heterogeneous mixture containing some insoluble impurities, hydrocarbons, and numerous other compounds acquired from the geologic formation, potentially including naturally occurring radioactive materials (NORM) and certainly, a wide range of metals.[21,22] Before samples were prepared, the PW was mixed to improve consistency. The results associated with release of formaldehyde from proppants in the presence of PW can be seen in Fig. 4.4C. Proppants PU1 and PU2 measured between 4 to 11 mg g^{-1} for both heated and room temperature samples with the exception of the 4 h room temperature sample for proppant PU1, which measured to be 20 ± 10 mg g^{-1}. Proppant PF1 samples at room temperature ranged from 14 to 18 mg g^{-1}, with the highest measurement of formaldehyde at 15 h. Heated samples

from proppant PF1 ranged from 24 to 42 mg g^{-1} with the largest value measured at 4 h. PW results for heated samples of proppant PF1 measured roughly half of the concentration measured in PWI, while the room temperature samples were comparable. Proppant PF2 ambient and heated samples ranged from 140 to 200 mg g^{-1} and stayed relatively close in concentration. At the 15 and 25 h intervals, the room temperature measurement for formaldehyde for proppant PF2 did not show a statistically significant difference from the concentration measured from the heated sample. This trend for proppant PF2 in the PW matrix was comparable to the trend observed in PWI.

Overall, matrix interference was seen in the measurement of formaldehyde leaching from PF1 upon heating, but little effect was seen for PF2. This interference could be from the hydrocarbons or metals present in the PW. To compare the differences between the four different proppants and the effect heating has on their ability to leach formaldehyde in produced water, paired t-tests were performed. It was found that PF1 and PU2 had greater values for their t-statistical (3.1683 and 4.1612, respectively) than t-critical (2.7764) indicating that the heating had a significant effect on the release of formaldehyde, while PF2 and PU1 had t-statistical values (0.4591 and 0.5890, respectively) smaller than their t-critical (2.7764), indicating no significant effect. If PF1 was less cured, the excess formaldehyde would leach into the matrix in PWI, but the presence of additional metal complexes from the PW could catalyze the polymerization more rapidly, thus accounting for the decrease in formaldehyde concentration.

Further experiments were performed to quantitatively determine the behavior of proppants under lab-simulated downhole conditions. Subsurface conditions were mimicked by the addition of shale core to the matrix in addition to the proppant and PW. Typical components found in shale core include silica, quartz (SiO_2), smectite ($(Na,Ca)_{0.33}(Al, Mg)_2(Si_4O_{10})(OH)_2 \cdot nH_2O$), calcite ($CaCO_3$), dolomite ($CaMg(CO_3)_2$), feldspars ($KAlSi_3O_8$–$NaALSi_3O_8$–$CaAl_2SiO_8$), pyrite ($FeS_2$), siderite ($FeCO_3$), clay minerals, organic matter, copper, and phosphates.[23] TOCs for the Barnett Shale have been measured to range between 2–6%.[23]

4.5.4 Proppants measured in produced water and shale core

The addition of the shale core to the produced water and proppant mixture resulted in a suppression in the detection of the formaldehyde derivative. Fig. 4.4D shows the results of these experiments. Proppants PU1 and PU2 for room temperature and heated samples leached around 4 mg g^{-1}. Proppant PF1 at room temperature measured from 4 to 6 mg g^{-1}, and the heated samples ranged from 6 to 10 mg g^{-1}, with the highest value measured at 20 h. Room temperature samples for proppant PF2 ranged from 6 to 42 mg g^{-1}, and the concentrations leached from heated samples varied from 10 to 28 mg g^{-1}. The heterogeneous nature of the PW and the shale core could account for the inconsistency in the measurements. The high complexity of the composition of the shale core and the PW likely catalyze the oxidation of formaldehyde to formic acid. In previous work, it was determined by DFT calculations and temperature programmed desorption that a Cu-Al_2O_3 catalyst could completely oxidize formaldehyde at room temperature.[24] A complex originating from

the shale core could be oxidizing the formaldehyde in a similar fashion at ambient and heated conditions. It is also possible that another pathway is present; the decrease could also be a result of biodegradation or sorption processes.

4.5.5 VOCs from proppants

The HS-GC-MS was also used to investigate all the volatile and semi-volatile compounds that leached from the proppants. Samples were prepared as previously described, using DIW/PWI/PW and analyzed either immediately after prepping or after 24 h of heating at 93 °C with intermittent agitation. PW and PWI samples were additionally tested and the resulting chromatograms compared. Proppant PF1 did not return any leaching compounds after immediate analysis, but after heating for 24 h, displayed a small peak corresponding to ethanol. Proppant PF2 did not give any indication of leaching detectable compounds in these experiments either at room temperature or at elevated temperature. PU1 indicated a small peak for ethanol upon immediate analysis and an even larger peak for ethanol upon heating for 24 h. PU2 did not return a response for any compounds leaching upon immediate analysis, while the heated sample did indicate a small peak for ethanol.

4.6 Conclusion

The approaches developed here, particularly the HS-GC-MS, provided for identification and quantitation of formaldehyde in complex matrices, where other methods tested (LC-UV and HS-GC-VUV) fell short. The EPA method for formaldehyde detection of the 2,4-DNPH derivative using LC-UV has limitations with respect to specificity and for the analysis of complex matrices. The LC-UV method tended to underestimate the concentration of formaldehyde present. To compensate

for this, two other methods were investigated to monitor the proppant propensity to leach chemicals. These methods, both more selective, also had their own set of limitations. Additional studies may be conducted to better understand the behavior of the derivatization procedure, as well as the conversion of formaldehyde to formic acid in the presence of metals, NORM, hydrocarbons, and minerals. In the future, a model could also be constructed to establish the fate of the leached formaldehyde taking into account biodegradation in downhole conditions. The analytical data provided in this report would be useful for such determinations.

This is insightful information for real world applications, as the screening of proppants for leachates could be useful in selecting appropriate and more environmentally friendly prop- pants. In industrial applications, production wells can use up to 10 million gallons of water per well,[25] and up to 4 million pounds of proppant per well.[26] This equates to a ratio of 1 g of proppant to approximately 20 mL of water. While these real- world conditions could be replicated in lab, the quantities of formaldehyde would be under the limit of detection. As such, this study provides a scaled down investigation into the behavior of proppant leachates. This information could prove to be valuable for future HF endeavors and in the reuse of PW for further HF procedures.

The overall objective of this research was to determine the proclivity of RCP to leach formaldehyde and other compounds under lab-simulated downhole conditions to better understand the potential environmental impact of using such RCPs during hydraulic fracturing. A common finding when dealing with produced water and other complex samples is that standard methods, like EPA methods, do

not often return reliable results. Special considerations are needed to effectively adapt known standard methods for produced water and related analysis. Based on these findings, these results would be important for drilling companies to take into consideration when choosing a proppant. To the authors' knowledge, this is the first work presenting the study of leachates from RCP under lab-simulated geothermal reservoir conditions, in this case focusing on the effect of temperature. Further studies could also be performed to examine the effect of elevated pressures (also in combination with elevated temperatures) on the leaching of formaldehyde and other chemicals of concern from the proppants.

Conflicts of interest

Disclaimer: KAS is a member of the scientific advisory board for VUV Analytics, Inc.

Acknowledgements

The authors wish to acknowledge monetary support for this research by Apache Corporation. Further acknowledgements are given to the Shimadzu Institute for Research Technologies at the University of Texas at Arlington, for access to research instrumentation, and Solaris Midstream Partners for access to produced water.

4.7 References

1.F. Liang, M. Sayed, G. A. Al-Muntasheri, F. F. Chang and L. Li, A comprehensive review on proppant technologies, Petroleum, 2016, 2, 26–39.
2. K. D. Pangilinan, A. C. C. de Leon and R. C. Advincula, Polymers for proppants used in hydraulic fracturing, J. Pet. Sci. Eng., 2016, 145, 154–160.
3. G. A. Kahrilas, J. Blotevogel, E. R. Corrin and T. Borch, Downhole transformation of the hydraulic fracturing fluid biocide glutaraldehyde: implications for flowback and produced water quality, Environ. Sci. Technol., 2016, 50, 11414–11423.
4. K. Mazerov, Environmentally friendly proppant technology to improve hydraulic fracturing efficiency, Drilling Contractor, May 2013, online.
5. J. Koplan, A Formaldehyde, https://www.atsdr.cdc.gov/ toxprofiles/tp111-c6.pdf.

6. Y. Lin, P. Wang, L. Hsieh, K. Ku, Y. Yeh and C. Wu, Determination of linear aliphatic aldehydes in heavy metal containing waters by high performance liquid chromatography using 2,4-dinitrophenylhydrazine derivatization, J. Chromatogr. A, 2009, 1216, 6377–6381.
7. R. J. Kieber and K. Mopper, Determination of picomolar concentrations of carbonyl compounds in natural waters, including seawater, by liquid chromatography, Environ. Sci. Technol., 1990, 24, 1477–1481.
8. Method 1667, Revision A: Formaldehyde Isobutyraldehyde, and Furfural by Derivatization Followed by High Performance Liquid Chromatography; U. S. Environmental Protection Agency, U. S. Government Office of Water, 1998.
9. R. Dator, A. Carra, L. Maertens, V. Guidolin, P. W. Villalta and S. Balbo, A high resolution/accurate mass (HRAM) data-dependent MS^3 neutral loss screening, classification, and relative quantitation methodology for carbonyl compounds in saliva, J. Am. Soc. Mass Spectrom., 2017, 608– 618.
10. P. Prabhu, Detection and quantiflcation for formaldehyde by derivatization with pentafluorobenzylhydroxyl amine in pharmaceutical excipients by static headspace GC/MS, Perkin Elmer Application Note, 2011.
11. Z. Li, L. K. Jacobus, W. P. Wuelflng, M. Golden, G. P. Martin and R. A. Reed, Detection and quantification of low- molecular-weight aldehydes in pharmaceutical excipients by headspace gas chromatography, J. Chromatogr. A, 2006, 1–10.
12. M. del Barrio, J. Hu, P. Zhou and N. Cauchon, Simultaneous determination of formic acid and formaldehyde in pharmaceutical excipients using headspace GC/MS, J. Pharm. Biomed. Anal., 2006, 41, 738–743.
13. B. D. A. D. Daoudy, M. Ammar Al-Khayat, F. Karabet and M. Amer Al-Mardini, A robust static headspace GC-FID method to detect and quantify formaldehyde impurity in pharmaceutical excipients, J. Anal. Methods Chem., 2018, 1– 8.
14. K. A. Schug, I. Sawicki, D. D. Carlton Jr, H. Fan, H. M. McNair, J. P. Nimmo, P. Kroll, J. Smuts, P. Walsh and D. Harrison, Anal. Chem., 2014, 86, 8329–8335.
15. I. Santos and K. A. Schug, Recent advances and applications of gas chromatography vacuum ultraviolet spectroscopy, J. Sep. Sci., 2017, 40, 138–151.
16. J. Schenk, J. X. Mao, J. Smuts, P. Walsh, P. Kroll and K. A. Schug, Analysis and deconvolution of dimethylnaphthalene isomers using gas chromatography vacuum ultraviolet spectroscopy and theoretical computations, Anal. Chim. Acta, 2016, 945, 1–8.
17. H. Fan, J. Smuts, L. Bai, P. Walsh, D. W. Armstrong and K. A. Schug, Gas chromatography-vacuum ultraviolet spectroscopy for analysis of fatty acid methyl esters, Food Chem., 2016, 194, 265–271.
18. H. Fan, J. Smuts, P. Walsh, D. Harrison and K. A. Schug, Gas chromatography vacuum ultraviolet spectroscopy for multiclass pesticide identi□cation, J. Chromatogr. A, 2015, 1389, 120–127.
19. J. K. Fink, 4-Phenol/Formaldehyde Resins: Reactive Polymers: Fundamentals and Applications, William Andrew, New York, 2018, 3rd edn.

20. M. F. Striegel, The effects of gas phase formaldehyde on selected inorganic materials found in museums, Objects Specialty Group Postprints. 1992, pp. 1–12.
21. J. B. Thacker, D. D. Carlton, Z. L. Hildenbrand, A. F. Kadjo and K. A. Schug, Chemical analysis of Flowback and Produced Water from Unconventional Drilling Operations. Water, 2015, pp. 1568–1579.
22. Z. L. Hildenbrand, I. C. Santos, T. Liden, D. D. Carlton, E. Varona-Torres, M. S. Martin, M. L. Reyes, S. R. Mulla and K. A. Schug, Characterizing variable biogeochemical changes during the treatment of produced oil□eld waste, Sci. Total Environ., 2018, 1519–1529.
23. K. R. Bruner and R. Smosna, A comparative study of the Mississippian Barnett Shale, Fort Worth Basin, and Devonian Marcellus Shale, Appalachian Basin, US department of energy, 2011, pp. 24–26.
24. Z. Chang-bin, S. Xiao-yan, G. Hong-wei and H. Hong, Elimination of formaldehyde over Cu–Al2O3 catalyst at room temperature, J. Environ. Sci., 2005, 429–432.
25. D. Kargbo, R. Wilhelm and D. Campbell, Natural gas plays in the Marcellus Shale: Challenges and potential opportunities, Environ. Sci. Technol., 2010, 44, 5679–5684.
26. J. O. Robertson and G. V. Chilingar. Environmental aspects of oil and gas production, Whiley, 2017, p. 235.

CHAPTER FIVE: Characterization of Ethoxylated Alcohols in Friction Reducers using Matrix-Assisted Laser Desorption/Ionization – Time-of-Flight – Mass Spectrometry

Jamie L. York,[1] Robert H. Magnuson II,[1] Dino Camdzic,1 Kevin A. Schug[*1]

1. Department of Chemistry and Biochemistry, The University of Texas at Arlington, Arlington, TX, USA

5.1 Abstract

Rationale: Matrix-assisted laser desorption/ionization time-of-flight mass spectrometry (MALDI-TOF-MS) provides detailed information for the analysis of ethoxylated alcohols and polymers. In this study, five friction reducers used in commercial hydraulic fracturing processes were analyzed in their as-received form to identify their ethoxylated alcohol content. The friction reducers were then subjected to lab-simulated downhole conditions. Characterization of friction reducers before and after being subjected to reactive conditions can provide fingerprints associated with produced oilfield waste for source apportionment and information on the stability of these key hydraulic fracturing additives.

Methods: Five different industrially used friction reducers were analyzed for their ethoxylated alcohol content using MALDI-TOF-MS. Three different matrices were assessed for optimal response: α-cyano-4-hydroxycinnamic acid, 2,5-dihydroxybenzoic acid, and 2,5- dihydroxybenzoic acid with 2,2,2-trifluoroethanol (2,5-DHB+E). Reaction times, temperatures, and sample matrices (deionized water, produced water inorganic, produced water, and produced water + shale core) were varied to assess changes in molecular weight distribution and polydispersity of the ethoxylated alcohols relative to their as-received content.

Results: A preference for the 2,5-DHB+E matrix was observed. The friction

reducers were found to contain ethoxylated alcohols with carbon chain lengths of 12 and 14 with degrees of ethoxylation ranging from 6 to 18. Upon being subjected to 100 °C for 24 hours, the ethoxylated alcohols tended to polymerize further, returning higher average molecular weights. Less polymerization was seen in more complex matrices, as supported by dispersity calculations.

Conclusions: Ethoxylated alcohol content was effectively determined in friction reducers using MALDI-TOF-MS. Although this is not a new technique to characterize ethoxylated alcohols, it has proven to be a quick and effective way to determine ethoxylated alcohol content in friction reducers in complex oilfield matrices. This technique can be used as a rapid and straightforward way to determine ethoxylated alcohol content in friction reducers and hydraulic fracturing wastewater for fingerprinting.

Keywords: hydraulic fracturing; unconventional oil and gas extraction; polydispersity; enhanced oil recovery

5.2 Introduction

Nonionic surfactants are used in a wide variety of household products and industrial applications, including hydraulic fracturing, one step in the unconventional oil and gas extraction process. One class of nonionic surfactants is nonylphenol ethoxylates and it is estimated in the US that 300-400 million pounds are consumed per year.1 Nonylphenol ethoxylates can be harmful to aquatic life and, once in the environment, degrade into nonylphenol.[1,2,3,4] Nonylphenol itself is also harmful to marine life, is bio-accumulative, and is an endocrine disruptor.[2,4] The use of precursors that degrade to octyl- or nonylphenols is disclosed in 50% of hydraulic fracturing procedures,[4] but these precursors are being phased out and replaced with

less ecotoxic compounds as industries are becoming more environmentally conscience. Alcohol ethoxylates are a class of nonionic surfactants that are more readily biodegradable and less harmful to aquatic life;[1,5] they are considered a good alternative to nonylphenol ethoxylate surfactants.

Nonionic surfactants can be detected and analyzed using a number of different methods. In previous work, ethoxylated alcohols were successfully characterized by derivatizing the alcohol ethoxylate to the corresponding alcohol ethoxysulfate and subsequent analysis using liquid chromatography-mass spectrometry.[6] Ethoxylated alcohols with C12-C18 have been detected using a comprehensive 2D LC system equipped with hydrophilic interaction chromatography (HILIC) conditions in the first dimension and a reversed phase column in the second dimension with an evaporative light scattering detector.[7] While this is an effective method for identification, it is very complex and requires special instrumentation. Previous work with the detection of ethoxylated alcohols has also used liquid chromatography tandem mass spectrometry methods for detection.[1,8] For complex samples containing copious amounts of salt, metals, and undissolved particles, such in the case of produced water with added shale core, these methods to detect ethoxylated alcohol content would require excessive clean-up of the samples before their injection into the instrument.

Friction reducers are a critical additive in hydraulic fracturing fluid and serve to reduce the friction and backpressure in oil and gas extraction wells when pumping at high flow rates, to increase production. The generic composition of a friction reducer consists of high molecular weight emulsion polymers, a hydrocarbon

external phase, and surfactants.[9] Matrix-assisted laser desorption/ionization – time-of-flight – mass spectrometry (MALDI- TOF-MS) has shown promise in the detection of polyethylene glycol and polydimethylsiloxane components in complex matrices, as demonstrated in the detection of prophylactic lubricants in the presence of biological fluids.[10] The focus of this research was to identify the ethoxylated alcohols contained in five different industrial friction reducers used in the hydraulic fracturing process using MALDI-TOF-MS, without sample clean-up. Once the initial ethoxylated alcohol content was determined, the behavior of the ethoxylated alcohols was monitored at lab-simulated downhole conditions to draw conclusions about how these chemical additives behave once downhole. The overall goal was to look at degradation products or increased polymerization and to calculate polydispersity. The polydispersity will indicate if these additives degrade into potentially harmful components, which could contaminate nearby water supplies, or if they polymerize and thus become less soluble in solution.

5.3 Experimental

Five commercial friction reducers (undisclosed manufacturer) and shale core taken from 9208-9209 feet below the surface (undisclosed location) were provided by Apache Corporation (Houston, TX, USA). Produced water was collected near Midland (TX, USA). Furthermore, a surrogate for produced water (termed here as produced water inorganic (PWI)) was prepared in house and consisted of $BaCl_2$ (1.88 mmol/L), $CaCl_2$ (39.63 mmol/L), $MgCl_2$ (9.51 mmol/L), $SrCl_2$ (2.97 mmol/L), Na_2SO_4 (0.02 mmol/L), $NaHCO_3$ (15.19 mmol/L), and NaCl (1,896.31 mmol/L) with a salinity of 12%.[11] α-Cyano-4- hydroxycinnamic acid (99%), 2,5-dihydroxybenzoic

acid (98%), trifluoroacetic acid (99%), and BrijC10 (Mn~683) were purchased from Sigma-Aldrich (St. Louis, MO, USA). LC-MS grade acetonitrile was purchased from Honeywell (Morris Plains, NJ, USA) and 2,2,2- trifluoroethanol (99.8%) was purchased from Fisher Scientific (Waltham, MA, USA). A stainless steel 384 well MALDI plate DE1580TA was used for all experiments (Shimadzu Biotech, Columbia, MD, USA).

5.3.1 Sample preparation

A standard for ethoxylated alcohols was analyzed using a 10 mg/mL mixture of BrijC10 in methanol. This was used to gain insight on how the ethoxylated alcohols in the friction reducers would become ionized with the various matrices examined by MALDI- TOF-MS. α- Cyano-4- hydroxycinnamic acid (CHCA) matrix was analyzed and a solution of 30/70 v/v ACN/0.1% trifluoracetic acid in water (TA30) was made up and saturated with CHCA. BrijC10 standard was spotted on the plate (1 µL) and allowed to dry, followed by spotting of the MALDI matrix (1 µL). 2,5-Dihydroxybenzoic acid (2,5-DHB) was also examined and a solution of 10 mg/mL of 2,5-DHB was constructed in TA30 solution. 1 µL of the 10 mg/mL BrijC10 standard was spotted on the plate and allowed to dry followed by 1 µL of MALDI matrix, following the dried droplet method. An additional experiment with the 2,5-DHB matrix was performed by spotting 1 µL of standard, 1 µL of MALDI matrix, and 1 µL of 2,2,2-trifluoroethanol (TFE), allowing the sample spot to dry between each application. The latter method was chosen for all further analyses. Friction reducer (approximately 250 µL) was added to a 3-dram screw cap vial with 1750 µL of solvent. The solvents included deionized water (DIW), produced water inorganic

(PWI)[11], or produced water (PW). Experiments were performed to also examine the behavior of ethoxylated alcohols contained in friction reducers in the presence of shale core and produced water. For these experiments ~250 µL of friction reducer, 1750 µL produced water, and one gram of shale core was added to a screw cap vial. Samples were tested immediately after preparation to determine initial content of ethoxylated alcohols. Samples were also allowed to rest either at room temperature or heated to 100 °C for 4 hours or 24 hours to determine behavior over time and with a differential of temperature. The samples were plated for MALDI by spotting approximately 1 µL of sample, 1 µL of MALDI matrix, and 1 µL TFE, allowing the sample to dry between each application.

5.3.2 Data Collection and Processing

The samples were analyzed using a Shimadzu AXIMA Confidence MALDI-TOF- mass spectrometer (Shimadzu Scientific Instruments, Inc., Columbia, MD, USA) equipped with an N_2 laser at the BioMolecular Imaging Center at the University of Texas at Arlington (Arlington, TX, USA). Spectra were acquired using 100 laser shots per sample spot. Prior to analyzing the data, the instrument was externally calibrated using the monoisotopic mass $[M+H]^+$ of *m/z* 190.0426 for CHCA and the monoisotopic fragment ion of *m/z* 757.3997 for bradykinin. Each sample was analyzed in triplicate and each mass spectrum was normalized to a scale of 0-1. The top 70% of signals were tabulated for each sample analyzed and these values and their abundance were used to calculate the weight average molecular weight (M_w) and the number average molar mass (M_n). The results for the weight average

molecular weight and number average molar mass were used to calculate the dispersity (Đ, formally PDI).

5.4 Results and Discussion

5.4.1 Sample Preparation Method Development

Three different sample preparation techniques, based on the use of CHCA, 2,5-DHB, and 2,5-DHB+E matrix compositions, were surveyed for their efficiency to ionize the polymer standard, Brij C10, using MALDI-TOF-MS. Brij C10 is a commercial name given to the polyethylene glycol hexadecyl ether. This compound is a linear carbon 16-ethoxylated alcohol, with an average degree of ethoxylation of 10. There is no information as to the manufacturing companies of the friction reducers supplied (intentionally blinded), but the material safety data sheets (MSDS)12-17 stated that the friction reducers contain ethoxylated alcohols of carbon chain length 10-16 but provided no information on the degree of ethoxylation. Brij C10 was chosen as the standard because this was within range of the expected carbon chain length of the ethoxylated alcohols contained in the friction reducers.

Different matrices were tested with this standard to find the most appropriate matrix to facilitate ionization in the MALDI experiments. α- Cyano- 4-hydroxycinnamic acid (CHCA) was evaluated and promoted very limited ionization in the sample. 2,5- dihydroxybenzoic acid (2,5-DHB) was prepared as described and returned more enhanced ionization of the sample than previously seen with CHCA. Another MALDI matrix combination consisting of 2,5-DHB and 2,2,2-trifluoroethanol (2,5-DHB+E) was also evaluated. This matrix combination provided the best results

for intensity and spectral resolution and a comparison of 2,5-DHB and 2,5-DHB+E can be seen in Figure 5.1.

MALDI-MS can have limited use in the analysis of synthetic polymers because of solubility issues between the polymer and solvents used for MALDI, especially for high molecular weight polymers.[18] 2,5-DHB is a hydrophilic MALDI matrix and interacts well with the alcohol groups on the ethoxylated alcohols. The addition of the TFE could facilitate greater interaction between the friction reducer and the MALDI matrix. The addition of TFE in sample preparation has been demonstrated for MALDI mass spectrometry imaging of high molecular weight proteins up to 70,000 Da[19], but its use has yet to be reported in a MALDI sample preparation protocol for the analysis of synthetic ethoxylated alcohols. TFE is probably not participating in the ionization of the analyte but instead solubilizing the ethoxylated alcohols, as seen previously with Nylon-6,20 allowing the analyte and MALDI matrix to co-crystalize. Due to the volatility of the TFE, it presumably evaporates before the MALDI analysis is performed and thus is probably not participating in the ionization of the analyte.

5.4.2 Data Acquisition and Analysis

Samples were analyzed by MALDI-TOF-MS in triplicate with varying laser power; a laser power of 100 µJ was chosen for the analysis of the samples. The samples were prepped and analyzed immediately to identify the initial polymer content. It was found that the five testable friction reducers contained two different ethoxylated alcohols (Figure 5.2) of carbon chain lengths 12 (black) and 14 (yellow)

with degrees of ethoxylation ranging from 6 to 18, and were detected as sodium adduct ions.

In order to perform data analysis on the mass spectra of the friction reducers to determine the initial content, the mass spectra were normalized on a scale of 0 to 1 and the top 70% of abundant hits taken into consideration to avoid low-abundance compounds and working with extremely convoluted mass spectra. The number average molecular mass (M_n) was calculated by taking the sum of the products of the normalized abundance and the *m/z* ($\sum N_i M_i$) and dividing it by the sum of the normalized abundance ($\sum N_i$), as shown in Equation 1. The weight average molecular weight (M_w) was calculated by taking the sum of the normalized abundance multiplied by the square of the *m/z* ($\sum N_i M_{i2}$) and dividing it by the sum of the product of the normalized abundance and the *m/z* ($\sum N_i M_i$), as shown in Equation 2. The difference between the two calculations is that the Mn is dependent on the number of polymer chains, and the M_w is dependent on the size of the chains.[18]

$$M_n = \sum_i \frac{N_i M_i}{N_i} \qquad \text{Equation 1}$$

$$M_w = \sum_i \frac{N_i M_i^2}{N_i M_i} \qquad \text{Equation 2}$$

Weight average molecular weights (M_w) were calculated for each analysis and compiled for each ethoxylated alcohol polymer found in the friction reducers for each condition tested. The full results of these calculations for all the friction reducers can be seen in the supporting information. Some friction reducers are more difficult to spot onto the plate than others and returned no results for some of the parameters

tested. Returning no results was more frequent for the C14 ethoxylated alcohol, which was in less abundance than the C12. The lack of results could also be attributed to the nonuniformity of the laser hitting the plate and the complexity of the sample matrix. The two polymers for the five friction reducers contained carbon chain lengths of 12 and 14. The ethoxylated alcohol with carbon chain length 12 was overall more polymerized and in higher abundance than the polymer with 14 carbons and had an overall higher weight average molecular weight. An example of the results of these calculations for ethoxylated alcohols containing 12 carbons in friction reducer 3 in each of the sample matrices can be seen in Figure 5.3.

When the friction reducers were analyzed in water matrix, due to polymerization they returned higher weight average molecular weights than the other three matrices tested (i.e. PWI, PW, PW+ shale). Heating the samples for 4 h at 100 °C showed variable results for the different sample matrices tested, but heating for 24 h tended to polymerize the ethoxylated alcohols and shift the weight average molecular weight to higher values. An example of this can be seen in Figure 5.4 where the mass spectrum for friction reducer 3 immediately tested in DIW was overlaid with the results tested after 24 h of heating in DIW. A shift can be seen in the abundance of the higher molecular weight compounds upon heating, indicating that it is probable that the polymers generally extend their length, and thus probably do not break down when exposed to temperatures encountered in downhole conditions. However, the presence of degradation products was not observable using the developed method, due to significant low molecular weight interferences in the MALDI mass spectra.

The weight average molecular weights tended to be higher (more polymerization) in water than in other complex sample matrices. This phenomenon has been observed previously when dealing with these matrices,[11] and is probably due to competing reactions taking place that result in less polymerization of the ethoxylated alcohol. Although the complex sample matrix tended to hinder polymerization when tested immediately at room temperature compared with the water matrix, upon heating for 24 hours a trend was observed in most cases that polymerization occurs in all matrices.

The implications of this could be that as the friction reducers are exposed to downhole conditions, they become less water soluble as they polymerize further. This indication of the stability of the ethoxylated alcohols means that they are not significantly decomposing into their precursor ethylene oxides. Ethylene oxides are a human carcinogen and in high exposures can result in seizures, loss of consciousness, coma, and damage to the liver and kidneys.[21] From these results, no evidence regarding the decomposition of ethoxylated alcohols (and the potential release of ethylene oxides) in these friction reducers was observed, even after exposing them to lab-simulated subsurface conditions.

5.4.3 Dispersity

The dispersity was also calculated for the polymer distributions observed. Dispersity, or Đ, is the degree of non-uniformity of distribution of a polymer, and is determined by calculating the weight-average molar mass (M_w) and dividing it by number-average molar mass (M_n) (Equation 3). For samples that are monodisperse, the Mn will equal the Mw.18 The result of these calculations, Đ, determines the

degree of non-uniformity or change under the different conditions to which the friction reducers were exposed, such as different sample matrix (water, PWI, PW, PW+ shale core), amount of time left to rest, and temperature variation.

$$Đ = \frac{M_w}{M_N} \quad \text{Equation 3}$$

Đ was calculated for the friction reducers and their results are tabulated in the supporting information. Although these are polydisperse polymers, containing a wide variety of chain lengths from 6 to 18 monomers, their Đ values only ranged from 1.002 to 1.058. The physical properties of polymers depend heavily on their chain length; as they become more polymerized, they often become less water-soluble and more viscous. Since these polymers do not exhibit a wide range of Đ values, this indicates negligible change under stress conditions with the various different matrices tested. Figure 5.5 was constructed by taking the Đ values for carbon chain length 12 of friction reducer 2 for each of the sample matrices tested. Upon heating the samples for 24 h, the Đ value tended to shift to higher values in water and produced water, but only negligible change was observed in PWI and PW+ shale for friction reducer 2. Other exceptions to this can be seen for friction reducers 3 and 4, which have higher Đ values (and associated higher variability) for the C12 and the C14 polymer, respectively, tested at 4 h at room temperature (see supporting information). The large error bars could be due to the viscosity of the samples, causing it to be very challenging to spot accurate amounts of them onto the plate. Inhomogeneities in crystallized sample spots could have also contributed to the increased variability.

It was overall observed that in the presence of more complex matrices (i.e. PWI, PW, and PW+ Shale), the ethoxylated alcohols tended to have lower weight average molecular weights and lower dispersity values. As previously discussed, this could be due to competing reactions occurring among the contents of the more complex sample matrices.[11]

5.5 Conclusions

This method has proven to be a rapid, inexpensive, green, and effective method for the qualitative characterization of ethoxylated alcohol polymer content in friction reducers. Minimal sample preparation was needed to analyze these complex samples using MALDI- TOF-MS. Since this method only needed microliters of sample and MALDI matrix per analysis, it is greener than other methods of analysis, such as LC/MS, which generates more waste due to the use of larger volumes of solvents and more extensive sample preparation. The MALDI matrix chosen in the sample preparation procedure proved to have a great effect on the efficiency of analyzing and detecting the ethoxylated alcohol content. The carbon chain length of the polymers was determined to be C12 to C14, which matched nicely with the MSDS sheets for each one of the friction reducers. This method could be implemented as an approach to detect ethoxylated alcohol polymer content in produced water and wastewater for fingerprinting. To the authors' knowledge, this is the first time that ethoxylated alcohols from friction reducers have been characterized using MALDI. In the future, high molecular weight polymers including polyacrylamide and acrylic acid polymers, which are in a majority of friction reducers, could also potentially be targeted for characterization by a variation of this method.

The residual acrylamide content in these friction reducers is of interest, as is an improved understanding of the fate of these and other ingredients at downhole conditions.

Acknowledgements

Monetary support for this work provided by Apache Corporation is gratefully acknowledged. The authors would also like to acknowledge the Shimadzu Institute for Research Technologies at the University of Texas Arlington for instrumentation support, and Solaris Midstream Partners for access to produced water.

5.6 References

1. DeArmond PD, DiGoregorio AL. Rapid liquid chromatography−tandem mass spectrometry-based method for the analysis of alcohol ethoxylates and alkylphenol ethoxylates in environmental samples. *J Chromatogr A*. 2013;1305:154−163. doi:10.1016/j.chroma.2013.07.017.
2. United States Environmental Protection Agency (EPA). Risk management for nonylphenol and nonylphenol ethoxylates. Assessing and managing chemicals under TSCA. https://www.epa.gov/assessing-and-managing-chemicals-under-tsca/risk- management-nonylphenol-and-nonylphenol-ethoxylates. Accessed July 13, 2018.
3. Shang DY, Macdonald RW, Ikonomou MG. Persistence of nonylphenol ethoxylate surfactants and their primary degradation products in sediments from near a municipal outfall in the Strait of Georgia, British Columbia, Canada. *Environ Sci Technol*. 1999;33(9):1366−1372. doi:10.1021/es980966z.
4. Elsner M, Hoelzer K. Quantitative survey and structural classification of hydraulic fracturing chemicals reported in unconventional gas production. *Environ Sci Technol.* 2016;50(7):3290−3314. doi:10.1021/acs.est.5b02818.
5. Human & Environmental Risk Assessment (HERA). Human & Environmental Risk Assessment on ingredients of European household cleaning products. Alcohol ethoxylates, Version 2.0, 2009. https://www.heraproject.com/files/34-f-09%20hera%20ae%20report%20version%202%20-%203%20sept%2009.pdf Accessed July 20, 2018.
6. Cassani G, Pratesi C, Faccetti L, et al. Characterization of alcohol ethoxylates as alcohol ethoxy sulfate derivatives by liquid chromatography-mass spectrometry. *J Surfactants Deterg.* 2004;7(2):195-202. doi:10.1007/s11743-017-2015-z.
7. Elsner V, Schmitz OJ, Wulf V, Naegele E. Separation of homologous series of technical detergents with the Agilent 1290 infinity 2D-LC solution coupled with evaporative light scattering detector. Agilent application note, 2014.

https://www.agilent.com/cs/library/applications/5991-2775EN.pdf. Accessed August 1, 2018.
8. Thurman EM, Ferrer I, Blotevogel J, Borch T. Analysis of hydraulic fracturing flowback and produced waters using accurate mass: identification of ethoxylated surfactants. *Anal Chem*. 2014;86(19):9653−9661. doi:10.1021/ac502163k.
9. Durham D. Hydraulic fracturing chemicals overview, Proceedings of the 251st American Chemical Society National Meeting and Exposition, San Diego, CA, 2016.
10. Spencer SE, Kim SY, Kim SB, Schug KA. Matrix-assisted laser desorption/ionization-time of flight mass spectrometry profiling of trace constituents of condom lubricants in presence of biological fluids. *Forensic Sci Int.* 2011;207(1- 3):19-26. doi:10.1016/j.forsciint.2010.08.010.
11. Schenk J, Carlton DD, Smuts J, et al. Lab-simulated downhole leaching of formaldehyde from proppants by high performance liquid chromatography (HPLC), headspace gas chromatography- vacuum ultraviolet (HS-GC-VUV), and headspace gas chromatography- mass spectrometry (HS-GC-MS). *Environ Sci: Process Impacts.* 2018. doi:10.1039/c8em00342d.
12. *Friction Reducer A*; MSDS; Undisclosed Manufacturer, Jan 22, 2016
13. *Friction Reducer B*; MSDS; Undisclosed Manufacturer, Jan 22, 2016
14. *Friction Reducer C*; MSDS; Undisclosed Manufacturer, Jan 22, 2016 15.
15. *Friction Reducer D*; MSDS; Undisclosed Manufacturer, Jan 22, 2016 16.
16. *Friction Reducer E*; MSDS; Undisclosed Manufacturer, Jan 22, 2016 17.
17. *Friction Reducer F*; MSDS; Undisclosed Manufacturer, Jan 22, 2016
18. Carraher CE. *Introduction to polymer chemistry*. 4th ed. Boca Raton, FL: Taylor & Francis Group; 2017.
19. Franck J, Longuespee R, Wisztorski M. MALDI mass spectrometry imaging of proteins exceeding 30,000 daltons. *Med Sci Monit.* 2010;16(9):293-299.
20. Montaudo G, Montaudo SM, Puglisi C, Samperi F. Characterization of polymers by Matrix-assisted Laser Desorption/Ionization Time-of-flight Mass Spectrometry: Molecular Weight Estimates in Samples of Varying Polydispersity. *Rapid Commun Mass Spectrom.* 1995;9:453-460
21. Agency for toxic substances & disease registry (ATSDR). Toxic substances portal- ethylene oxide. 2014. https://www.atsdr.cdc.gov/mmg/mmg.asp?id=730&tid=133. Accessed June 5, 2018.

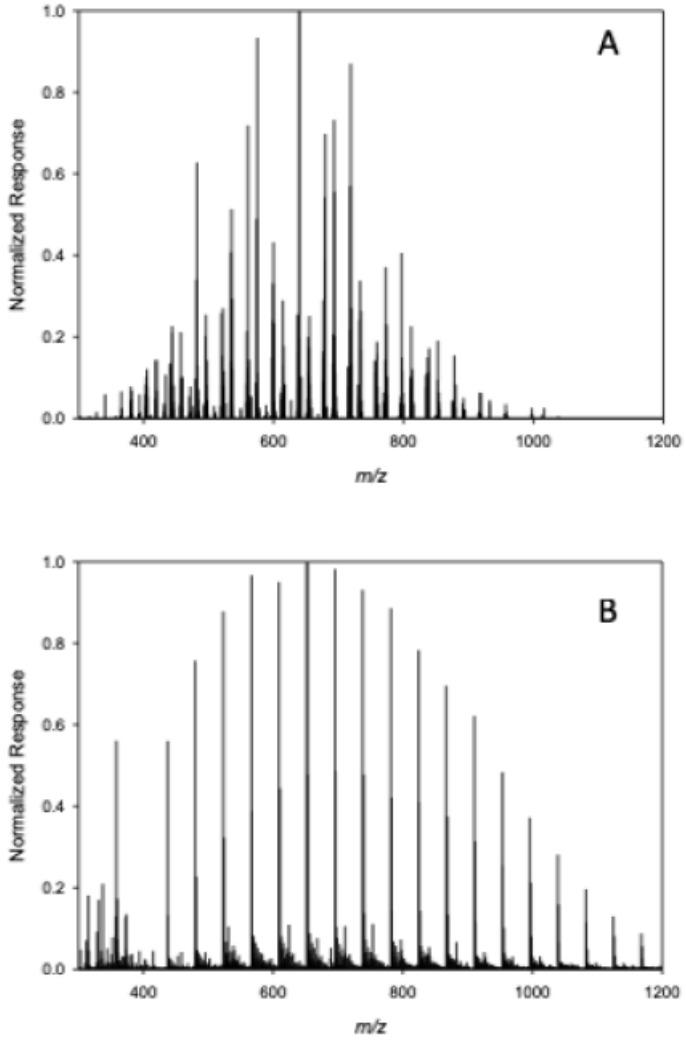

Figure 5.1 MALDI matrix comparison on BrijC10 standard A) 2,5-Dihydroxybenzoic acid (2,5-DHB) B) 2,5-Dihydroxybenzoic acid with 2,2,2-trifluoroethanol (2,5-DHB+E).

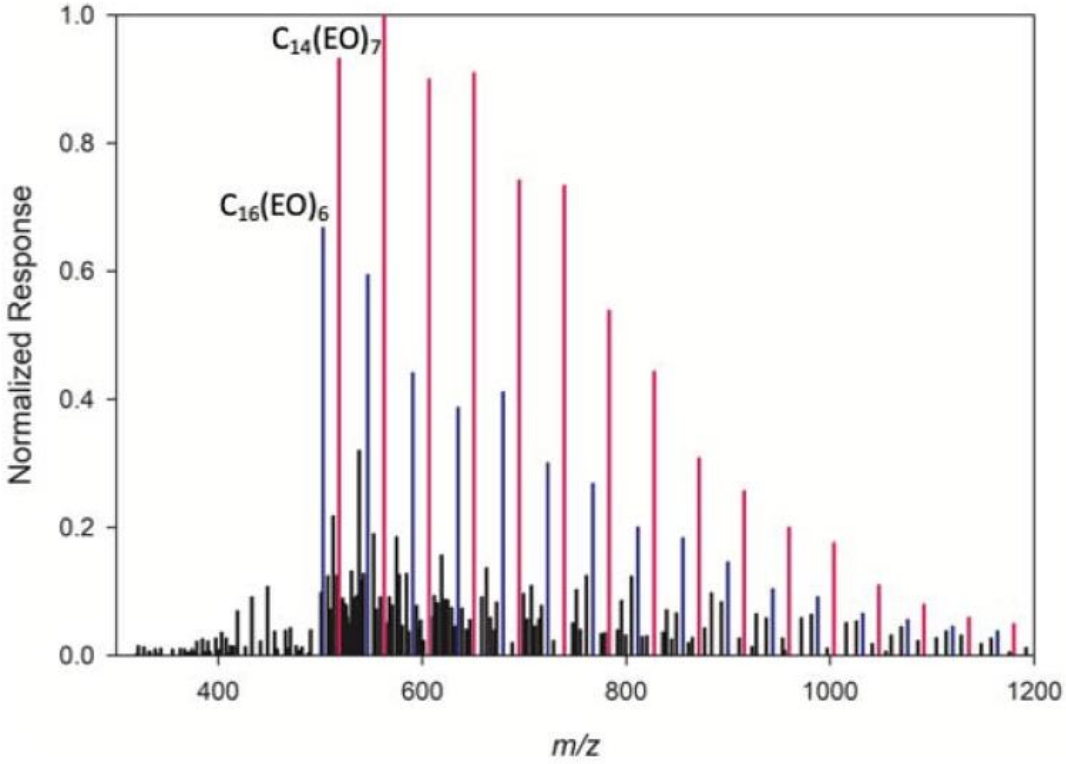

Figure 5.2 Example MALDI mass spectrum of friction reducer 4 ethoxylated alcohol polymer containing 12 carbons (blue) and 14 carbons (green) highlighted.

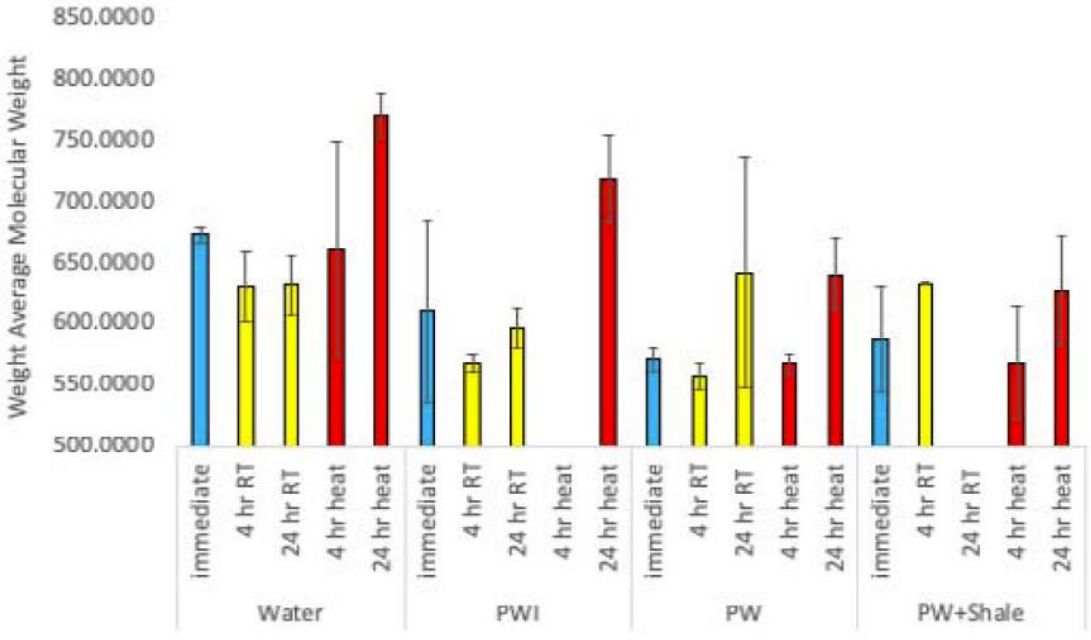

Figure 5.3 Weight average molecular weight calculated for friction reducer 3 for C12 polymer content in water, PWI, PW, and PW+Shale core.

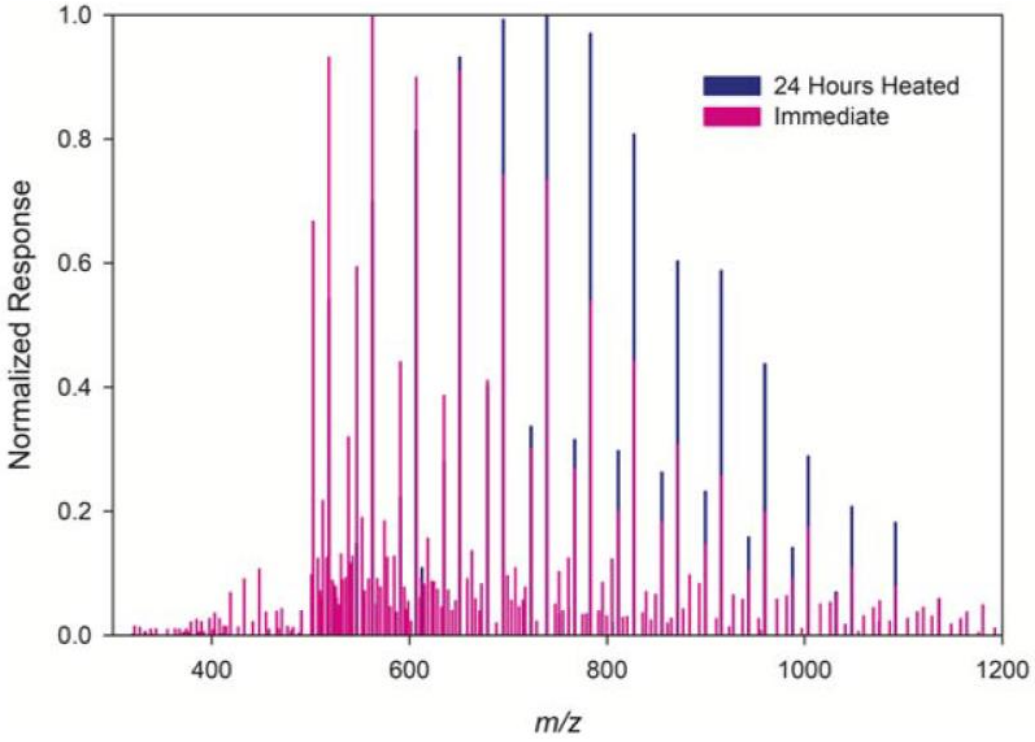

Figure 5.4 MALDI mass spectra for immediate testing and testing after 24 hours at 100 °C overlaid to highlight the shift to higher molecular weight upon heating for 24 hours.

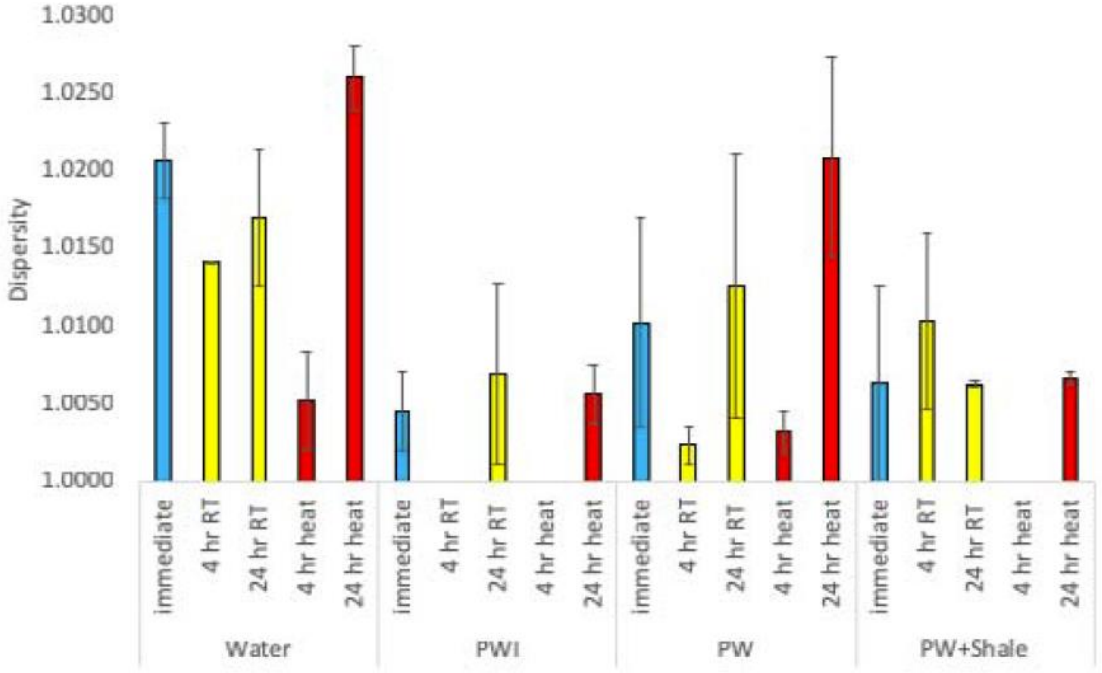

Figure 5.5 Dispersity calculated for friction reducer 2 for C12 ethoxylated alcohol polymer content in water, PWI, PW, and PW+Shale core.

5.7 SUPPLIMENTAL INFORMATION

Characterization of Ethoxylated Alcohols in Friction Reducers using Matrix-Assisted Laser Desorption/Ionization – Time-of-Flight – Mass Spectrometry

Jamie L. York,[1] Robert H. Magnuson II,[1] Dino Camdzic,[1] Kevin A. Schug*[1,2]

1. Department of Chemistry and Biochemistry, The University of Texas at Arlington, Arlington, TX, USA

2. Affiliate of the Collaborative Laboratories for Environmental Analysis and Remediation (CLEAR), The University of Texas at Arlington, Arlington, TX, USA

Table 5S1. Calculated values for weight average molecular weight for ethoxylated alcohols containing 12 carbons and 14 carbons in triplicate with their calculated standard deviation in deionized water.

Weight Average Molecular Weight for Water Matrix					
Friction Reducer	Time Tested	C12	STDEV	C14	STDEV
1	immediate	653.2	28.2	562.1	31.5
	4 hr RT	664	13	595	4.4
	24 hr RT	643	30.1	563.9	24.2
	4 hr heat	613	0.7	561.8	0.8
	24 hr heat	750	20.2	ND	ND
2	immediate	635.7	14	538.3	2.7
	4 hr RT	607.6	1.2	521.3	0.2
	24 hr RT	625	22.2	537.6	18
	4 hr heat	560.7	22.9	510.1	13
	24 hr heat	689.7	8.3	609.5	28.4
3	immediate	672.8	6.5	570.6	25.8
	4 hr RT	631	28.7	527.9	10.7
	24 hr RT	631.8	23.6	532.4	10.9
	4 hr heat	661.9	87.9	529	32.5
	24 hr heat	770.3	17.4	ND	ND
4	immediate	675.3	28.8	634.3	49.1
	4 hr RT	683.6	49.4	721.8	62.7
	24 hr RT	717.6	24.9	697.7	49
	4 hr heat	735	16.1	744.8	25.2
	24 hr heat	674.4	17.8	671.9	37.3
5	immediate	657.8	37.3	577	50
	4 hr RT	707	17.8	ND	ND
	24 hr RT	671.7	32	ND	ND
	4 hr heat	702.5	59.6	ND	ND
	24 hr heat	667.7	12.2	583.1	10.1

Table 5S2. Calculated values for weight average molecular weight for ethoxylated alcohols containing 12 carbons and 14 carbons in triplicate with their calculated standard deviation in produced water inorganic.

Weight Average Molecular Weight for Produced Water Inorganic (PWI) Matrix					
Friction Reducer	Time Tested	C12	STDEV	C14	STDEV
1	immediate	639.1	14.2	566.7	17.8
	4 hr RT	591.2	32.6	541.4	40.1
	24 hr RT	664.4	29.5	595.7	34
	4 hr heat	564	19.9	512.3	8.2
	24 hr heat	629.8	53.5	556.5	57.7
2	immediate	562.1	21.1	518	2.6
	4 hr RT	ND	ND	ND	ND
	24 hr RT	569.2	24	521.4	2.9
	4 hr heat	ND	ND	ND	ND
	24 hr heat	570.5	9.8	512.5	8.9
3	immediate	610.4	74.1	594	124.2
	4 hr RT	568	8	ND	ND
	24 hr RT	597.2	16.3	527.1	15
	4 hr heat	ND	ND	ND	ND
	24 hr heat	718.7	35.5	612.4	44.9
4	immediate	656	21.5	660.2	32.1
	4 hr RT	624.7	62.4	ND	ND
	24 hr RT	566.6	44.5	ND	ND
	4 hr heat	589.5	59.5	ND	ND
	24 hr heat	768	132.3	ND	ND
5	immediate	665.3	28.2	584.3	30.9
	4 hr RT	647.1	26.5	573.4	12.4
	24 hr RT	559.6	36.5	513.5	9.7
	4 hr heat	592	22.9	525.5	11.5
	24 hr heat	634.9	34.6	603	44.8

Table 5S3 Calculated values for weight average molecular weight for ethoxylated alcohols containing 12 carbons and 14 carbons in triplicate with their calculated standard deviation in produced water.

Weight Average Molecular Weight for Produced Water (PW) Matrix					
Friction Reducer	Time Tested	C12	STDEV	C14	STDEV
	immediate	663.6	46.5	602.5	31
	4 hr RT	615.4	40.8	591.8	101.1
	24 hr RT	647.3	31.9	568	21.9
	4 hr heat	564.9	43.5	529.3	19.8
1	24 hr heat	675.3	36.1	592.9	48.8
	immediate	594.8	32.8	520.3	2.6
	4 hr RT	548.8	11.7	513	9.3
	24 hr RT	609.2	51.6	548.9	23.9
	4 hr heat	555.2	12.1	513.5	9.7
2	24 hr heat	652.9	24.6	587.1	24.9
	immediate	570.7	9.5	523.9	8.5
	4 hr RT	556.5	10.8	507.3	8.4
	24 hr RT	641.9	94.3	579.3	71.7
	4 hr heat	567.3	7.8	518.4	1.3
3	24 hr heat	640.5	28.8	560.3	7.6
	immediate	625.9	13	587.2	47.4
	4 hr RT	654.9	40.2	575.4	17.6
	24 hr RT	601.8	53.8	ND	ND
	4 hr heat	599.8	21.8	542.6	27.2
4	24 hr heat	723.4	17.5	649.6	43.9
	immediate	648.1	24	ND	ND
	4 hr RT	655	40.3	582.1	28.8
	24 hr RT	602.4	10.5	556.2	20
	4 hr heat	599.9	21.7	535.6	15.5
5	24 hr heat	723.5	17.4	645.1	55.2

Table 5S4 Calculated values for weight average molecular weight for ethoxylated alcohols containing 12 carbons and 14 carbons in triplicate with their calculated standard deviation in produced water and shale core.

Weight Average Molecular Weight for Produced Water + Shale Core (PW+S) Matrix					
Friction Reducer	Time Tested	C12	STDEV	C14	STDEV
1	immediate	641.1	60.8	574.6	46.9
	4 hr RT	568.4	8.6	519.9	1.4
	24 hr RT	639.1	43.3	590.9	41.8
	4 hr heat	624.9	48.9	567.1	55
	24 hr heat	713.2	50.9	639.1	27.9
2	immediate	570.3	36.4	531.6	19.4
	4 hr RT	587.3	23.7	536.8	13.7
	24 hr RT	578.3	3.1	564.4	6.9
	4 hr heat	ND	ND	526.7	27.1
	24 hr heat	573.9	2.5	533.4	11.4
3	immediate	587.7	43	535.9	20.3
	4 hr RT	632.7	1	577.1	44.3
	24 hr RT	ND	ND	ND	ND
	4 hr heat	568.3	45.7	533.5	15.2
	24 hr heat	627	45.5	566	33.9
4	immediate	553.9	32.4	528.9	18.9
	4 hr RT	ND	ND	ND	ND
	24 hr RT	654.2	12	624.2	27.2
	4 hr heat	ND	ND	ND	ND
	24 hr heat	598.3	35.1	601.7	41.6
5	immediate	636.2	55.9	553.2	30.1
	4 hr RT	621.1	59.6	561.4	33.7
	24 hr RT	626.9	25.3	577.8	30.4
	4 hr heat	647.3	62.8	566.5	50.9
	24 hr heat	666.0	72.7	630.8	53.7

Table 5S5 Calculated values for dispersity for ethoxylated alcohols containing 12 carbons and 14 carbons in triplicate with their calculated standard deviation in deionized water.

Dispersity in Water Matrix					
Friction Reducer	Time Tested	C12	STDEV	C14	STDEV
	immediate	1.026	0.003	1.009	0.005
	4 hr RT	1.002	0.029	1.01	0
	24 hr RT	1.003	0.024	1.013	0.008
	4 hr heat	1.013	0.002	1.006	0.001
1	24 hr heat	1.017	0.019	ND	ND
	immediate	1.021	0.002	1.004	0
	4 hr RT	1.014	0	1.002	0
	24 hr RT	1.017	0.004	1.004	0.003
	4 hr heat	1.005	0.003	1.001	0.001
2	24 hr heat	1.026	0.002	1.003	0.004
	immediate	1.024	0.001	1.009	0.004
	4 hr RT	1.058	0.068	1.003	0.001
	24 hr RT	1.013	0.009	1.003	0.001
	4 hr heat	1.018	0.015	1.003	0.004
3	24 hr heat	1.033	0.004	ND	ND
	immediate	1.024	0.004	1.019	0.008
	4 hr RT	1.024	0.006	1.062	0.065
	24 hr RT	1.028	0.004	1.019	0.014
	4 hr heat	1.028	0.003	1.025	0.002
4	24 hr heat	1.021	0.003	1.009	0.009
	immediate	1.021	0.007	1.006	0.005
	4 hr RT	1.026	0.001	ND	ND
	24 hr RT	1.022	0.006	ND	ND
	4 hr heat	1.024	0.006	ND	ND
5	24 hr heat	1.026	0.001	1.006	0.006

Table 5S6 Calculated values for dispersity for ethoxylated alcohols containing 12 carbons and 14 carbons in triplicate with their calculated standard deviation in produced water inorganic.

Dispersity in Produced Water Inorganic (PWI) Matrix					
Friction Reducer	Time Tested	C12	STDEV	C14	STDEV
	immediate	1.019	0.002	1.008	0.002
	4 hr RT	1.011	0.007	1.007	0.009
	24 hr RT	1.023	0.004	1.012	0.004
	4 hr heat	1.005	0.003	1.001	0.001
1	24 hr heat	1.017	0.009	1.007	0.007
	immediate	1.005	0.003	1.002	0
	4 hr RT	ND	ND	ND	ND
	24 hr RT	1.007	0.006	1.002	0
	4 hr heat	ND	ND	ND	ND
2	24 hr heat	1.006	0.002	1.001	0.001
	immediate	1.013	0.011	1.017	0.027
	4 hr RT	1.006	0.001	ND	ND
	24 hr RT	1.012	0.004	1.003	0.003
	4 hr heat	ND	ND	ND	ND
3	24 hr heat	1.031	0.004	1.01	0.007
	immediate	1.02	0.004	1.026	0.011
	4 hr RT	1.016	0.01	ND	ND
	24 hr RT	1.007	0.007	ND	ND
	4 hr heat	1.012	0.01	ND	ND
4	24 hr heat	1.022	0.004	ND	ND
	immediate	1.023	0.004	1.01	0.004
	4 hr RT	1.019	0.004	1.009	0.003
	24 hr RT	1.006	0.005	1.001	0.001
	4 hr heat	0	0	ND	ND
5	24 hr heat	1.017	0.006	1.017	0.009

Table 5S7 Calculated values for dispersity for ethoxylated alcohols containing 12 carbons and 14 carbons in triplicate with their calculated standard deviation in produced water.

Dispersity in Produced Water (PW) Matrix					
Friction Reducer	Time Tested	C12	STDEV	C14	STDEV
	immediate	1.021	0.007	1.008	0.005
	4 hr RT	1.014	0.007	1.018	0.023
	24 hr RT	1.02	0.004	1.009	0.002
	4 hr heat	1.006	0.007	1.004	0.003
1	24 hr heat	1.024	0.006	1.014	0.009
	immediate	1.01	0.007	1.002	0
	4 hr RT	1.002	0.001	1.001	0.001
	24 hr RT	1.013	0.009	1.006	0.003
	4 hr heat	1.003	0.001	1.001	0.001
2	24 hr heat	1.021	0.007	1.014	0.005
	immediate	1.006	0.002	1.002	0.001
	4 hr RT	1.003	0.001	1.001	0.001
	24 hr RT	1.017	0.014	1.011	0.012
	4 hr heat	1.002	0.004	1.002	0
3	24 hr heat	1.018	0.004	1.007	0
	immediate	1.018	0	1.012	0.007
	4 hr RT	1.022	0.007	1.01	0.002
	24 hr RT	1.012	0.009	ND	ND
	4 hr heat	1.012	0.004	1.006	0.006
4	24 hr heat	1.03	0.001	1.021	0.005
	immediate	1.021	0.006	ND	ND
	4 hr RT	1.022	0.007	1.011	0.004
	24 hr RT	1.013	0.002	1.008	0.004
	4 hr heat	1.012	0.004	1.004	0.003
5	24 hr heat	1.03	0.001	1.019	0.006

Table 5S8 Calculated values for dispersity for ethoxylated alcohols containing 12 carbons and 14 carbons in triplicate with their calculated standard deviation in produced water and shale core.

Dispersity in Produced Water + Shale Core (PW+S) Matrix					
Friction Reducer	Time Tested	C12	STDEV	C14	STDEV
	immediate	1.019	0.01	1.009	0.007
	4 hr RT	1.006	0.002	1.002	0
	24 hr RT	1.019	0.008	1.013	0.006
	4 hr heat	1.017	0.01	1.01	0.01
1	24 hr heat	1.031	0.007	1.02	0.003
	immediate	1.006	0.006	1.004	0.003
	4 hr RT	1.01	0.006	1.005	0.004
	24 hr RT	1.006	0	1.009	0.002
	4 hr heat	ND	ND	1.003	0.004
2	24 hr heat	1.007	0	1.004	0.003
	immediate	1.01	0.009	1.004	0.003
	4 hr RT	1.018	0.001	1.012	0.008
	24 hr RT	ND	ND	ND	ND
	4 hr heat	1.007	0.007	1.004	0.003
3	24 hr heat	1.019	0.012	1.009	0.007
	immediate	1.005	0.005	1.004	0.003
	4 hr RT	ND	ND	ND	ND
	24 hr RT	1.022	0.001	1.02	0.004
	4 hr heat	ND	ND	ND	ND
4	24 hr heat	1.011	0.008	1.019	0.01
	immediate	1.018	0.01	1.007	0.005
	4 hr RT	1.016	0.011	1.009	0.006
	24 hr RT	1.019	0.004	1.012	0.005
	4 hr heat	1.019	0.012	1.009	0.01
5	24 hr heat	1.023	0.011	1.027	0.002

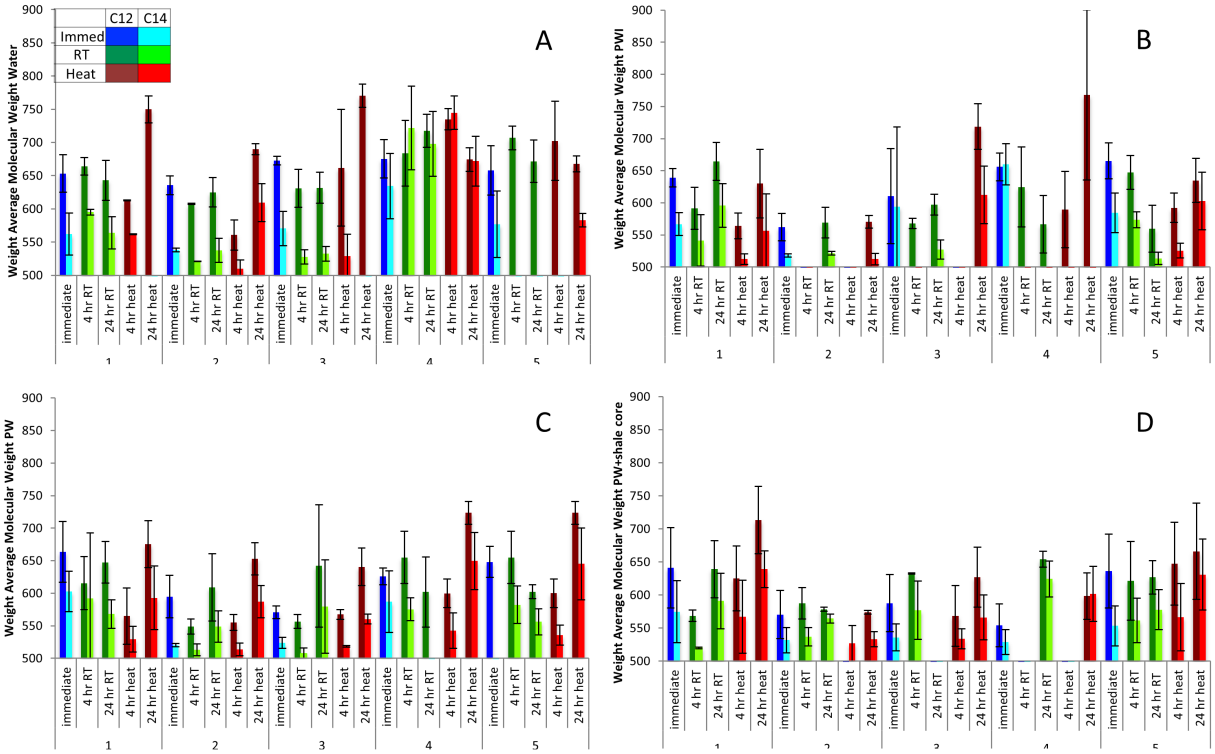

Figure 5S1 Weight average molecular weight calculated for the five testable friction reducers for polymer content in A) water B) PWI C) PW D) PW+ shale core.

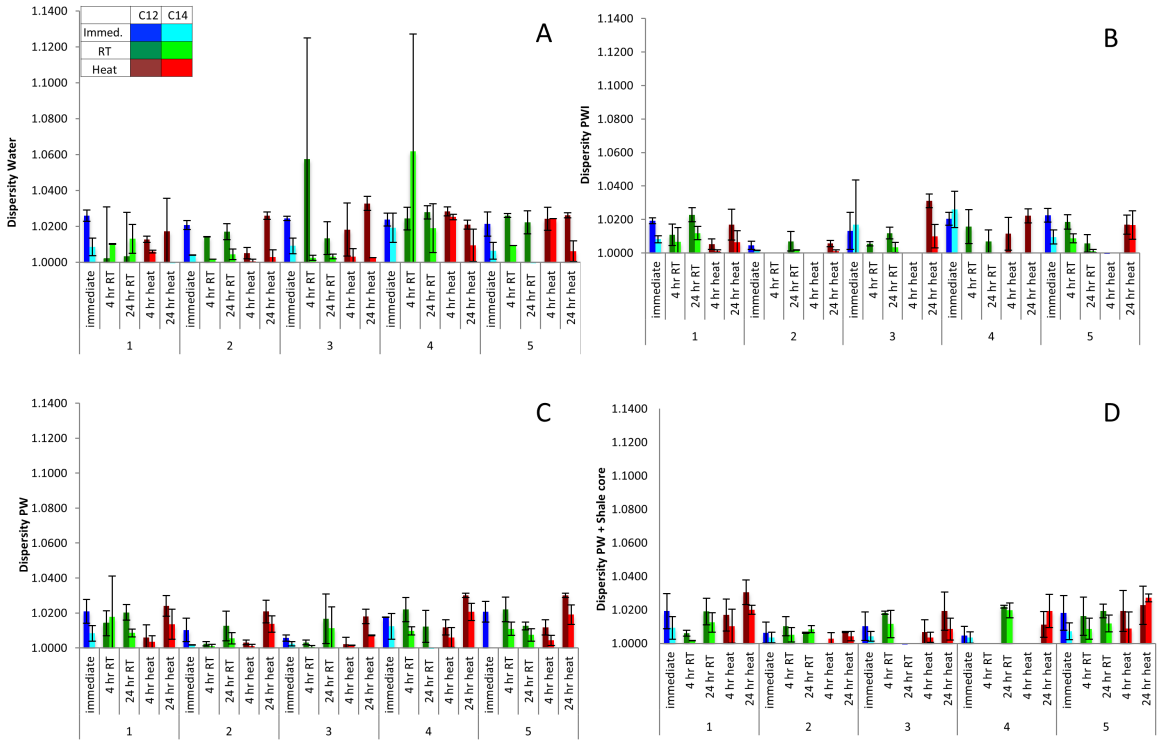

Figure 5S2 Dispersity calculated for the five testable friction reducers for ethoxylated alcohol polymers in A) water B) PWI C) PW D) PW+ shale core.

CHAPTER SIX: Identification and deconvolution of carbohydrates with gas chromatography-vacuum ultraviolet spectroscopy

Jamie Schenk[a], Gabe Nagy[b], Nicola L.B. Pohl[b], Allegra Leghissa[a], Jonathan Smuts[c], Kevin A. Schug[a,*]

[a] Department of Chemistry & Biochemistry, The University of Texas at Arlington, Arlington, TX 76019, United States

[b] Department of Chemistry, Indiana University, Bloomington, IN 47405, United States

[c] VUV Analytics, Inc., Cedar Park, TX 78613, United States

Keywords: Covariance analysis Sugars, Saccharides, Cold medicine, Sugar substitutes

6.1 ABSTRACT

Methodology for qualitative and quantitative determination of carbohydrates with gas chromatography coupled to vacuum ultraviolet detection (GC-VUV) is presented. Saccharides have been intently studied and are commonly analyzed by gas chromatography-mass spectrometry (GC–MS), but not always effectively. This can be attributed to their high degree of structural complexity: α/β anomers from their axial/equatorial hydroxyl group positioning at the C1-OH and flexible ring structures that lead to the open chain, five-membered ring furanose, and six-membered ring pyranose configurations. This complexity can result in convoluted chromatograms, ambiguous fragmentation patterns and, ultimately, analyte misidentification. In this study, mono-, di, and tri-saccharides were derivatized by two different methods—permethylation and oximation/pertrimethylsilylation—and analyzed by GC-VUV. These two derivatization methods were then compared for their efficiency, ease of use, and robustness. Permethylation proved to be a useful

technique for the analysis of ketopentoses and pharmaceuticals soluble in dimethyl sulfoxide (DMSO), while the oximation/ pertrimethylsilylation method prevailed as the more promising, overall, derivatization method. VUV spectra have been shown to be distinct and allow for efficient differentiation of isomeric species such as ketopentoses and reducing versus non-reducing sugars. In addition to identification, pharmaceutical samples containing several compounds were derivatized and analyzed for their sugar content with the GC-VUV technique to provide data for qualitative analysis.

6.2 Introduction

Whereas carbohydrate separation, classification, and identification has received considerable attention in recent years, the analytical toolbox remains bare in large part due to the high degree of structural complexity of this class of analytes.[1] This complexity arises from the number of carbon atoms in the molecule overall and in the individual closed ring (pyranose/furanose) structures, the stereochemistry of the ring substituents including the anomeric configurations (α/β), and the varying functional groups. This incredible diversity of structure in turn translates into a diversity of functions in humans, plants, and the food and pharmaceutical industries.[2-5]

Given this diversity, the separation and identification of a wide assortment of carbohydrates, with a specific emphasis on isomeric differentiation, is needed. Nuclear magnetic resonance (NMR) remains the gold standard for structural assignment, but requires milligram scales of sample as a rule and its deconvolution of coupling constants or *J* values from a mixture of saccharides is non-trivial.[6]

Traditional liquid chromatography (LC) suffers from column stability, regeneration times, reproducibility of retention times, cost, and the availability of suitable stationary phases.[2] Hydrophilic interaction liquid chromatography, ligand exchange chromatography, and other LC methods have been shown to be inefficient for separation of all carbohydrates or complicated isomeric mixtures, even on various stationary phases.[7] High-performance anion-exchange chromatography requires strong concentrations of sodium hydroxide, which makes it challenging to couple to other analytical techniques and/or detectors, and is limited to samples that are resistant to base.[8]

Mass spectrometry[1,6] has shown promise for the individual discrimination of hexose and pentose isomers through the measurement of dissociation rates, but has not been shown to resolve isomeric mixtures. Ion mobility spectrometry-mass spectrometry has been used to discriminate individual glucose isomers[9] but when analyzing isomers, two mobility peaks may not necessarily indicate the presence of two unique isomers, but instead may indicate the presence of two ion conformations. Gas chromatography coupled with mass spectrometry detection suffers similar drawbacks, namely significant coelution and inability to resolve complex mixtures due to similarities in carbohydrate electron ionization mass spectra.

A modern bench-top vacuum ultraviolet detector (VUV) has been introduced that may be able to overcome these shortcomings and be used for the differentiation of mixtures of carbohydrate isomers. Fig. 6.1 shows a generalized schematic of the GC-VUV instrument.[10]

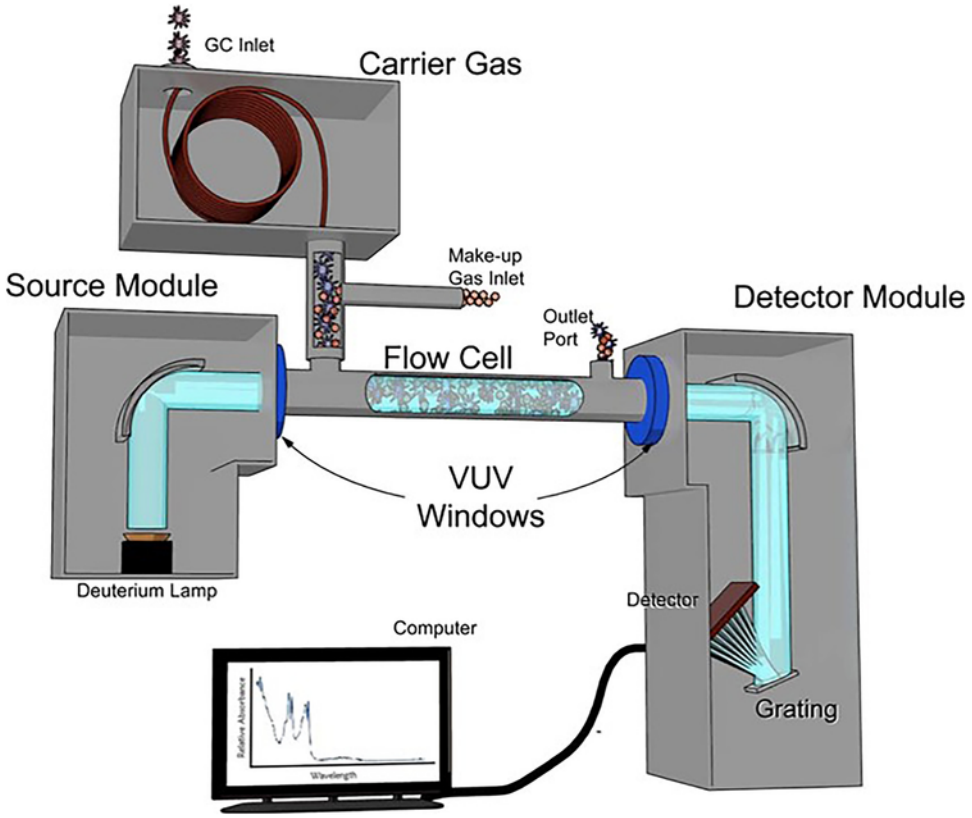

Figure 6.1 Schematic of the gas chromatography- vacuum ultraviolet (GC-VUV) instrument. Reprinted with permission from the American Chemical Society, copyright 2014.[10]

Analytes elute from the GC column and are passed through a heated transfer line into a flow cell. Reflective optics direct light from a deuterium lamp source through the flow cell and to a diffraction grating, which diffracts the light (120–240 nm) for detection by a charge-coupled device (CCD), with a maximum sampling rate of 100 Hz. Perhaps most novel is the fact that the natural additivity of absorbance spectra allows for deconvolution of coeluting peaks.[10,11] These and other merits of the VUV detector have been exemplified previously in the analysis of permanent gases[12], pesticides[13], fatty acids[14,15], terpenes[16], and hydrocarbon fuels.[10,11,18] The ability to rapidly deconvolve species in an automated fashion from chromatographic separations of complex mixtures—a process termed time interval deconvolution—

has also been demonstrated for PIONA (paraffins, isoparaffins, olefins, naphthenes, and aromatics) analysis of gasolines[19] and polychlorinated biphenyl-containing Aroclor mixtures.[20]

The aim of this study was to evaluate the potential of GC-VUV for effective separation, deconvolution, and determination of isobaric and isomeric carbohydrate analytes. Herein, methods are described for the rapid differentiation of mono-, di-, and trisaccharides that have been derivatized by permethylation and oximation/pertrimethylsilylation (O/TMS), so as to become sufficiently volatile and thermally stable for GC analysis. Mixtures of derivatized carbohydrates were analyzed and deconvolutions were performed on compounds that coeluted to separate the compounds for quantitative and qualitative analysis. Covariance calculations were performed to evaluate theoretical detection limits for deconvolutions to compare with experimental measurements. Furthermore, experiments were performed to identify carbohydrates present in samples of over-the-counter cold medicines and prescription medications.

6.3 Material and methods

6.3.1 Materials

D-(−)-ribose (99%), D-(+)-xylose (99%), D-(+)-glucose (99.5%), D-(−)-arabinose (98%), D-(−)-fructose (99%), D-(+)-galactose (99%), D-(+)-mannose (99%), sucrose (99.5%), β-lactose (99%), D-(+)-cellobiose (98%), melibiose (98%), maltitol (98%), D-(+)-turanose (98%), lactulose (98%), sodium hydroxide (98%), iodomethane (99%), pyridine anhydrous (99.8%), hexamethyldisilazane (99%), hydroxylamine hydrochloride (99%), isomaltotriose (98%), D-(+)-melezitose hydrate

(99%), D-(+)-raffinose pentahydrate (98%), 1-kestose (98%), and dimethylsulfoxide (99.5%) were all purchased from Sigma-Aldrich (St. Louis, MO). D-ribose, L-ribose, D-arabinose, L-arabinose, D-xylose, L-xylose, D-lyxose, L-lyxose, D-allose, L-allose, D-altrose, L-altrose, D-glucose, L-glucose, D-mannose, L-man- nose, D-gulose, L-gulose, D-idose, L-idose, D-galactose, L-galactose, D-talose, L-talose, D-ribulose, L-ribulose, D-xylulose, L-xylulose, D-psicose, L-psicose, D-sorbose, L-sorbose, D-fructose, L-fructose, D-tagatose, and L-tagatose were obtained from Carbosynth (Berk- shire, UK) and Sigma Aldrich (Milwaukee, WI, USA). L-ribulose, D-xylulose, L-idose, and D-allose were purchased from Carbosynth (Berkshire, UK). All samples were analyzed at the University of Texas at Arlington (Arlington, TX).

6.3.2 Instrumentation

A Shimadzu GC-2010 gas chromatograph (Shimadzu Scientific Instruments, Inc., Columbia, MD) was coupled with a VGA-100 VUV detector (VUV Analytics, Inc., Cedar Park, TX). The GC-VUV set up was used to collect data from derivatized carbohydrate samples at a data acquisition rate of 10 Hz. The transfer and flow cell temperatures were set to 300 °C and nitrogen was used as the makeup gas at 0.25 psi. An Rtx-5 column (30 m × 0.25 mm × 0.25 μm) obtained from Restek Corporation (Bellefonte, PA) was used at a constant velocity of 30 cm/s with a helium carrier gas. The injection port was set to 270 °C with an 8.5:1 split ratio for permethylated samples and 50:1 split for O/TMS samples with a 1.0 μL injection volume.

The GC oven profile for all permethylated monosaccharaides was set to 70 °C for 1 min, followed by a 20 °C/min ramp to 210 °C and held for 8 min, then a 20 °C/min ramp to 300 °C and held for 10 min. The GC oven profile for all O/TMS

mono- and disaccharides and per- methylated disaccharides was set to 100 °C for 5 min, followed by 10 °C/min ramp to 300 °C and held for 5 min. The GC oven profile for all trisaccharide analysis was set to 200 °C for 15 min, followed by 15 °C/min ramp to 270 °C, then 1 °C/min ramp to 290 °C, then a 15 °C/min ramp to 330 °C and held 15 min. Samples of medicines were analyzed using an oven program initially set at 100 °C for 5 min, followed by a 10 °C/min ramp to 270 °C, followed by a 1 °C/min ramp to 290 °C, followed by a 15 °C/min ramp to 330 °C and held for 15 min. Needle wash solvent was chloroform for permethylated samples and dichloromethane (DCM) for O/TMS samples.

6.3.3 Permethylation of standards

Each monosaccharide was weighed on a balance (4–5 mg). DMSO (0.5 mL) was added and stirred until the sample was completely dissolved. Powdered NaOH (12 mg) was added, followed immediately by methyl iodide (0.1 mL). The reaction was capped and then stirred for 1 h at ambient temperature. The reaction was diluted with deionized water (2 mL) and chloroform (2 mL). The organic layer was washed three times with deionized water, dried over sodium sulfate, and concentrated. The permethylation method followed previously de- scribed methods in the literature.[21,22] The structures of permethylated carbohydrates are shown in the electronic Supplementary Information document, Figs. 6S1–S3.

6.3.4 Oximation/pertrimethylsilylation of standards

Monosaccharides were accurately weighed out (5 mg) and dissolved samples (1 mg/mL in methanol:water 30:70, v/v) were concentrated under reduced pressure at 50 °C until dry. Anhydrous pyridine (1.8 mL) was added (containing 2.5 g of

hydroxylamine per 100 mL of pyridine) and heated to 70 °C for 30 min. Samples were cooled and hexamethyldisilazane (HMDS) (0.9 mL) and trifluoroacetic acid (TFA) (0.1 mL) were added. Once HMDS and TFA were added, the samples were heated to 100 °C for 60 min. Samples were centrifuged and the supernatant was used for analysis. The oximation/ pertrimethylsilylation procedure followed previously described methods in the literature.[23-27] The structures of O/TMS-derivatized carbohydrates are shown in the electronic Supplementary Information document, Figs. 6S4–S7.

6.3.5 Medication preparation and analysis

Tri-sprintec (one pill) and Theraflu (0.5g) medication were crushed into a fine powder and dissolved into DMSO (2 mL). Toluene (2 mL) was added to induce precipitation of the sugar. The content was centrifuged and the precipitant dried and derivatized using the permethylation method as described above. Chloraseptic Max lozenge was crushed as finely as possible and dissolved into 2 mL of ethanol. The solution was washed three times with ethyl acetate and concentrated to dryness before derivatization. Derivatization was performed using the O/TMS method described above.

6.4 Results and discussion

6.4.1 Selection of derivatization techniques

To increase the volatility of small carbohydrates and make them amenable to gas chromatography, two derivatization methods, permethylation and oximation/pertrimethylsilylation (O/TMS), were tested in conjunction with analysis by the described GC-VUV system. Permethylation is one of the most common

derivatization methods used for carbohydrate analysis, especially for N/O-glycans (Fig. 6.2A).[28] In this reaction, each hydroxyl group is protected with a methyl group, thereby eliminating the donor protons that decrease analyte volatility. However, permethylation may yield complex chromatograms, with up to six peaks per saccharide present, based on the fact that in solvent, monosaccharides exist in an equilibrium of various structures that includes α/β anomer mutarotation, furanose/pyranose five/six membered rings, and acyclic configurations (anhydrous and/or hydrate). As an added obstacle, any incomplete methylation reactions can further complicate the chromatograms with additional peaks corresponding to various partially methylated products.

To simplify the chromatographic responses for each saccharide, and in an attempt to simplify chromatograms of mixtures, oximation/ pertrimethylsilylation derivatization was also evaluated. Oximation/ pertrimethylsilylation (O/TMS) derivatization eliminates the issue of having α/β anomers and furanose/pyranose ring configurations pre sent in the sample. O/TMS derivatives only produce E (anti) and Z (syn) conformations for reducing sugars and only one conformation for non-reducing sugars.[29] The reason for the presence of only two conformations is due to the two-step derivatization process in which oximation of the free carbonyl group is performed first to form a sugar oxime, before the pertrimethylsilylation step (Fig. 6.2B).[25] This two-step process effectively locks the sugar into the acyclic configuration for monosaccharides before the derivatization, ensuring that only two forms are ultimately present in the sample.[30] The silyl donor, HMDS, was chosen because of its fast rate of reaction, stability, and high yield of derivatives.[31] It has

been previously reported that the more abundant peak corresponds to the thermodynamically-favored E (anti) isomer and that the Z (syn) corresponds to the minor peak for aldohexoses.[23,24,32] The O/TMS method also has the advantage of being a diagnostic technique for reducing sugars; if one peak is seen when analyzing an unknown analyte, this is indicative of a non-reducing sugar and can be invaluable in de novo sequencing applications of larger polysaccharides from biological or other sources. Both derivatization methods were assessed for their ability to facilitate analysis and deconvolution of mono-, di-, and trisaccharides using GC-VUV.

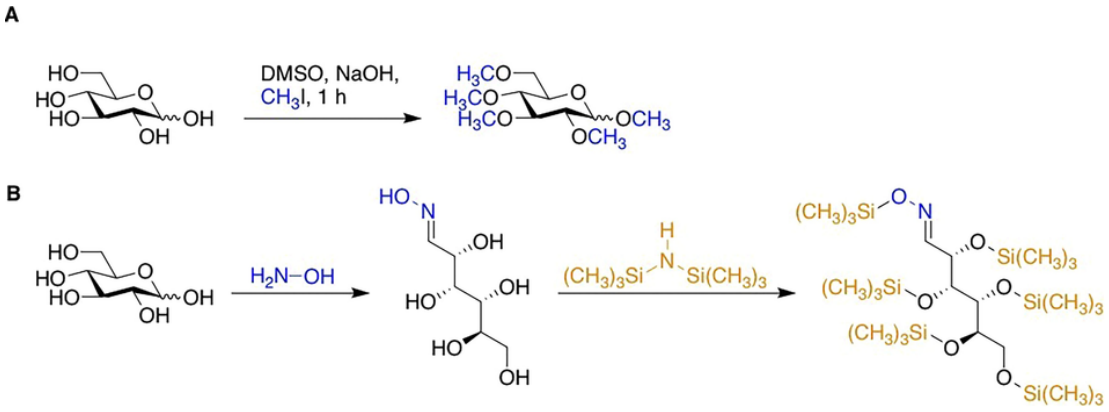

Figure 6.2 Derivatization reactions for A) permethylation of D-glucose and B) O/TMS of D-glucose.

6.4.2 Permethylation

The permethylation method and subsequent analysis of the aldopentoses showed that each monosaccharide contained at least three unique structural peaks in each chromatogram. Coelution and shouldering issues were observed for arabinose and xylose as shown in Fig. 6.3A. In order for deconvolutions to be performed, the coeluted peaks must be composed of known compounds and their pure absorbance spectra must be entered into the VUV library. Since the

coeluting/shouldering peaks could not be separated and their pure spectra obtained, they could not be deconvolved. It may be possible to further improve resolution by the use of an increased polarity stationary phase column such as an Equity-1701 or SPB-624 but these attempts were beyond the scope of this presented work.

Ketopentoses produced two peaks for xylulose and one peak for ribulose (Fig. 6.3B) suggesting that ketopentoses can be effectively analyzed by this method. Aldohexoses yielded complicated chromatograms with up to four peaks per sugar due to the significant relative abundance of various configurations for each saccharide (Fig. 6.3C). Of the aldohexoses, talose was retained the longest, possibly due to the C2 and C4 axial OHs, which causes a 1,3-syn-diaxial repulsion.[33] Glucose was the shortest-retained aldohexose, possibly due to all the hydroxyl groups being in the equatorial position, and perhaps a more elongated structure. Ketohexoses exhibited up to three peaks per sugar with some shouldering and coelution present in tagatose (Fig. 6.3D). Since the pure absorbance spectrum of these shouldered peaks could not be obtained, no deconvolutions were performed to separate them from the main peak. Further separation of the shouldering peaks may be possible with the use of a more polar stationary phase, such as those previously suggested.

Seven disaccharides were also examined in these experiments. The two non-reducing sugars tested, sucrose and maltitol, gave only one peak, as expected (Fig. 6.4A). Four trisaccharides were studied and the permethylated sample of melezitose revealed three peaks, suggesting that full permethylation was not achieved (Fig. 6.4B).

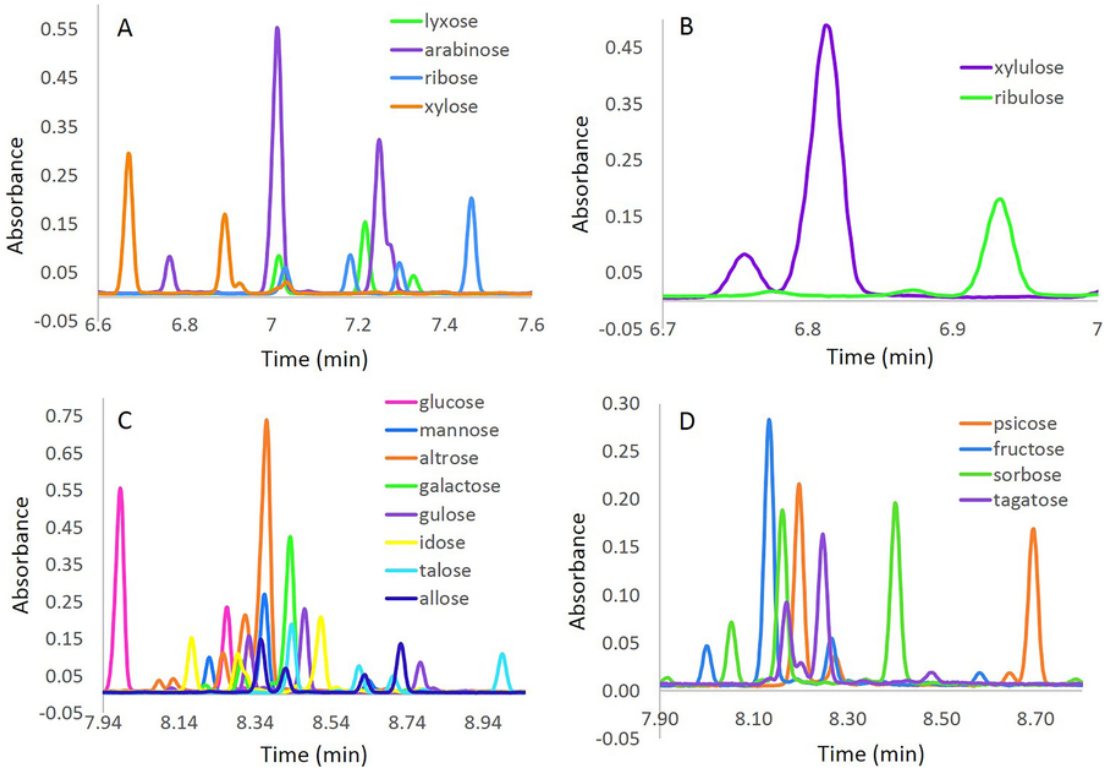

Figure 6.3 Chromatograms for permethylated A) aldopentoses, B) ketopentoses, C) aldohexoses, and D) ketohexoses.

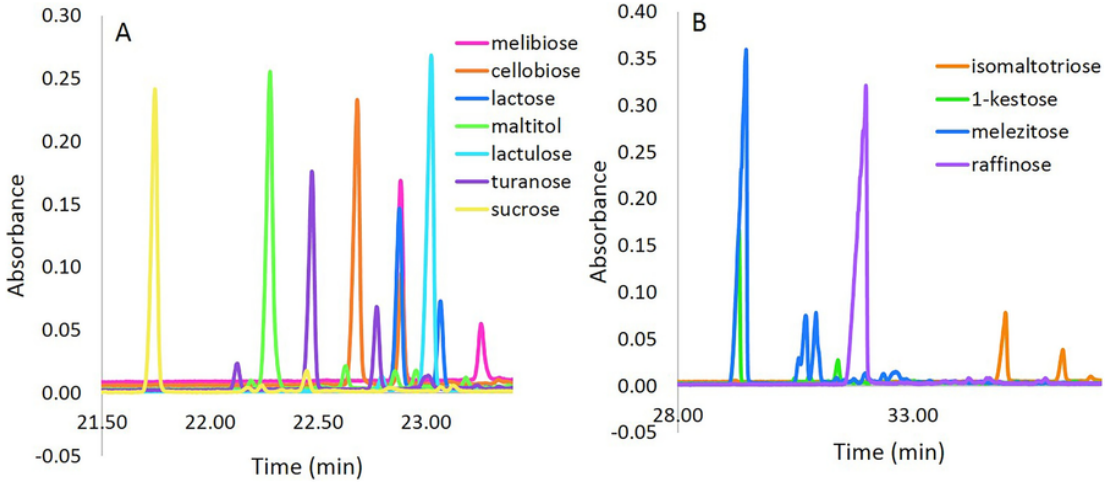

Figure 6.4 Chromatograms for permethylated A) disaccharides and B) trisaccharides.

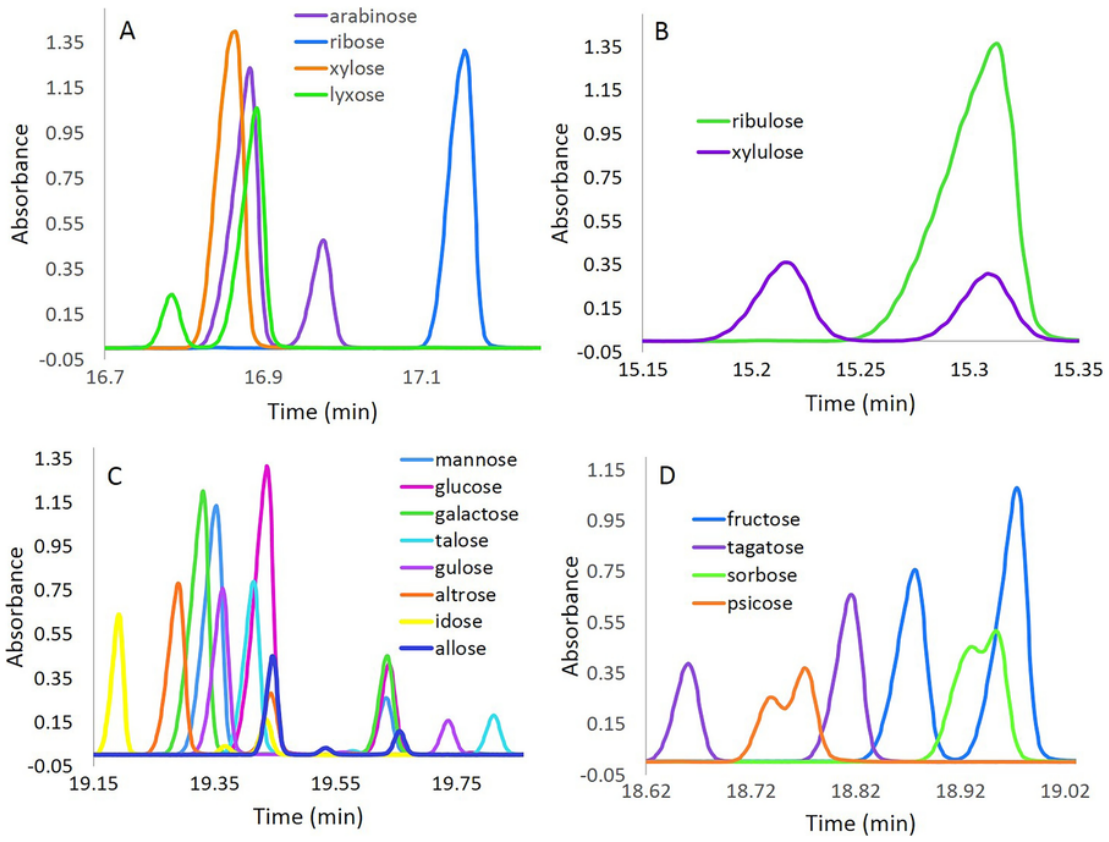

Figure 6.5 Chromatograms for trimethylsilyl oximated A) aldopentoses, B) ketopentoses, C) aldohexoses, and D) ketohexoses.

6.4.3 Oximation/pertrimethylsilylation

O/TMS-Derivatized aldopentose samples showed only one pre- dominant conformation present for xylose and ribose, while two peaks for arabinose and lyxose were observed (Fig. 6.5A). Ketopentoses presented two peaks for xylulose and one peak for ribulose (Fig. 6.5B). The aldohexoses yielded two strong peaks per saccharide (Fig. 6.5C). Ketohexoses gave two peaks per sugar present and coelution was observed for the E- and Z-conformations of sorbose and psicose (Fig. 6.5D). After the pure spectra were entered into the VUV library, the coeluted peaks were deconvoluted into their respective contributions to the sample as seen in Fig. 6.6A and B. Deconvolutions are performed in the Model and Analyze VUV software

application. The program fits absorbance spectra of coeluting compounds to the coeluted peak following Beer's law and returns a deconvolved chromatogram. The deconvolved signal noise in these demonstrations corresponds to their high spectral similarity. Since the absorbance for each of the compounds greatly resemble one another, the deconvolutions have poorer signal to noise ratios than desired.

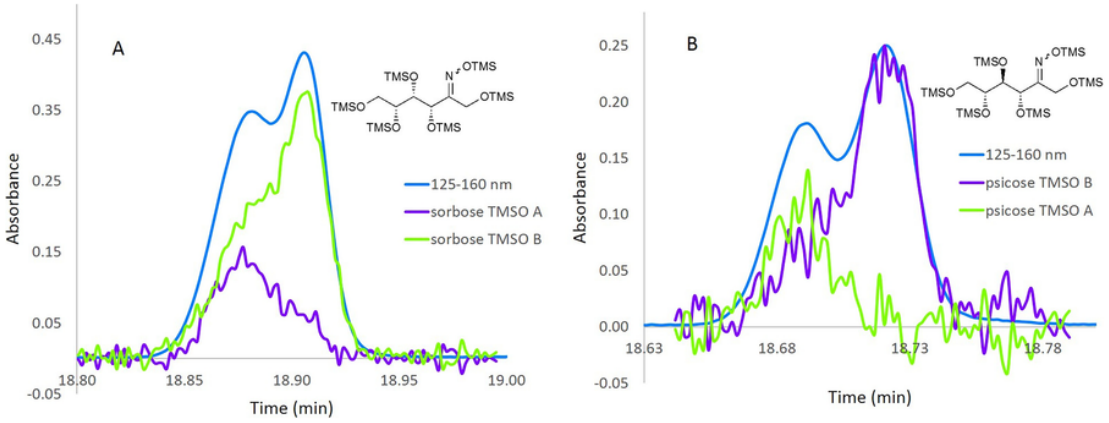

Figure 6.6 Deconvolutions performed on overlapping conformations of O/TMS-derived A) sorbose and B) psicose.

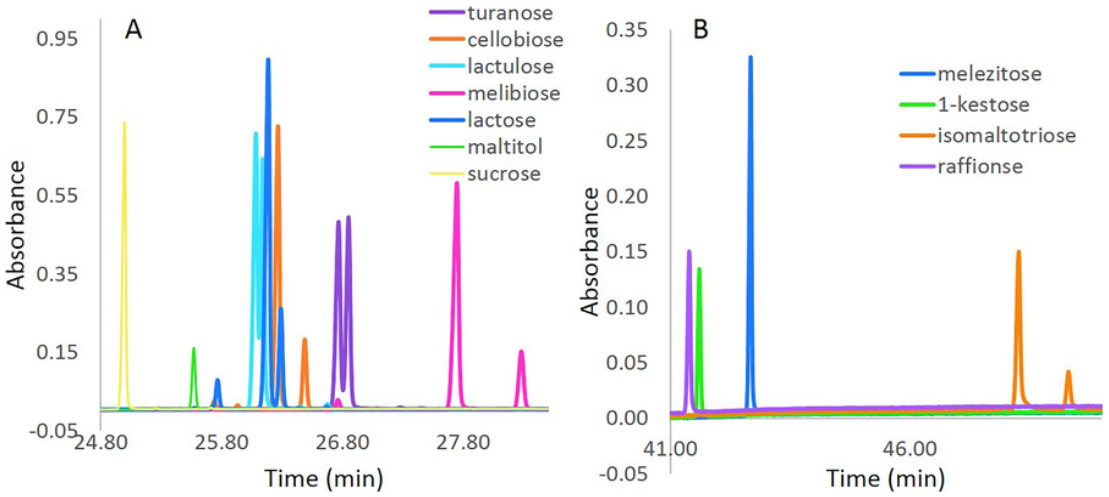

Figure 6.7 Chromatograms for trimethylsilyl oximated A) disaccharides and B) trisaccharides.

The disaccharides and trisaccharides each yielded two peaks for reducing sugars and one peak for the non-reducing sugars (Fig. 6.7). The reason that non-reducing sugars provide only one peak is because they do not form oximes, causing them to elute sooner than reducing sugars.[18] Structures for these compounds can be found in Supplementary Information Figs. 6S6 and S7 . Lactulose and turanose had partial coelution of their E- and Z-configurations and deconvolutions were performed as seen in Fig. 6.8A and B. In both of these cases, the E and Z absorbance spectra that are being deconvolved share a great resemblance and therefore cause the signal of the individual components to be quite noisy.

6.4.4 Spectral similarity and covariance calculations

Absorbance spectral similarity can be measured by determining the sum of square of residuals (SSR) between two spectra desired to be compared [11,34]. To perform these calculations, experimental spectra were searched in the VUV library and the top matches were calculated for their SSR value. The smaller the SSR value, the more similar the spectra.

These calculations were performed for O/TMS-derived sucrose (α-D-glucopyranosyl-(1 → 2)-β-D-fructofuranoside) relative to other O/TMS sugars. Sucrose has the smallest residual of 0.00110 indicating that sucrose is the most similar match from the library. SSR calculations for self-comparison of spectra do not result in zero due to the presence of some background noise. 1-Kestose (β-D-fructofura- nosyl-(2 → 1)-β-D-fructofuranosyl-(2 → 1)-α-D-glucopyranoside) is the second top match for sucrose from the VUV library and was characterized by a residual of 0.00494, when the spectra were compared. Although 1-kestose is a

trisaccharide, the very similar absorbance spectra can be described by comparing the two structures. The structure of sucrose is comprised of one monomer of glucose with a glycosidic linkage to one monomer of fructose. 1-Kestose is comprised of one monomer of glucose and one monomer of fructose linearly bonded in the same fashion as sucrose, but with a second monomer of fructose added as a branch. Melezitose (α-D-glucopy- ranosyl-(1 → 3)-β-D-fructofuranosyl-(2 → 1)-α-D-glucopyranoside) was the third top match for sucrose and yielded a residual of 0.00816. Melezitose also contains a monomer of glucose connected to a monomer of fructose linearly, but has a second glucose monomer bonded in a branched fashion. Overall, these SSR values are very similar and are all in the same degree of magnitude. Such a result indicates that it would be difficult to deconvolve these peaks over a wide range of relative abundance if they coeluted chromatographically.

As a reference from previous work, 1,2-dimethylnapthalene and 1,3-dimethylnaphthalene (DMN), two structural isomers, were analyzed by GC-VUV and shown to have an SSR value of 0.82.[11] For these compounds, it was shown that they could be deconvolved in overlapping peaks that differed in relative abundance up to a ratio of 99:1 (or for 100s of pg of one isomer in the presence of 10s of ng of the other isomer). The DMN isomers had significantly higher SSR values because of the pronounced absorption features and significant associated shifts with the changing position of methyl group substitution on the aromatic ring. In comparison to the DMNs, the sugars are much less responsive to absorbance measurements and have higher spectral similarities, as indicated by low SSR values. Thus, while overlapping sugar signals could be deconvolved, it is expected that a limit of relative

abundance that could be accommodated by such a treatment would be more limited than the case evaluated previously for DMN isomers.

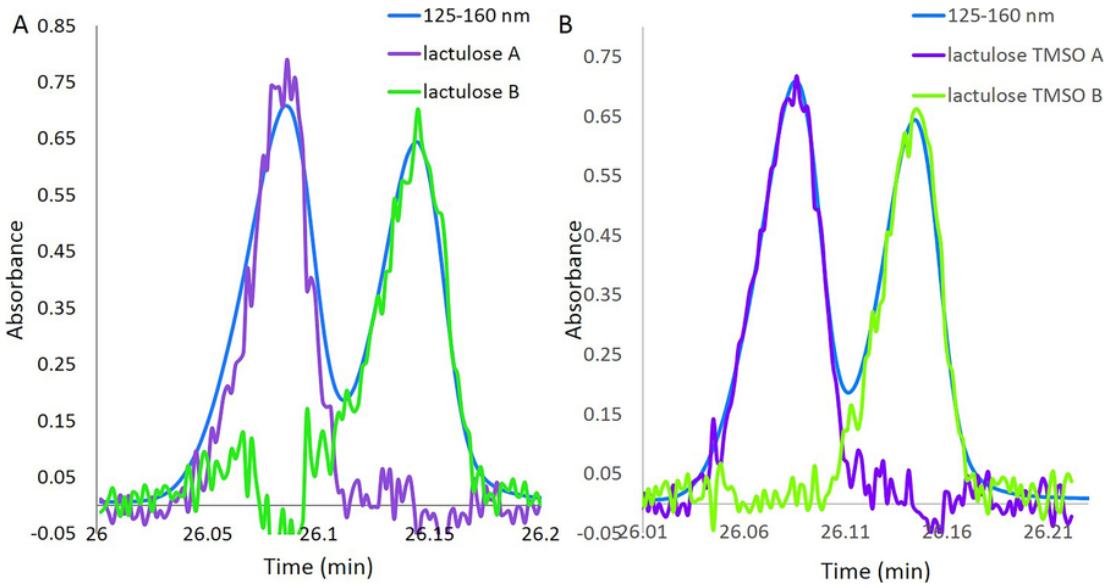

Figure 6.8 Deconvolutions performed on overlapping conformations of O/TMS-derived A) lactulose and B) turanose.

Disaccharides with common monomers were also compared for similarity in spectra by performing comparative SSR calculations. Sucrose (α-(1 → 2) linkage) and turanose (α-(1 → 3) linkage), containing glucose and fructose monomers, were compared visually according to their absorbance spectra in Fig. 6.9A and B for permethylated and O/TMS-derivatized compounds, respectively. The SSR calculation for the O/TMS derivatized analytes was performed and when turanose A was compared to itself, a small residual of 0.000136 was calculated. The next closest SSR spectra, turanose B, returned a residual of 0.00658 when compared to turanose A, indicating significant dissimilarity between the spectra for E- and Z-conformations. Sucrose was calculated to have the most dissimilar absorbance spectra of the compounds compared with turanose A and produced a residual of 0.257.

Next, the two compounds containing a galactose and glucose moiety, lactose (β −(1 → 4) linkage) and melibiose (α-(1 → 6) linkage), were compared according to their absorbance spectra, as shown in Fig. 6.9C and D for permethylated and O/TMS-derivatives, respectively. SSR calculations were carried out for the O/TMS derivatization method. Melibiose A was first compared to itself resulting in a residual value of 0.00268. Lactose A delivered the second closest SSR value to melibiose A with an SSR of 0.0108 indicating that it is the next closest spectra contained in the VUV library. For reference, when O/TMS-derivatized sucrose spectra are compared to 2,6-dimethylnaphthalene, an SSR of 212.97 is obtained.

Theoretical covariance analysis calculations allowed an estimate of the amounts of two compounds that can be deconvolved from one another.[35] Covariance calculations take into account how each compound is affected by the other due to similarity in spectra, analyte concentration, and amount on column, when the spectra are assumed to be overlapped. No additional experimental analysis is necessary if a registered cross-section for each analyte is present in the VUV library. A cross section is obtained by measuring a standard of known concentration and determining the number of molecules on column, under conditions of known injection volume, flow rate, sampling rate, and split ratio.[36] The output for covariance calculation is the standard deviation of the specified masses. In this case, covariance calculations were performed between an O/TMS-derivatized monosaccharide, glucose, and a disaccharide, sucrose. 10σ was chosen as the threshold to determine deconvolution conditions because it is roughly two to three times above the noise floor and estimated to be a suitable limit of quantitation (LOQ)

for these calculations. Calculations were performed with 19.6 ng of glucose and sucrose (50:50 ratio). The 10σ response for each was 0.259 ng (75:1) and 0.392 ng (50:1), respectively. The correlation factor was −0.988, indicating a strong correlation (although anti) between the two spectra (highest value +/−1), which indicates that the spectra are very similar. The covariance calculations are based on assumptions, due to error, in measured absorbance values and should only serve as an estimate in what to expect for the performance of the instrument's deconvolution capabilities.

For reference, when O/TMS-derivatized glucose and 2,6-dimethylnaphthalene are compared at a 50:50 ratio (19.6 ng of each on-column), a correlation factor of −0.657 was obtained. This shows that the spectra for the compounds are not strongly correlated. The 10σ response for glucose and 2,6-dimethylaphthalene was 34.8 pg (560:1) and 61.5 pg (150:1), respectively. Such a situation represents approximately an order of magnitude greater deconvolution capability than for the sucrose and glucose case. A sensitivity test was performed by analyzing a representative sample for the monosaccharides, glucose, and a representative for disaccharides, sucrose, at different concentrations until the response measured 3σ above the baseline. The concentration for glucose and sucrose was found to be 0.0392 ng on-column.

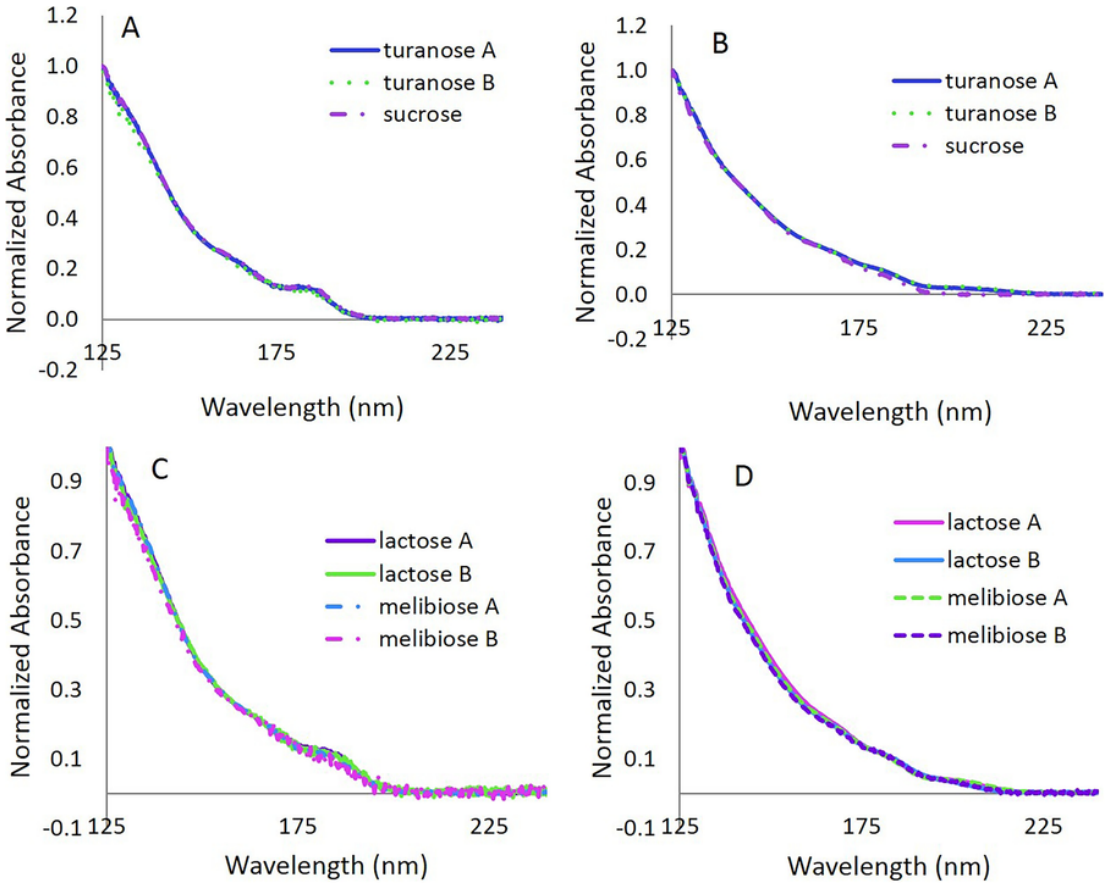

Figure 6.9 Absorbance spectra for sucrose and turanose with common monomers glucose and fructose compared using A) permethylation and B) O/TMS-derivatization methods. Absorbance spectra for lactose and melibiose with common monomers galactose and glucose compared using C) permethylation and D) O/TMS-derivatization methods.

6.4.5 Deconvolutions, sugar substitutes, and sugar detection

Mixed samples were prepared and analyzed by common elution time, taking into account common relative abundances in nature. Two mixtures were constructed for GC-VUV analysis: one that contained ribose, arabinose, and xylose and the other with glucose, galactose, and mannose. These two samples were derivatized by both methods and analyzed. Any peaks that contained multiple coeluting compounds were deconvolved as shown in Fig. 6.10; the results are tabulated in Tables 6.1 and 6.2. The permethylated sample of arabinose, xylose, and ribose seen in Fig. 6.10A

returned 11 peaks with a great deal of coelution. The O/TMS-derivatized example of the same analyte (Fig. 6.10B) showed only 3 distinct peaks for the three compounds with coelution in only ones of those peaks, which was routinely deconvolved. The amount on-column was computed and compared to the determined percent deconvolution, and their relative difference was calculated. The absolute difference was then divided by the amount on-column and these results were tabulated for the permethylated samples and O/TMS-modified samples in Tables 6.1 and 6.2, respectively. The relative average of differences for ribose, arabinose, and xylose had corresponding values of 0.4, 0.6, and 1.0 for permethylated and 0.3, 1.7, and 1.5 for O/TMS-derivatized forms, respectively.

The second sample containing glucose, mannose, and galactose yielded 6 peaks for the permethylated sample and 3 peaks for the O/ TMS sample (Fig. 6.10C and D, respectively). Out of the three peaks, two of them contained coelutions. The first peak, comprised of galactose and mannose, was readily deconvolved, but the peak that contained three coeluting compounds was challenging to deconvolute because of the similarity between the three spectra. Relative averages computed for glucose, galactose, and mannose returned values of 0.3, 0.4, and 0.5 for permethylated and 0.6, 0.4, and 1.5 for O/TMS-derivatized forms. With the O/TMS derivatization method, chromatograms were more straightforward to analyze because of fewer peaks for each analyte as compared to permethylation; both methods returned the same order of magnitude of error, with the permethylation method being slightly more accurate.

In order to probe the potential of GC-VUV in the determination of artificial sweeteners, a sample of sucralose, the most consumed artificial sweetener in the United States,[37] was derivatized by both permethylation and O/TMS, and subsequently analyzed (Fig. 6.11A and B, respectively). Note that sucralose itself is synthesized by replacement of three sucrose hydroxyl substituents with chlorine atoms. It was observed that the analytes are similar in absorbance spectral pattern but are still sufficiently distinct. One can note that the normalized spectra for the derivatized sucrose and sucralose overlap (touches or crosses) at some points; this is a good visual indication that the spectra are well differentiable with the VUV software. SSR were calculated to compare sucralose A to itself and the result returned a 0.00345 residual. The second highest match to sucralose A was sucrose, which was characterized by a SSR of 4.35, indicating that these analytes are easily differentiable based on VUV analysis.

Since GC-VUV proved successful in the analysis of the carbohydrate-based artificial sweetener sucralose, the proposed method was next tested for its suitability for the qualitative determination of carbohydrate content in three pharmaceutical products: the prescription medication Tri-Sprintec, Chloraseptic max lozenges, and over the counter apple cinnamon Theraflu. Sample preparation for extraction of the sugar, and solubility of the compound being analyzed, played a large role in which derivatization method was most suitable. Any method that utilized DMSO was better fit for per methylation and any method that used methanol was better applicable for O/TMS derivatization. Without the use of stringent anhydrous techniques, the solvent used in permethylation, DMSO, often contains enough water to hydrolyze

the hexamethyldisilazene reagent, thereby lowering yields of the trimethylsilyl ethers formed. Although the samples were concentrated under reduced pressure before derivatization, full removal of DMSO was challenging. The samples of prescription medication, Tri-Sprintec, and over the counter apple cinnamon Theraflu were more soluble in DMSO and therefore the samples were analyzed via permethylation. Tri-sprintec tablet analysis identified peaks for lactose A and lactose B as seen in Fig. 6.12A. The analysis of apple cinnamon Theraflu cold medicine, as shown in Fig. 6.12B, allowed for identification of a peak corresponding to sucrose and three other unknown peaks. The three other peaks were searched against the library and identified as permethylated raffinose (SSR = 0.00137), permethylated lactulose (SSR = 0.00141), and permethylated sucrose (SSR = 0.00583). Chloraseptic max lozenges were soluble in ethanol and consequently analyzed by O/TMS derivatization. GC-VUV analysis showed one large peak corresponding to sucrose (Fig. 6.11C).

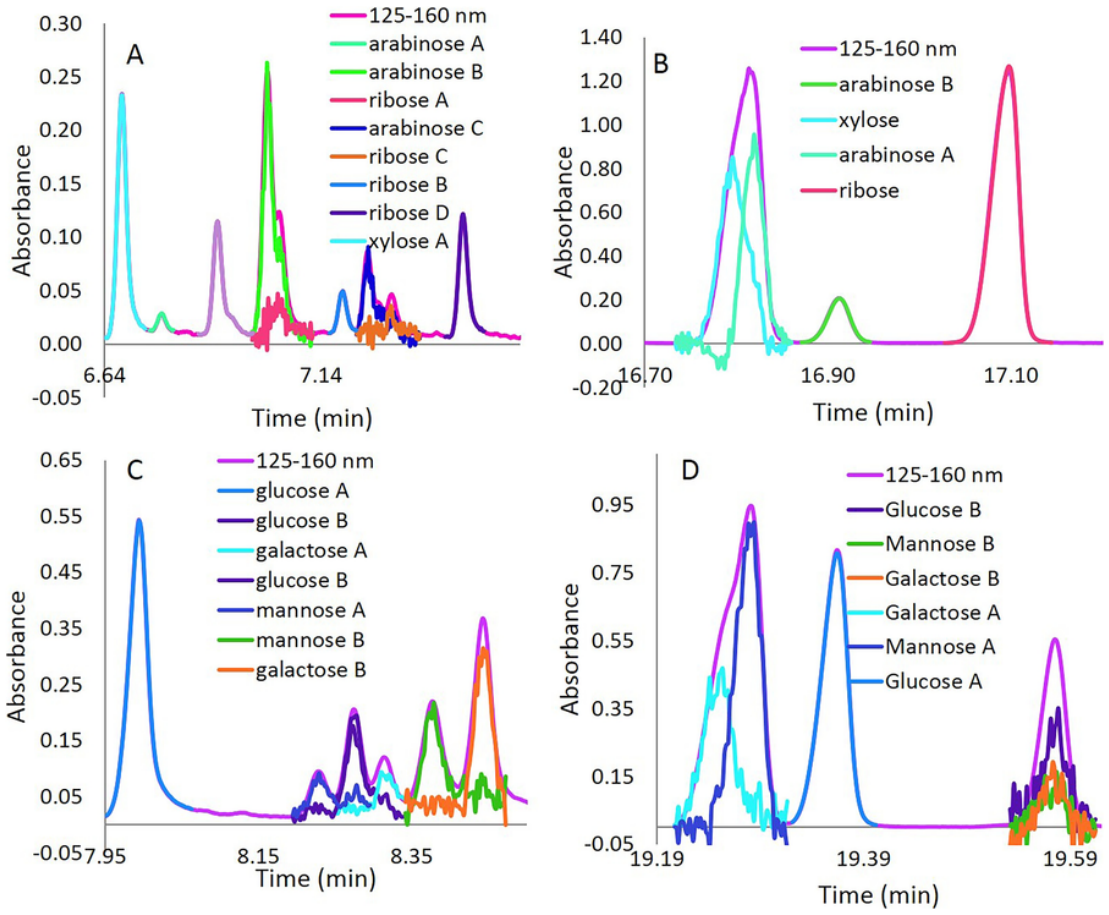

Figure 6.10 Deconvolutions performed on mixed samples of the aldopentoses arabinose, xylose, and ribose using A) permethylation and B) O/TMS-derivatization methods. Mixed samples of the aldohexoses glucose, galactose, and mannose deconvolved using C) permethylation and D) O/TMS-derivatization methods.

Table 6.1 Permethylated mixed sample deconvolution. Calculated amount on column and experimentally recovered percent after deconvolutions performed. Calculation of absolute difference between amount on column and deconvolution determined percent, absolute difference, and relative difference.

Permethylated		amount on column (ng)	determined (ng)	abs diff (ng)	relative difference (%)
1	glucose	59.0	58.1	0.9	1.5
	galactose	26.2	31.2	5.0	19
	mannose	26.4	23.2	3.2	12
2	glucose	35.6	30.7	4.9	14
	galactose	46.9	50.2	3.3	7.0
	mannose	32.1	33.6	1.5	4.6
3	glucose	33.9	29.1	4.8	14
	galactose	44.6	40.7	3.9	8.7
	mannose	24.8	33.5	8.7	35
1	ribose	31.9	35.9	4.0	13
	arabinose	45.1	48.9	3.8	8.4
	xylose	31.6	23.7	7.9	25
2	ribose	50.6	48.7	1.9	3.7
	arabinose	31.7	40.9	9.2	29
	xylose	30.8	22.7	8.1	26
3	ribose	29.6	37.7	8.1	28
	arabinose	28.1	35.8	7.7	27
	xylose	30.9	15.1	15.8	51

Table 6.2 TMSO mixed sample deconvolution. Calculated amount on column and experimentally recovered percent after deconvolutions performed. Calculation of absolute difference between amount on column and deconvolution determined percent, absolute difference, and relative difference.

TMSO		amount on column (ng)	determined (ng)	abs diff (ng)	relative difference (%)
1	glucose	39.4	28.6	10.8	28
	galactose	34.7	26.2	8.5	24
	mannose	27.6	46.9	19.3	70
2	glucose	37.5	33.5	4.0	11
	galactose	32.0	31.9	0.1	0.17
	mannose	39.9	56.9	17.0	43
3	glucose	31.7	25.6	6.1	19
	galactose	43.2	38.3	4.9	11
	mannose	26.5	37.5	11.0	42
1	ribose	25.2	23.9	1.3	5.3
	arabinose	23.2	42.5	19.3	83
	xylose	31.4	13.5	17.9	57
2	ribose	32.9	39.7	6.8	21
	arabinose	25.2	30.4	5.2	21
	xylose	35.9	23.9	12.0	34
3	ribose	24.5	24.4	0.1	0.46
	arabinose	24.9	41.7	16.8	67
	xylose	30.3	13.5	16.8	55

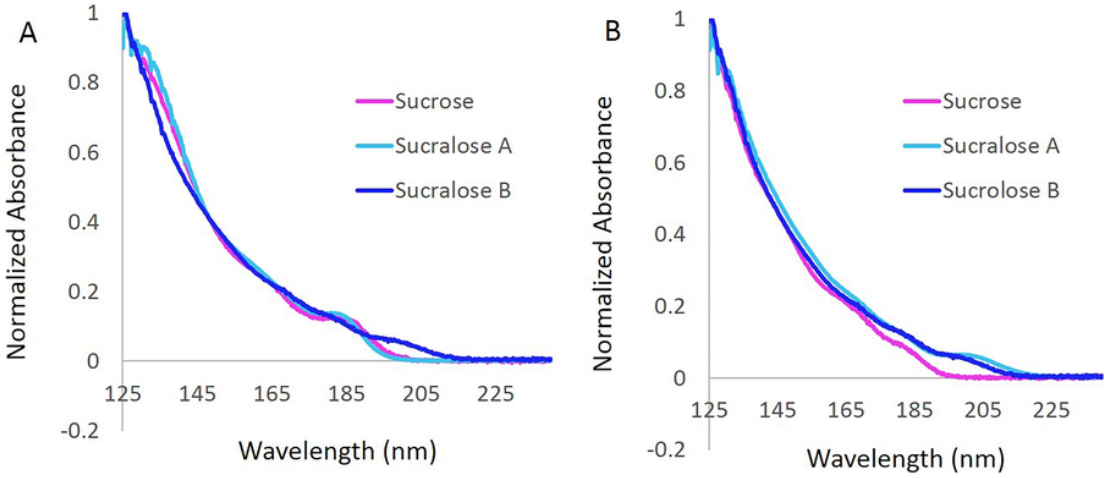

Figure 6.11 Comparison of absorbance spectra between sucralose and sucrose using A) permethylation and B) O/TMS derivatization techniques.

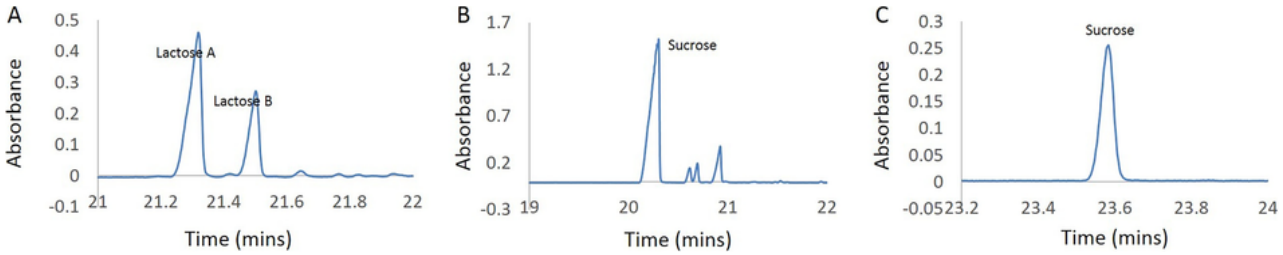

Figure 6.12 Pharmaceuticals tested for their carbohydrate content: A) Permethylated Tri-Sprintec tablets; B) permethylated Theraflu; and C) O/TMS-derivatized Chloraseptic Max Lozenges.

6.5 Conclusions

Herein it has been demonstrated that GC-VUV, in combination with various derivatization techniques, is capable of the differentiation of mixtures of carbohydrate isomers based on compound-specific ab- sorption spectra. Due to the inherent structural similarity amongst various carbohydrate isomers, the ability to resolve and deconvolve complex saccharide mixtures present a distinct advantage of this herein presented GC-VUV methodology over reported mass spectrometry techniques. In comparison to the commonly used GC–MS method for carbohydrate analysis, this described GC-VUV protocol has the major advantage of producing unique, characteristic compound spectra. The GC–MS technique is hindered by its inability to distinguish compounds with very close or identical fragmentation patterns, especially when compounds coelute. By using VUV we can now see coeluting compound distinction between the carbohydrate isomers at an appreciable level. Deconvolutions could be performed for compounds that coeluted, given pure absorption spectra could be obtained, closing the gap on a missing feature in previous techniques for carbohydrate analysis. This method provides valuable information for complex samples with multiple saccharides coeluting that may go unnoticed when GC–MS is used.

The two different derivatization methods examined proved to be useful in various situations. Permethylation proved to be a valid method for the analysis of ketopentoses and medications soluble in DMSO, whereas the O/TMS-derivatization method proved to be the more promising method overall. Idose had the shortest retention time for the O/TMS-derivatization method while glucose had the shortest

retention time for the permethylation method. These two compounds are diastereomers, with D-glucose having equatorial hydroxyl (OH groups) at carbons C-2, C-3, and C-4, while D-idose has all axial OH groups at C-2, C-3, and C-4. This suggests that the ring opening re- action has a large effect on the retention index for the idose configuration. Enantiomeric differentiation of these carbohydrate isomers is a proposed future direction, perhaps through the use of chiral derivatization agents or chiral stationary phases.

This presented work provides the first time that carbohydrates of any kind have been analyzed with a GC-VUV system. It has clearly demonstrated that challenging analytes existing in multiple solution-phase stereochemical configurations, as well as only having minor structural differences amongst their axial/equatorial OH group positioning, are amenable to analysis by this presented technique. This method is potentially suitable for a wide variety of fields, including the food and pharmaceutical industries. The wide breadth of analytes studied illustrates that the methodology is applicable to a range of carbohydrates, varying in their hydroxyl group orientation, as well as monosaccharide constituents and glycosidic linkages in di/ tri-saccharides. The quantitative and qualitative analysis of complex carbohydrate mixtures is indeed attainable, even for coeluting isomers.

Conflict of interest

Disclaimer: KAS is a member of the Scientific Advisory Board for VUV Analytics, Inc.

Uncited reference

[17].

Acknowledgements

Support for this work was provided by VUV Analytics, Inc. Joan and Marvin Carmack

Chair funds for partial support of this work (N.L.B.P) and the Joan and Marvin

Carmack Chair fund graduate fellowship (G.N.) are also acknowledged.

6.6 References

1. G. Nagy, N.L.B. Pohl, Complete hexose isomer identification with mass spectrometry, J. Am. Soc. Mass Spectrom. 26 (2015) 677–685.
2. H. Liu, L. Zhao, L. Fan, L. Jiang, Y. Qiu, Q. Xia, J. Zhou, Establishment of a nanofiltration rejection sequence and calculated rejections of available monosaccharides, Sep. Technol. 163 (2016) 319–330.
3. J.R. Bergquist, C.A. Puig, C.R. Shubert, R.T. Groeschl, E.B. Habermann, M.L. Kendrick, D.M. Nagorney, R.L. Smoot, M.B. Farnell, M.J. Truty, Carbohydrate antigen 19-9 elevation in anatomically resectable: early-stage pancreatic cancer is independently associated with decreased overall survival and an indication for neoadjuvant therapy: a national cancer database study, J. Am. Coll. Surg. 233 (2016) 52–65.
4. T. Dingjan, I. Spendlove, L.G. Durrant, A.M. Scott, E. Yuriev, P.A. Ramsland, Structural biology of antibody recognition of carbohydrate epitopes and potential uses for targeted cancer immunotherapies, Mol. Immunol. 67 (2015) 75–88.
5. X. Zhang, W. Lu, J. Shen, Y. Jiang, E. Han, X. Dong, J. Huang, Carbohydrate derivative-functionalized biosensing toward highly sensitive electrochemical detection of cell surface glycan expression as cancer biomarker, Biosens. Bioelectron. 74 (2015) 291–298.
6. G. Nagy, N.L.B. Pohl, Monosaccharide identification as a first step toward de novo carbohydrate sequencing: mass spectrometry strategy for the identification and differentiation of diastereomeric and enantiomeric pentose isomers, Anal. Chem. 87 (2015) 4566–4571.
7. J.D. Oliver, M. Gaborieau, E.F. Hilder, P. Castignolles, Simple and robust determination of monosaccharides in plant fibers in complex mixtures by capillary electrophoresis and high performance liquid chromatography, J. Chromatogr. A 1291 (2013) 179–186.
8. D.P. Ward, M. Cárdenas-Fernández, P. Hewitson, S. Ignatova, G.J. Lye, Centrifugal partition chromatography in a biorefinery context: separation of monosaccharides from hydrolysed sugar beet pulp, J. Chromatogr. A 1411 (2015) 84–91.
9. M.M. Gaye, G. Nagy, N.L.B. Pohl, D.E. Clemmer, Multidimensional analysis of 16 glucose isomers by ion mobility spectrometry, Anal. Chem. 88 (2016) 2344–2355.
10. K.A. Schug, I. Sawicki, D.D. Carlton, H. Fan, H.M. McNair, J.P. Nimmo, P. Kroll, J. Smuts, P. Walsh, D. Harrison, Vacuum ultraviolet detector for gas chromatography, Anal. Chem. 86 (2014) 8329–8335.

11. J. Schenk, J.X. Mao, J. Smuts, P. Walsh, P. Kroll, K.A. Schug, Analysis and deconvolution of dimethylnaphthalene isomers using gas chromatography vacuum ultraviolet spectroscopy and theoretical computations, Anal. Chimica Acta 945 (2016) 1–8.
12. L. Bai, J. Smuts, P. Walsh, H. Fan, Z. Hildenbrand, D. Wong, D. Wetz, K.A. Schug, Permanent gas analysis using gas chromatography with vacuum ultraviolet detection, J. Chromatogr. A 1388 (2015) 244–250.
13. H. Fan, J. Smuts, P. Walsh, D. Harrison, K.A. Schug, Gas chromatography–vacuum ultraviolet spectroscopy for multiclass pesticide identification, J. Chromatogr. A 1389 (2015) 120–127.
14. H. Fan, J. Smuts, L. Bai, P. Walsh, D.W. Armstrong, K.A. Schug, gas chromatography – vacuum ultraviolet spectroscopy for analysis of fatty acid methyl esters, Food Chem. 194 (2016) 265–271.
15. C.A. Weatherly, Y. Zhang, J.P. Smuts, H. Fan, C. Xu, K.A. Schug, J.C. Lang, D.W. Armstrong, Analysis of long-chain unsaturated fatty acids by ionic liquid gas chromatography, J. Agric. Food Chem. 64 (2016) 1422–1432.
16. C. Qiu, J. Smuts, K.A. Schug, Analysis of terpenes and turpentines using gas chromatography with vacuum ultraviolet detection, J. Sep. Sci. 40 (2017) 869–877.
17. B.M. Weber, P. Walsh, J.J. Harynuk, Determination of hydrocarbon group-type of diesel fuels by gas chromatography with vacuum ultraviolet detection, Anal. Chem. 88 (2016) 5809–5817.
18. T.M. Groeger, B. Gruber, D. Harrison, M.R. Saraji-, M. Mthembu, A.C. Sutherland, R. Zimmermann, A fast vacuum ultraviolet absorption array spectrometer as a fast and selective detector for comprehensive two-dimensional gas chromatography: concept and first results, Anal. Chem. 88 (2016) 3031–3039.
19. P. Walsh, M. Garbalena, K.A. Schug, Rapid analysis and time interval deconvolution for comprehensive fuel compound group classification and speciation using gas chromatography – vacuum ultraviolet spectroscopy, Anal. Chem.
88 (2016) 11130–11138.
20. C. Qiu, J. Cochran, J. Smuts, P. Walsh, K.A. Schug, Gas chromatography-vacuum ultraviolet detection for classification and speciation of polychlorinated biphenyls in industrial mixtures, J. Chromatogr. A 1490 (2017) 191–200.
21. I. Ciucanu, Per-O-methylation reaction for structural analysis of carbohydrates by mass spectrometry, Anal. Chim. Acta 576 (2006) 147–155.
22. I. Ciucanu, F. Kerek, A simple and rapid method for the permethylation of carbohydrates, Carbohydr. Res. 131 (1984) 209–217.
23. M.L. Sanz, J. Sanz, I. Martínez-Castro, Gas chromatographic–mass spectrometric method for the qualitative and quantitative determination of disaccharides and trisaccharides in honey, J. Chromatogr. A 1059 (2004) 143–148.
24. G. Peterson, Gas-chromatographic analysis of sugars and related hydroxy acids as acyclic oxime and ester trimethylsilyl derivatives, Carbohydr. Res. 33 (1974) 47–61.

25. A.I. Ruiz-Matute, O. Hernández-Hernández, S. Rodríguez-Sánchez, M.L. Sanz, I. Martínez-Castro, Derivatization of carbohydrates for GC and GC–MS analyses, J. Chromatogr. B 879 (2011) 1226–1240.
26. I. Molnár-Perl, K. Horváth, Simultaneous quantitation of mono-: di-and trisaccharides as their TMS ether oxime derivatives by GC–MS: I. In model solutions, Chromatographia 45 (1997) 321–327.
27. M. Brokl, A.C. Soria, I. Martínez-Castro, M.L. Sanz, A.I. Ruiz-Matute, Characterization of O-trimethylsilyl oximes of trisaccharides by gas chromatography–mass spectrometry, J. Chromatogr. A 1216 (2009) 4689–4692.
28. S. Kurz, K. Aoki, C. Jin, N.G. Karlsson, M. Tiemeyer, I.B.H. Wilson, K. Paschinger, Targeted release and fractionation reveal glucuronylated and sulphated N- and O-glycans in larvae of dipteran insects, J. Proteomics 126 (2015) 172–188.
29. I. Molnár-Perl, Role of chromatography in the analysis of sugars: carboxylic acids and amino acids in food, J. Chromatogr. A 891 (2000) 1–32.
30. G. Peterson, Gas-chromatographic analysis of sugars and related hydroxy acids as acyclic oxime and ester trimethylsilyl derivatives, Carbohydr. Res. 33 (1974) 47–61.
31. M.A. Adams, Z. Chen, P. Landman, T.D. Colmer, Simultaneous determination by capillary gas chromatography of organic acids sugars, and sugar alcohols in plant tissue extracts as their trimethylsilyl derivatives, Anal. Biochem. 266 (1999) 77–84.
32. W. Funcke, C. von Sonntag, Syn and anti-forms of some monosaccharide O-methyl oximes: a ^{13}C-n.m.r. and g.l.c. study, Carbohydr. Res. 69 (1979) 247.
33. V. Kräutler, M. Müller, P.H. Hünenberger, Conformation, dynamics, solvation and relative stabilities of selected ß-hexopyranoses in water: a molecular dynamics study with the gromos 45A4 force field, Carbohyd. Res. 342 (2007) 2097–2124.
34. L. Skultety, P. Frycak, C. Qiu, J. Smuts, L. Shear-Laude, K. Lemr, J.X. Mao, P. Kroll, K.A. Schug, A. Szewczak, C. Vaught, I. Lurie, V. Havlicek, Resolution of isomeric new designer stimulants using gas chromatography – vacuum ultraviolet spectroscopy and theoretical computations, Anal. Chim. Acta 971 (2017) 55–67.
35. W.H. Press, S.A. Teukolsky, W.T. Vetterling, B.P. Flannery, Numerical Recipes in C: The Art of Scientific Computing, second ed., Cambridge University Press, 1992.
36. L. Bai, J. Smuts, C. Qiu, P. Walsh, H.M. McNair, K.A. Schug, Pseudo-absolute quantitative analysis using gas chromatography – vacuum ultraviolet spectroscopy – a tutorial, Anal. Chim. Acta 953 (2017) 10–22.
37. A.C. Sylvetsky, K.I. Rother, Trends in the consumption of low-calorie sweeteners, Physiol. Behav. 164 (2016) 446–450.

6.7 SUPPLEMENTARY INFORMATION

Identification and Deconvolution of Carbohydrates using Gas Chromatography- Vacuum Ultraviolet Spectroscopy

Jamie Schenk,[1] Gabe Nagy,[2] Nicola L. B. Pohl,[2] Jonathan Smuts,[3] Allegra Leghissa,[1] Kevin A. Schug[1*]

1. Department of Chemistry & Biochemistry, The University of Texas at Arlington, Arlington, Texas 76019, US

2. Department of Chemistry, Indiana University, Bloomington, Indiana 47405, US

3. VUV Analytics, Inc., Cedar Park, Texas VUV Analytics, Inc., Cedar Park, Texas 78613, US

Contents:
Structures of derivatized sugar analytes

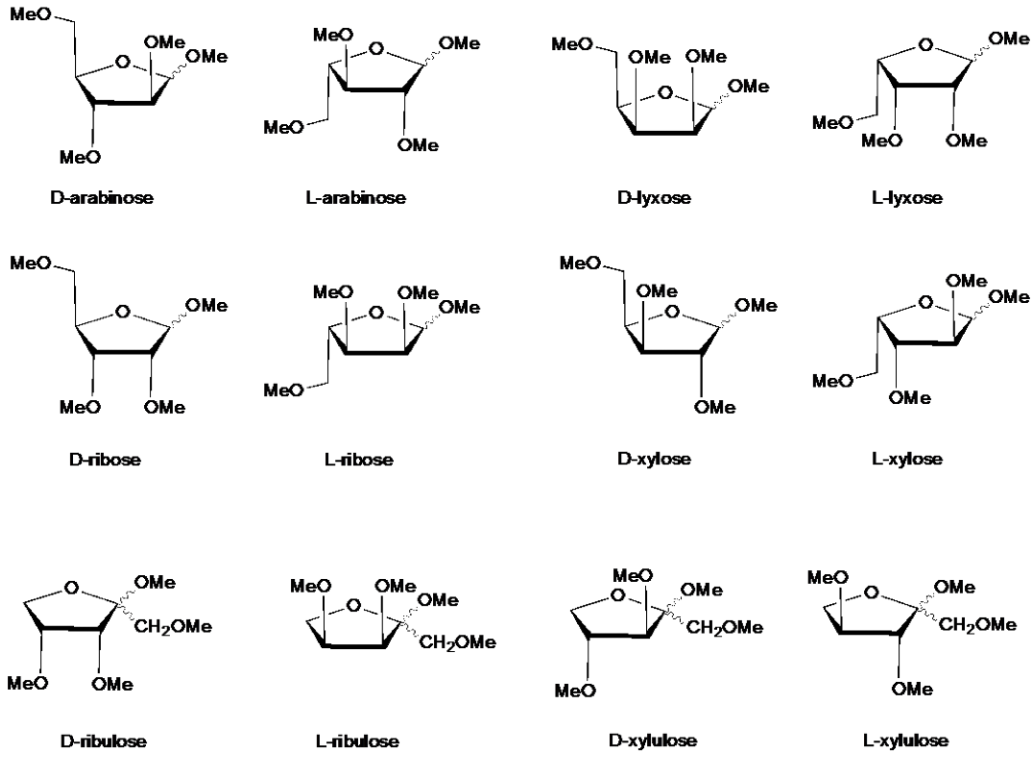

Figure 6S1. Permethylated aldopentoses and ketopentoses

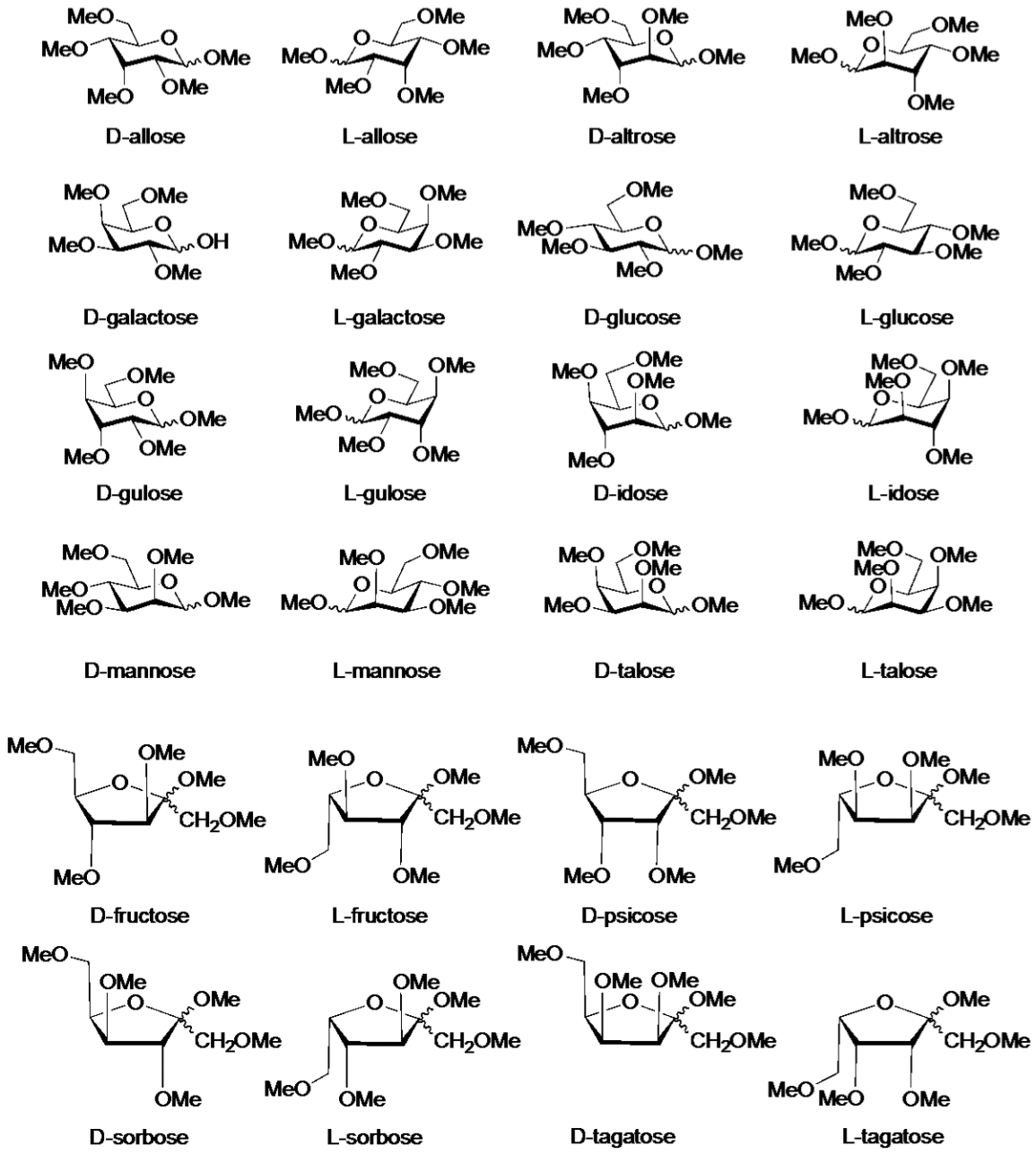

Figure 6S2. Permethylated aldohexoses and ketohexoses

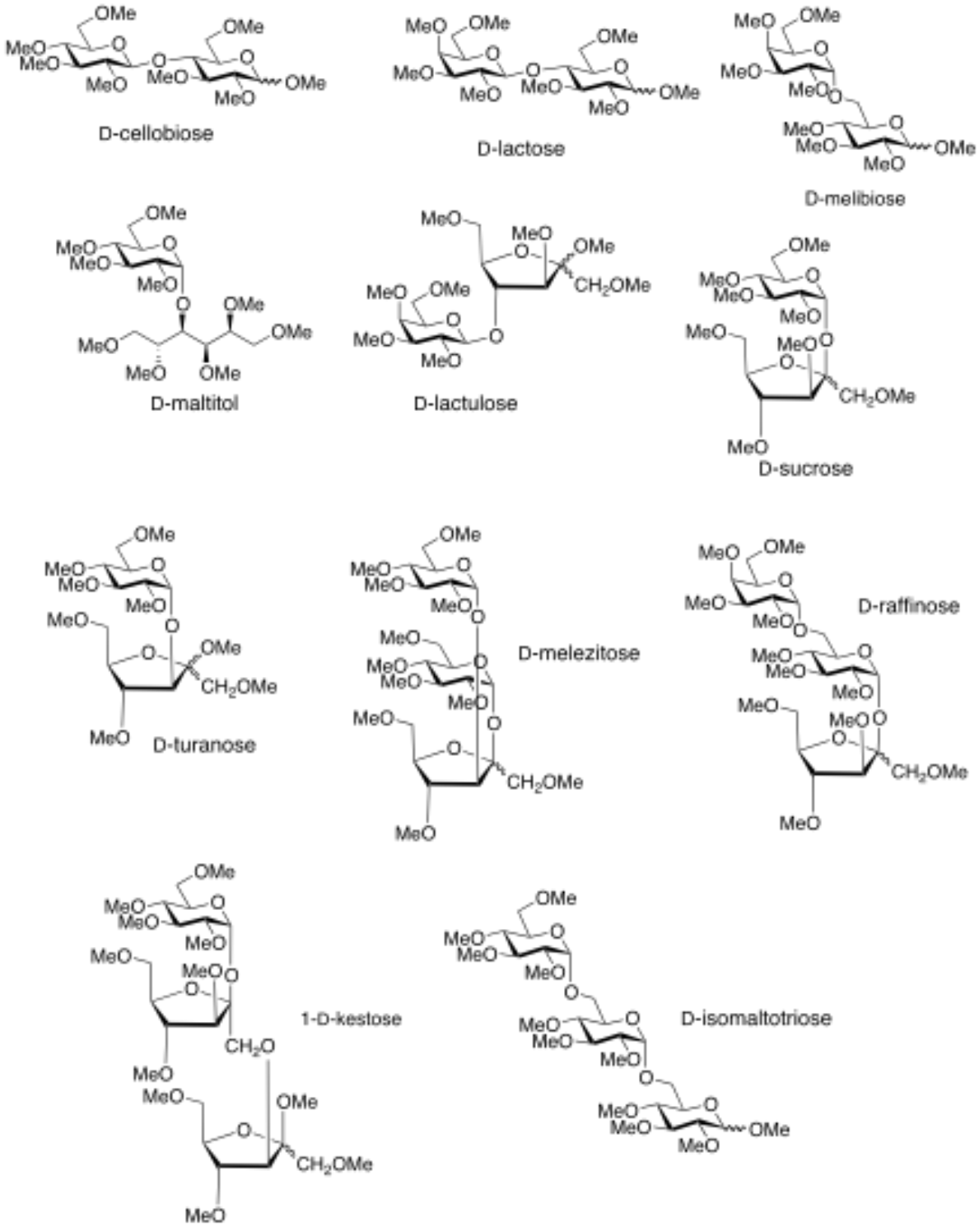

Figure 6S3. Permethylated disaccharides and trisaccharides

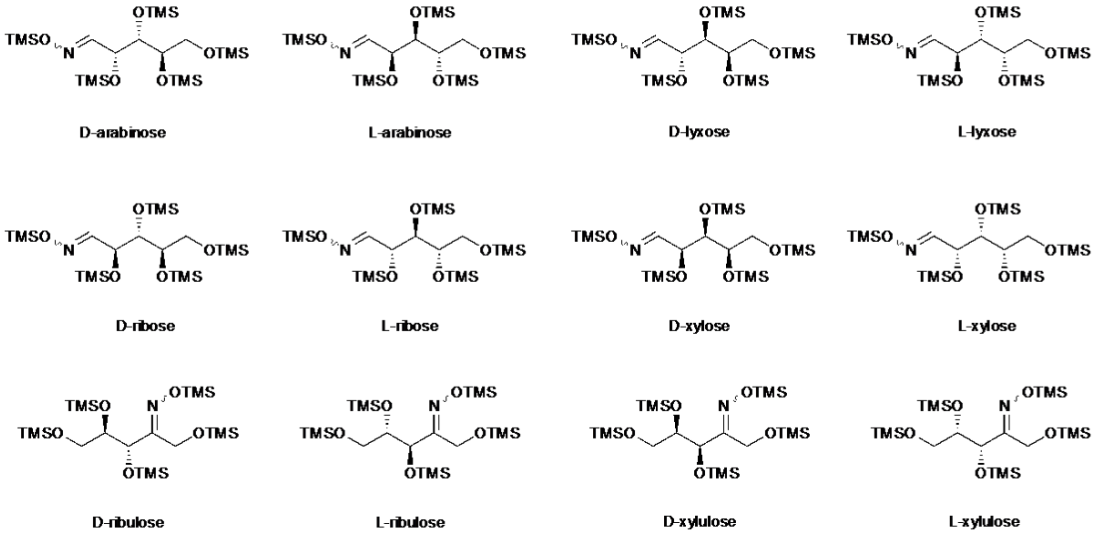

Figure 6S4. TMSO aldopentoses and ketopentoses

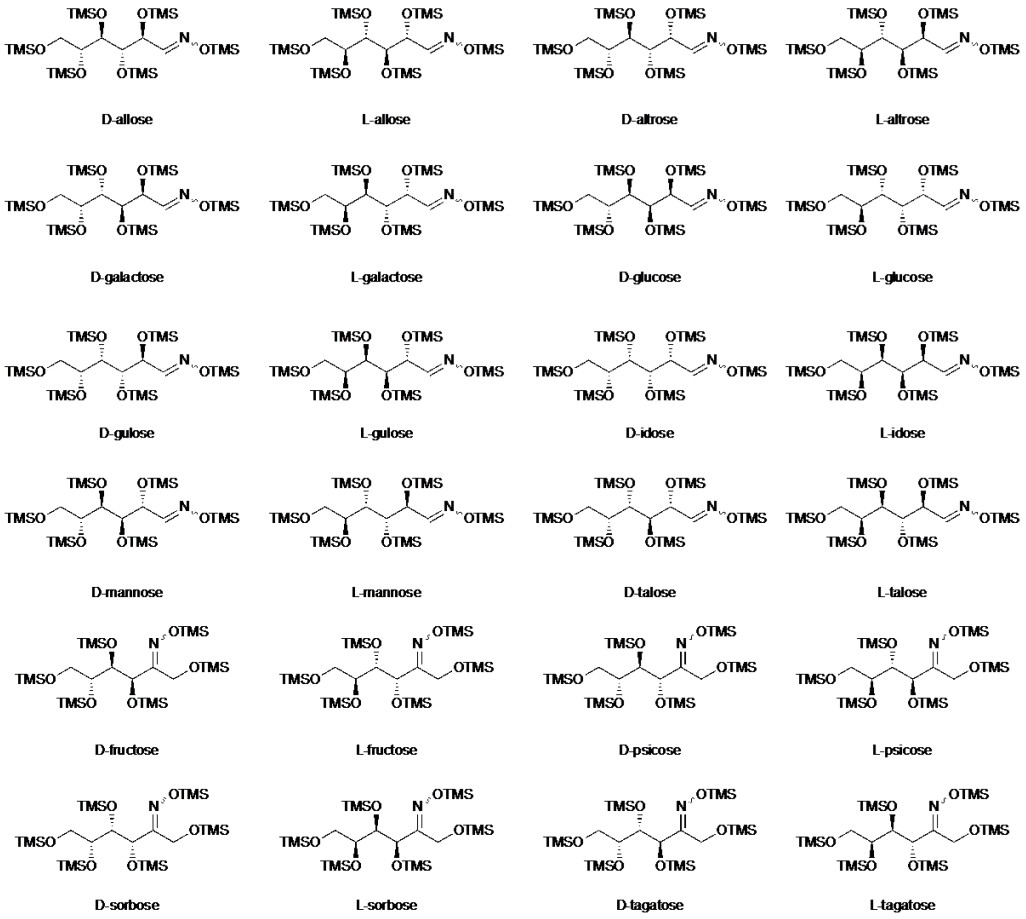

Figure 6S5. TMSO-derivatized aldohextoses and ketohexoses

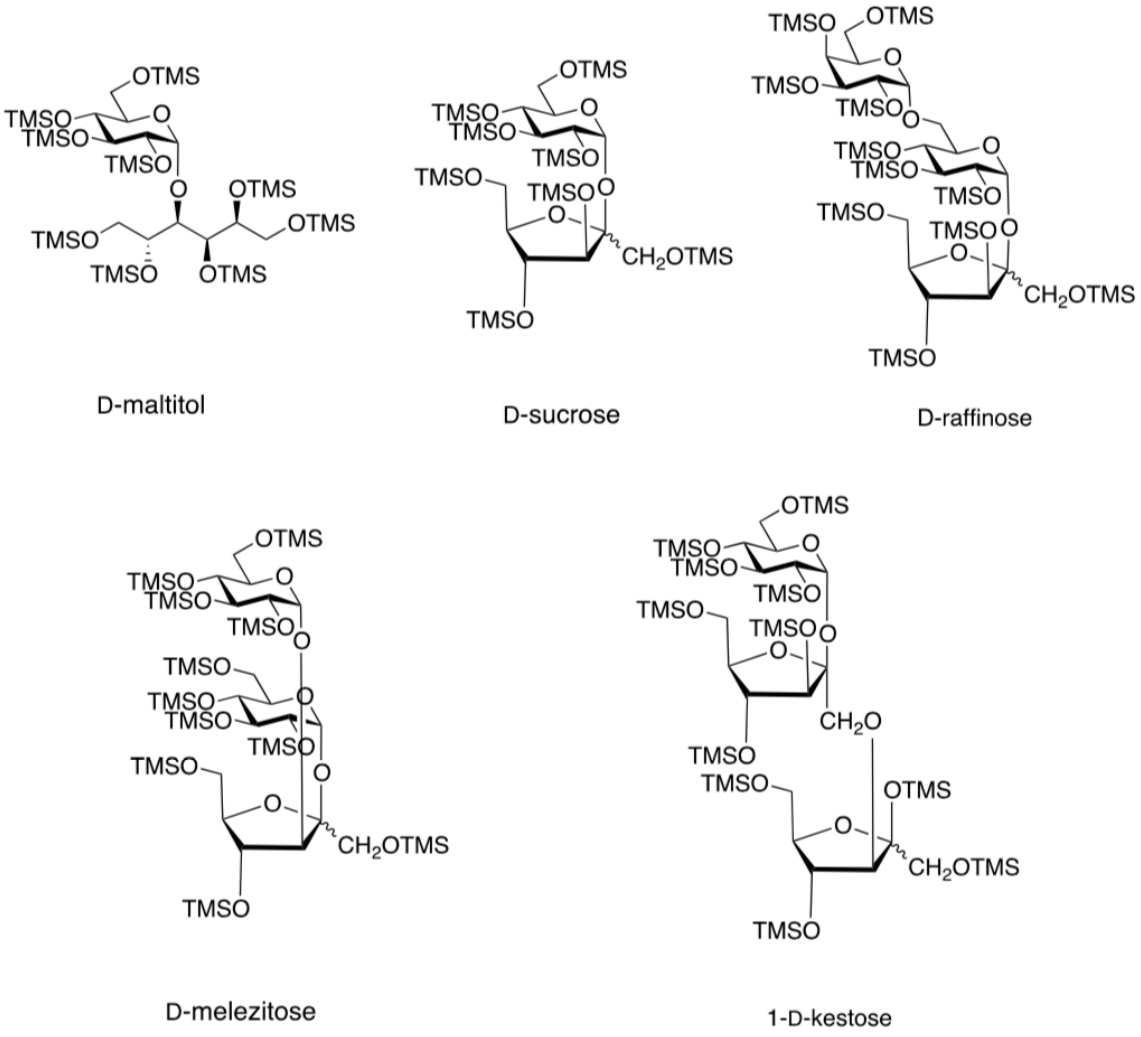

Figure 6S6. TMSO-derivatized non-reducing disaccharide and trisaccharide sugars

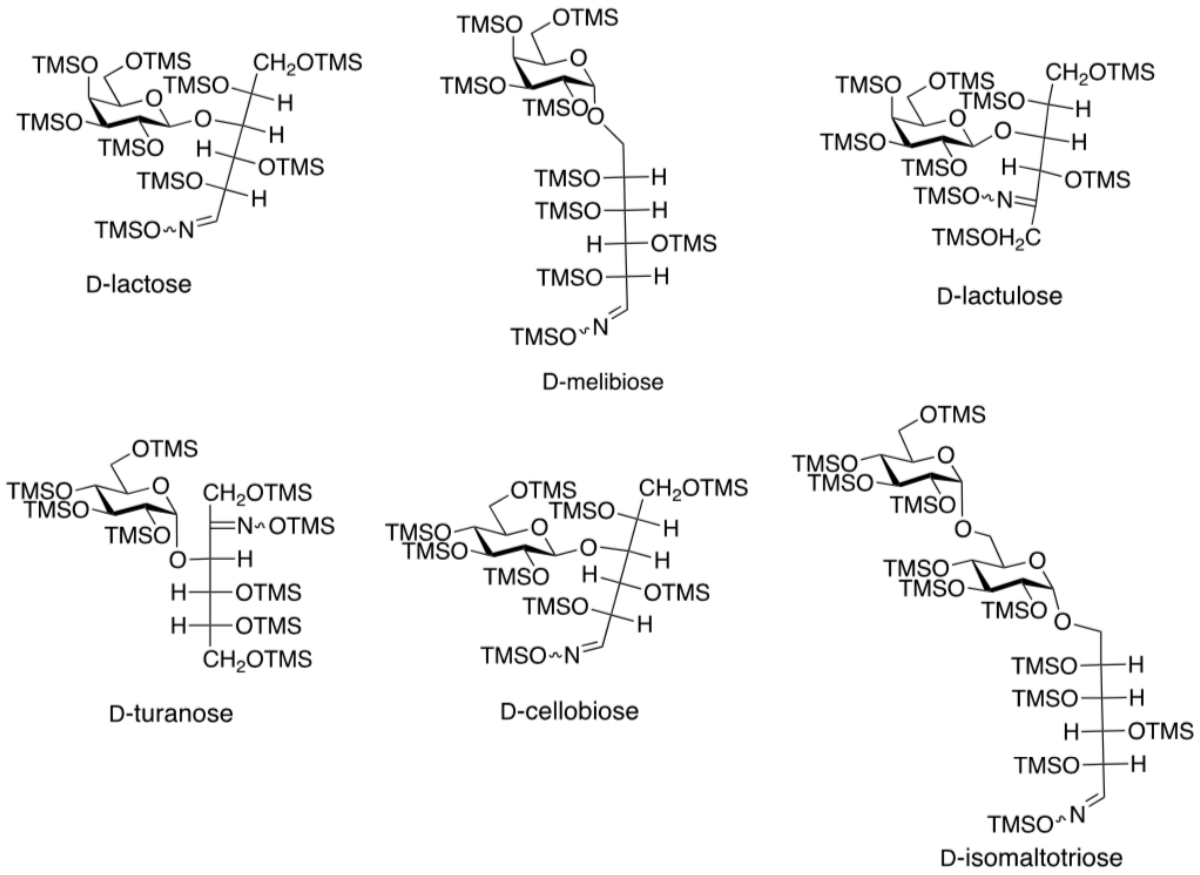

Figure 6S7. TMSO-derivatized reducing disaccharide and trisaccharide sugars.

CHAPTER SEVEN: Challenges associated with multi-compound class analysis in a complex food matrix: hormones, fat-soluble vitamins, and mycotoxin content in egg yolk by LC-MS/MS and correlation to hens living and feeding conditions

Jamie L. York,[1] Robert H. Magnuson II,[1] Kevin A. Schug[1*]

[1]Department of Chemistry and Biochemistry, The University of Texas at Arlington, Arlington, TX, USA

7.1 Abstract

Various types of chicken eggs are available in markets in the US and include eggs from cage, cage-free, free-range, and pasture-raised hens. Herein, the contents of hen egg yolk from various sources are examined for their mycotoxin, naturally occurring hormone, and fat-soluble vitamin content. These were quantified to correlate how their living conditions effect the contents of the egg. A method was developed for the multi-class analysis of egg yolk using a simple dilute and shoot sample preparation process coupled with on-line sample clean-up using a restricted access media column in line with LC-MS/MS. This methodology allows for quick and easy sample preparation and high throughput. While there are some limitations, the method displayed good linearity (R^2>0.99), with appropriate limits of detection (0.05-10 ng/g) and limits of quantitation (0.15- 30 ng/g) for all analytes tested. Overall, it was discovered that the hen's diet, rather than living conditions, had the greatest effects on the contents of the eggs, especially in the case of fat-soluble vitamin and mycotoxin content. Egg yolk has proven to be a very challenging complex matrix with many caveats to consider but overall, some dissimilarity was discovered in the various chicken eggs tested that distinguished the eggs based on their origins.

Keywords: LC-MS/MS, egg yolk, restricted access media, protein precipitation, standard addition

7.2 Introduction

Concerns for livestock welfare has allowed a window of opportunity for agricultural companies to sell the same product with multifarious marketing angles. Chicken eggs are no exception to this, and virtually all grocery stores in the United States offer a selection of egg products originating from hens from a variety of living conditions including caged, cage-free, free-range, and pasture-raised. In the US, the United States Department of Agriculture (USDA) oversees and stipulates the guidelines for hens living conditions. Although there are some terms the USDA does not enforce, secondary certifications such as “United Egg Producers” or “Certified Humane” can ensure that the guidelines set by the USDA are followed by the farmers .

There are various types of eggs that are available in grocery stores originating from different hen living conditions. Caged hen eggs typically do not require “caged” labeling on the carton. These hens are housed indoors in cages and, to be United Egg Producers Certified, the cages used must measure 67-86 square inches.[1] Cage-free eggs are defined as coming from hens that are housed indoors and have a minimum of 1-1.5 square feet per chicken of floor space.[1] Free-range chickens are defined by the USDA as hens that have access to the outdoors. This can sometimes be misleading, as in some cases, hens only have access to the outdoors for their head through a window and not full body access.[2] Secondary certification such as “Certified Humane” requires 2 square feet per bird. Further, they must have at least 6 hours outdoors per day, weather permitting, if they want to be considered as free-range.[2] Pasture-raised hens typically have at least 108 square

feet per bird to roam around.[2] This guideline is not regulated by the USDA, but can be validated if the eggs are certified by a secondary party, such as “Certified Humane”.

Eggs are an extremely complex matrix that contain many different compounds that can be of interest. Egg yolk has been reported to be composed of plasma, lipids, proteins, carbohydrates, fat-soluble vitamins, water-soluble vitamins, minerals, carotenoids, and amino acids.[3] Previously reported methods employ different sample preparation techniques, even for the same classes of compounds. In one example where free progesterones were targeted in eggs, sample preparation included the use of matrix solid-phase dispersion (MSPD) and further clean-up by solid-phase extraction (SPE) followed by subsequent analysis by LC-MS/MS.[4] In other methods investigating steroids in eggs, acetonitrile was used for extraction followed by zinc chloride addition to remove phospholipids, and additional clean-up by SPE before analysis by LC-MS/MS.[5,6] Zeng et al also targeted steroids in eggs and sample preparation included freeze-lipid filtration and liquid-liquid extraction before analysis on an LC-MS/MS.[7] In other research looking at mycotoxins, sample preparation included QuEChERS followed by analysis using LC-MS/MS.[8] For fat-soluble vitamins, one example of sample preparation includes multiple saponifications followed by extraction with solvent before being analyzed by HPLC using a fluorescence detector to detect Vitamin E isomers in food stuff, including eggs.[9] These examples all require laborious sample preparation techniques that can hinder throughput and become cumbersome for large sample

sets and there has yet to be a method reported for a multiclass compound analysis for these three classes.

Restricted access media (RAM) columns can allow for automation of sample clean-up of small molecules from macromolecules. The basic principle of RAM columns is somewhat analogous to size-exclusion chromatography. Sorbents can selectively extract small molecules due to the size of pores and the type of stationary phase contained in the pores (reversed phase, normal phase, anion exchange, cation exchange, etc.).[10] The most common types of sorbents include polymers, carbon nanotubes, and silica.[11] The external surfaces of these sorbents is modified with a hydrophilic group thus providing a non-retentive outer surface layer.[11] The non-retentiveness of the outer layer, size of pores, and type of stationary phase bound inside the pore allow for automated on-line sample clean-up of large biomolecule interferences from small molecule analytes.

The goal of these experiments was to perform a simplified version of sample preparation to investigate the ability to take sample preparation online using a restricted access media column. In this study, eggs that were from home raised, free-range, cage-free, and pasture-raised hens were compared to hens that were caged to determine if their contents had any effect on the way that these animals were raised with respect to their fat-soluble vitamin, hormone, and mycotoxin content. These experiments were performed using a RAM column for on-line sample clean-up to automate sample preparation before being analyzed by LC-MS/MS.

7.3 Materials and Methods

7.3.1 Samples and Reagents

Standards for retinol, all-trans retinal, retinoic acid, cholecalciderol (D3), ergocalciferol (D2), y-tocopherol, α-tocopherol, menatetrenone (MK4), β-estradiol, α-estradiol, estrone, cholesterol, progesterone, estriol, pregnenolone acetate, aflatoxin B1, aflatoxin B2, aflatoxin G1, aflatoxin G2, beauvericin, D3(6,19,19-d_3), progesterone-d_9, pregnolone-20, 21-$^{13}C_2$-16,16-d_2, cholesterol-2-3-4-$^{13}C_3$, 17β-estradiol-16,16,17-d_3, estrone-2,3,4-$^{13}C_3$, α-tocopherol-d_9, D2(6,19,19-d_3), and dextran-coated charcoal were purchased from Sigma-Aldrich (St. Louis, MO). Standards vitamin K1, 5α-dihydrotestosterone (DHT), androstenedione, dehydroepiandrosterone (DHEA), testosterone, androstane-3,17-dione-23,4-$^{13}C_2$, and 5α-dihydrotestosterone-d_3 were purchased from Cerilliant (Round Rock, TX). Mobile phase additives formic acid and ammonium formate were purchased from Sigma-Aldrich. LC-MS grade solvents water and methanol were purchased from Honeywell Burdick & Jackson (Muskegon, MI). Acetone was purchased from VWR (Radnor, PA). Dispersive solid phase extraction (dSPE) tubes were purchased from Restek (Bellefonte, PA) (catalog number 26219).

7.3.2 Preparation of Standard Solutions

Working standards were made up at 1 mg/mL, with the exception of cholesterol (200 mg/mL) and retinol (50 mg/mL). Progesterone, D2, and D3 working standards were made up in ethanol; pregnenolone was prepared in methanol. All other fat-soluble vitamins, hormones, cholesterol, and mycotoxins were diluted with chloroform. Working standards were kept in amber vials to prevent photosensitive

compounds from degrading and stored in the freezer. Standards were diluted with acetone to desired concentration. Structures for analytes can be found in Figure 7S1 of the supplementary information.

7.3.3 Preparation of Samples for LC-MS/MS

All eggs were purchased at the local market, except the eggs from chickens that were home raised and were collected from two local homeowners. Eggs were purchased/acquired and numbered in the following order: 1. Cage-free pasteurized grade AA; 2. Caged grade A; 3. Home raised; 4. Caged vegetarian fed grade A; 5. Free-range grade A; 6. Caged grade A; 7. Pasture-raised grade A; 8. Free-range organic grade A; 9. Pasture-raised organic soy-free grade A; 10. Cage-free grain fed grade A; 11. Cage-free grade AA; 12. Pasture-raised organic grade A; 13. Cage-free omega-plus grade AA; and 14. Home raised. Six egg yolks of the same source were pooled and homogenized by vortexing. For recovery experiments and LOD/LOQ determination one egg yolk from each egg (14 total) was taken to pool the samples and homogenized. Samples were prepared in amber 2 mL microcentrifuge tubes to prevent photodegradation of any compounds. The previously reported value for density of egg yolk[12] was used to calculate the equivalence of 300 µL of egg yolk in milligrams to add to the microcentrifuge tubes. 307.5 ± 5 mg of homogenized yolk was measured into microcentrifuge tubes and prepared for analysis by spiking with standards and diluting to a total volume of 1 mL with ice cold acetone. For recovery experiments, egg samples were spiked with concentrations of standard onto the egg yolk and diluted to their final volume (1 mL) with acetone to facilitate precipitation of proteins. The sample was vortexed then spun down in a centrifuge at 14,000 RPM

for 10 min before the supernatant was transferred to an LC vial and injected onto the instrument. For comparative analysis of the recovery experiments, spiked blanks were also prepared, where the egg yolk was diluted with acetone to promote protein precipitation, vortexed and centrifuged, supernatant transferred to LC vials, and spiked with standards before being injected onto the instrument.

7.3.4 LC-MS/MS Instrumentation and Conditions

All analysis was performed on a Shimadzu LC-MS/MS-8040 (Shimadzu Scientific Instruments, Inc. Columbia, MD) using ESI in positive mode as the source. The instrument was equipped with LC-20AD XR LC pumps, SIL-20AC XR autosampler, DGU-20A5 degasser, and CBM-20A communications bus module. A Restek Raptor Biphenyl (2.7 µ, 2.1 mm ID, 100 mm; Bellefonte, PA) analytical column and a Shim-pack MAYI-C4(HP) (10 mm x 4.6 mm, 50 µm) restricted access media trap column from Shimadzu were used. Mobile phases consisted of (A) 5 mM ammonium formate and 0.1 % formic acid in water, (B) 5 mM ammonium formate and 0.1 % formic acid in methanol, (C) 98/2% water/methanol mixture, and (D) acetone. Each analyte of interest was surveyed for optimal conditions and monitored by MRM. Representative precursor ions, product ions, collision energies, and retention times for each compound are listed in Table 7.1. The LC-MS/MS parameters for mobile phase conditions, flow rate, and valve positions are given in Figure 7.1.

Table 7.1. Retention times and optimized spectrometric conditions including precursor ion, product ions, and collision energies.

						Transitions		
Compound	**Retention Time (min)**	**Precursor Ion**	**CE**	**Product Ion 1**	**CE**	**Product Ion 2**	**CE**	**Product Ion 3**
α-Estradiol (+)	6.39	271	-13	253.15	-23	159	-21	156.9
β-Estradiol (+)	6.39	271.1	-14	252.95	-21	133.2	-	-
Estrone (+)	6.39	271.05	-12	253.15	-21	133.05	-20	159.15
5α -DHT-IS (+)	6.40	294.1	-17	221.1	-11	277.05	-11	236.05
Testosterone (+)	6.46	289.2	-25	109	-22	97.1	-45	79
Estriol (+)	6.49	289.15	-26	106.9	-13	253	-19	133
DHEA (+)	6.49	289.15	-8	271.05	-11	253.05	-20	213.1
Aflatoxin G2 (+)	6.51	331	-24	313.1	-31	245.1	-43	189.05
Estrone-IS (+)	6.51	275.05	-15	257.1	-24	135.05	-24	161.05
17β-Estradiol-IS (+)	6.52	275.1	-13	257.05	-23	134.95	-16	159.05
5α -DHT (+)	6.55	291.15	-15	255.2	-21	159.1	-18	105.1
Pregnenolone-IS (+)	6.66	321.15	-8	303.15	-14	285.3	-22	159
Aflatoxin G1 (+)	6.68	329	-27	243.05	-41	200	-23	311.05
Retinol (+)	6.71	269.2	-22	93.15	-48	77	-33	105
Retinoic acid (+)	6.74	301.2	-16	123.1	-33	81	-22	159.15
Androstenedione-IS (+)	6.83	290.15	-23	100.2	-26	111.9	-13	81.15
Androstenedione (+)	6.83	287.1	-25	97	-25	109	-45	79.1
Aflatoxin B2 (+)	6.85	315	-27	287.05	-29	259	-39	243.05
Aflatoxin B1 (+)	7.05	313	-24	285.05	-38	241.05	-32	269
Retinal (+)	7.15	285.15	-9	161.15	-11	175.3	-21	119.1
Progesterone-IS (+)	7.18	324.2	-25	100	-31	113.05	-22	306.2
Progesterone (+)	7.22	315.2	-24	109.05	-22	97.1	-50	79.15
Pregnenolone (+)	7.39	299.25	-11	281.2	-21	161.1	-28	131
D3-IS (+)	7.55	388.25	-12	370.25	-14	259.15	-21	110.1
Cholesterol-IS (+)	7.56	390.25	-11	372.35	-39	81	-37	95.1
D3 (+)	7.56	385.3	-12	367.25	-26	107.1	-23	159.1
y-Tocopherol (+)	7.59	417.35	-20	151.1	-42	123.1	-37	69.1
D2-IS (+)	7.60	400.3	-26	69	-11	382.3	-22	110.1
D2 (+)	7.62	397.3	-25	69.2	-22	107.1	-12	379.25
^{13}C Cholesterol (+)	7.65	370.2	-27	147.1	-33	95.15	-14	81.15
Beauvericin (+)	7.76	784.25	-54	134.05	-30	244.05	-28	262.05
α-Tocopherol-IS (+)	7.81	437.35	-20	171.1	-20	111.1	-37	69.1
α-Tocopherol (+)	7.83	431.4	-20	165.1	-27	69.15	-40	137.1
K2 (+)	8.99	445.3	-47	95.1	-22	187.05	-37	81.2
K1 (+)	9.17	451.25	-27	186.95	-50	57.1	-20	185.2

Time	Module	Command	Value	Action
0	pumps	B conc	50	loading RAM, washing analytical 0,1
0	pumps	D conc	0	
0	pumps	A + B flow	0.4	
0	pumps	C + D flow	0.02	
0	oven	L	0	
0	oven	R	1	
3	pumps	C + D flow	0.6	
3.01	oven	L	1	eluting RAM to analytical column 1,1
3.01	pumps	B conc	50	
3.01	pumps	C + D flow	0.02	
4.99	pumps	C + D flow	0.02	
5	oven	L	0	analytical separation and RAM cleaning with acetone 0,1
5	pumps	B conc	75	
5	pumps	C + D flow	0.6	
5.01	pumps	D conc	0	
5.01	pumps	B conc	85	
5.02	pumps	D conc	100	
11	pumps	B conc	100	
15	pumps	B conc	100	
15	pumps	C + D flow	0.6	
15	pumps	A + B flow	0.4	
15.01	oven	L	1	analytical column cleaning with acetone 1,0
15.01	oven	R	0	
15.01	pumps	C + D flow	0.2	
15.01	pumps	A + B flow	0.02	
25	pumps	D conc	100	equilibrating column and RAM with starting conditions of next run 0,1
25	oven	L	0	
25	oven	R	1	
25	pumps	B conc	100	
25	pumps	A + B flow	0.02	
25.01	pumps	D conc	0	
25.01	pumps	B conc	50	
25.01	pumps	A + B flow	0.4	
35	controller		stop	

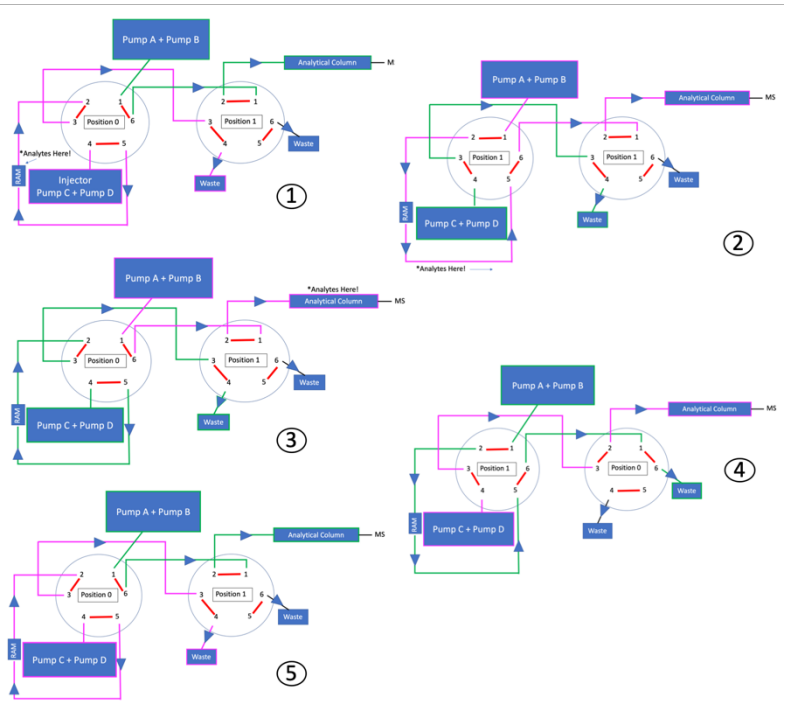

Figure 7.1. Instrument conditions for each diagram step including mobile phase flow rate, mobile phase concentration, and valve position with corresponding diagram of each step.

7.3.5 Method Validation

Matrix matched and solvent calibration curves for all the compounds in their expected concentrations in the egg matrix were constructed and linear regression was used to generate calibration curves on the LC-MS/MS instrumentation. A list of the calibration range, LOD, LOQ, and R^2 values are outlined in Table 7.2. Quantitation of each analyte in egg was performed by constructing a four-point standard addition curve and calculating area using an internal standard ratio for each analyte. Recovery experiments were performed by spiking known concentrations of analyte at low, medium, and high levels before precipitation and after precipitation of proteins from the egg matrix and their area ratios compared (Table 7.3). Further experiments were implemented with two-times dilution and 5-

times dilution with water of egg matrix to try to improve percent recovery and results are shown in Table 7.4.

Table 7.2. Linearity expressed as R^2 values, calibration curve levels, LOD, and LOQ for each analyte.

Analyte	Matrix Matched			
	R^2	Calibration Levels	LOD (ppb)	LOQ (ppb)
estriol	0.996	10- 500 ppb	5.00	15.00
dihydrotestosterone	0.991	1- 85 ppb	0.50	1.50
androstenedione	0.995	0.1- 500 ppb	0.05	0.15
dehydroepiandrosterone	0.990	1- 500 ppb	0.50	1.50
α -estradiol	0.990	0.1- 500 ppb	0.10	0.50
β -estradiol	0.991	0.1- 500 ppb	0.10	0.50
estrone	0.992	0.1- 500 ppb	0.10	0.30
pregnenolone	0.991	10- 100 ppb	5.00	15.00
retinol	Not linear			
retinoic acid	0.992	10-200 ppb	1.00	5.00
progesterone	0.993	1- 500 ppb	0.50	1.50
testosterone	0.992	0.1-100 ppb	0.10	0.50
aflatoxin G2	0.994	0.5- 500 ppb	0.50	1.50
retinal	0.991	5- 500 ppb	1.00	5.00
aflatoxin G1	0.992	0.1- 500 ppb	0.10	0.50
aflatoxin B2	0.992	0.5- 300 ppb	0.50	1.50
aflatoxin B1	0.992	0.5- 300 ppb	0.10	0.50
D2	0.994	20- 300 ppb	10.00	30.00
D3	0.993	20 - 300 ppb	10.00	30.00
beauvericin	0.990	0.5- 250 ppb	0.50	1.50
y-tocopherol	0.991	40 ppb- 50 ppm	1.00	5.00
α -tocopherol	0.996	40 ppb- 1 ppm	1.00	5.00
cholesterol N+1	Not linear			
K2	0.996	5 ppb- 10 ppm	1.00	5.00
K1	0.993	5- 800 ppb	1.00	5.00

Table 7.3. Spiked levels of analyte at low, medium, and high concentrations values, recovery percentages, and percent RSDs calculated.

Analyte	level	Concentration	% recovery no dilution	%RSD
estriol	low spiked	8 ppb	89	42
	med spiked	40 ppb	98	17
	high spiked	450 ppb	102	11
5-alpha-DHT	low spiked	8 ppb	100	25
	med spiked	28 ppb	81	12
	high spiked	90 ppb	76	22
Androstenedione	low spiked	0.8 ppb	94	20
	med spiked	40 ppb	111	16
	high spiked	400 ppb	93	7
DHEA	low spiked	0.8 ppb	118	46
	med spiked	40 ppb	115	35
	high spiked	400 ppb	89	3
alpha-estradiol	low spiked	0.8 ppb	108	30
	med spiked	40 ppb	97	10
	high spiked	400 ppb	80	13
beta-estradiol	low spiked	0.8 ppb	115	13
	med spiked	40 ppb	107	15
	high spiked	400 ppb	89	14
estrone	low spiked	0.8 ppb	111	16
	med spiked	40 ppb	114	13
	high spiked	400 ppb	82	15
pregnenolone	low spiked	8 ppb	103	35
	med spiked	80 ppb	114	19
	high spiked	5 ppm	101	4
retinol	low spiked	70 ppb	116	10
	med spiked	600 ppb	98	10
	high spiked	200 ppm	88	3
retinoic acid	low spiked	20 ppb	97	20

	med spiked	70 ppb	114	5
	high spiked	400 ppb	99	18
progesterone	low spiked	0.8 ppb	116	31
	med spiked	40 ppb	107	20
	high spiked	400 ppb	107	8
testosterone	low spiked	0.8 ppb	89	23
	med spiked	40 ppb	111	5
	high spiked	900 ppb	67	3
G2	low spiked	0.8 ppb	110	24
	med spiked	40 ppb	92	18
	high spiked	400 ppb	54	10
all-trans retinal	low spiked	8 ppb	120	41
	med spiked	80 ppb	199	20
	high spiked	900 ppb	107	8
G1	low spiked	0.8 ppb	90	17
	med spiked	40 ppb	110	4
	high spiked	400 ppb	80	2
B2	low spiked	0.8 ppb	91	21
	med spiked	40 ppb	115	19
	high spiked	400 ppb	110	6
B1	low spiked	0.8 ppb	113	9
	med spiked	40 ppb	106	16
	high spiked	275 ppb	89	11
D2	low spiked	40 ppb	66	17
	med spiked	200 ppb	71	16
	high spiked	900 ppb	40	7
D3	low spiked	40 ppb	109	40
	med spiked	200 ppb	108	34
	high spiked	900 ppb	41	5
Beauvericin	low spiked	0.8 ppb	118	9
	med spiked	140 ppb	135	15

	high spiked	275 ppb	113	11
y-tocopherol	low spiked	50 ppb	121	11
	med spiked	400 ppb	124	13
	high spiked	10 ppm	57	6
alpha-tocopherol	low spiked	50 ppb	133	8
	med spiked	400 ppb	120	4
	high spiked	10 ppm	95	8
cholesterol	low spiked	250 ppb	131	7
	med spiked	700 ppb	133	11
	high spiked	20 ppm	127	13
K2	low spiked	8 ppb	105	12
	med spiked	450 ppb	44	20
	high spiked	8 ppm	32	8
K1	low spiked	8 ppb	31	8
	med spiked	100 ppb	14	8
	high spiked	900 ppb	28	8

Table 7.4. Comparison of results from undiluted sample to 2x's and 5x's dilution with water at medium spiked concentration.

Analyte	level	concentration	%recovery no dilution	%recovery 2x	%recovery 5x
estriol	med spiked	40 ppb	97	82	66
5-alpha-DHT	med spiked	28 ppb	81	52	73
Androstenedione	med spiked	40 ppb	111	89	95
DHEA	med spiked	40 ppb	115	117	79
alpha-estradiol	med spiked	40 ppb	97	115	138
beta-estradiol	med spiked	40 ppb	107	115	131
estrone	med spiked	40 ppb	114	97	123
pregnenolone	med spiked	80 ppb	114	77	124
retinol	med spiked	600 ppb	98	90	99
retinoic acid	med spiked	70 ppb	114	62	81
progesterone	med spiked	40 ppb	107	94	112
testosterone	med spiked	40 ppb	111	82	85
G2	med spiked	40 ppb	92	59	66
all-trans retinal	med spiked	80 ppb	199	68	105
G1	med spiked	40 ppb	110	73	78
B2	med spiked	40 ppb	115	98	108
B1	med spiked	40 ppb	106	97	109
D2	med spiked	200 ppb	71	18	39
D3	med spiked	200 ppb	108	17	34
Beauvericin	med spiked	140 ppb	135	113	122
y-tocopherol	med spiked	400 ppb	124	103	78
alpha-tocopherol	med spiked	400 ppb	120	404	382
cholesterol	med spiked	700 ppb	133	497	567
K2	med spiked	450 ppb	44	12	21
K1	med spiked	100 ppb	14	6	9

7.4 Results and Discussion

7.4.1 Sample Preparation

Grading eggs is an essential part of the process before eggs make their way to the markets. The United States Department of Agriculture has developed an Egg Grading Manual to guide interested parties through the process. The outer portion is graded by inspecting the outside based on shape, texture, soundness, and cleanliness.[13] The inner portion is graded by a technique called candling where the egg is held up to a light in a dark room.[13] The inner factors an egg is graded on include the size of the air cell, distinctness of the yolk shadow, yolk size/shape, defects/germ development, and albumen.[13] A mixture of all these components give a final overall grade of AA, A, B, or rejects. A summary of these parameters can be seen in Table 7.5. Only eggs that were available at the local markets and home raised were analyzed for these experiments and because of this no B/reject graded eggs were analyzed. Currently, there are no methods implemented for detailed analytical quality control before eggs are sold on the market to test the presence or absence of compounds.

Early in the method development process, solvents to precipitate proteins were tested and included acetonitrile, acetonitrile with 0.2% formic acid, a mixture of chloroform/methanol 2:1, acetone, and methanol. These solvents were tested at room temperature, 1.6 °C, and -18 °C for their proclivity to precipitate protein from egg yolk. Acetonitrile, acetonitrile with 0.2 % formic acid, and acetone all qualitatively returned similar results, indifferent of temperature. Acetone was ultimately chosen because cholesterol, which is in great abundance in egg yolk, is not soluble in

acetonitrile at high concentrations. Consideration was also given to the amount of egg tested to ensure the concentration of target analytes would be within viable range of quantitation. The equivalence of 100, 200, and 300 µL of egg yolk sample were tested and ultimately the 300 µL sample size was chosen to ensure that minimum amount of egg was used in order to limit matrix effects but was concentrated enough to see the target analytes.

Much effort was given to produce a matrix of eggs that did not contain any analytes (blank) but had the same matrix effects as the native egg. A dispersive solid phase extraction (dSPE) mixture was tested that contained 150 mg $MgSO_4$, 50 mg primary and secondary amine (PSA), 50 mg C18-EC (end-capped), and 50 mg graphitized carbon black (GCB) and was not able to successfully remove all target analytes. Next, dextran-coated charcoal was surveyed for its ability to remove our target analytes and yield a blank matrix. The goal was to do this without significantly altering the matrix effects observed between the dilute and shoot samples and the dextran-coated charcoal treated sample. 50 mg of dextran-coated charcoal was added to the previously described method of sample preparation and analyzed. This method was able to remove all target analytes and was compared to the dilute/shoot method to determine variability in the matrix effects. This method greatly altered the matrix effects for the majority of the analytes and in return was not a valid method for obtaining a blank matrix. A summary of the slopes for each analyte in solvent, matrix matched, dSPE-treated, and dextrin-treated can be viewed in SI Table 7S1. These slopes were calculated by analyzing each sample matrix at seven different concentrations in triplicate and extrapolating the slope of the line. Even though

internal standards were used to calculate each of the analyte areas, a blank matrix would still ideally need to be obtained so the variability of analytes contained natively in the egg would not affect the analysis. Due to the inability to produce a blank matrix for matrix matching, standard addition was performed to quantify the concentration of target analytes in the egg yolk. The area for each analyte was calculated as a ratio using one of the internal standards.

Table 7.5. USDA summary of grading table for chicken eggs.[13]

	Egg Grading	Performed by	Grade AA	Grade A	Grade B	Reject
Exterior	Shape	inspection	ideal, practically normal	ideal, practically normal	abnormal	abnormal
	texture	inspection	slight ridges/rough areas	slight ridges/rough areas	ridges/thin spots	ridges/thin spots
	soundness	inspection	sound	sound	sound	check, leaker
	cleanliness	inspection	clean	clean	clean, slight stain	dirty
interior	air cell	candling	3.2 mm	4.8 mm	no limit	no limit
	disrinctness of yolk shadow	candling	ouline slightly defined	outline faily well defined	outline plainly visible	outline plainly visible
	yolk size/shape	candling	slightly defined	slightly defined	enlarged and flattened	enlarged and flattened
	defects/germ development	candling	practially free from defects	practially free from defects	clearly visibile germ development	blood due to germ development
	albumen	candling	clear, firm	clear, reasonably firm	weak, blood spots no more than 1/8 inch	weak, blood spots higher than 1/8 inch

7.4.2 Method Development and On-line Sample Clean-up

Multiple reaction monitoring (MRMs) were developed for each target analyte using the LC-MS/MS and a list of the optimized parameters can be seen in Table 7.1. An on-line restricted access media (RAM) trap column was used for further on-line sample processing prior to analytical measurement. RAM technology can have many benefits for analysis including automated sample preparation, higher throughput, increased sample loading, and on-line sample preconcentration.[14,15] Initially all sample clean-up was intended to be online, through the use of the RAM column, but it became inevitable that some of the proteins would precipitate out once the egg yolk matrix was diluted. As a result, the dilution was carried out to also accommodate significant protein precipitation in conjunction with use of the RAM column to rid the sample of remaining large biomolecule interferences. The RAM column accommodated 50 µL injections to enable trace amounts of analytes to be trapped and subsequently analyzed without detrimental effect to analyte peak shape

following chromatography. Although not performed in these experiments, the RAM column could also be loaded with multiple injections to detect ultra-trace levels of analyte and reach substantially lower limits of detection. An example of this was previously performed to detect Bisphenol A in human saliva by loading a RAM column with multiple injections for ultra-trace detection of analytes.[14] A multi-class analysis of compounds is also challenging when taking into account solubility of all target analytes. Careful consideration was given to ensure that all analytes were soluble, resulting in a mixture of final solvents in the sample that was injected. The loading solvent for these experiments consisted of 98/2% water/acetonitrile to achieve the tightest band possible of analytes at the head of the column and ensure no breakthrough of analytes. The analytes are relatively hydrophobic allowing for good trapping and no loss of analytes during the loading stage, as previously studied with four model compounds.[15] Also during the loading stage, a gradient flow rate was performed from 0.02- 0.6 mL/min to allow for analytes to enter the pores at a low flow rate and be retained before ramping up the flow rate to help wash the large biomolecules from the sample.[16] The RAM column method was perfected by testing the loading time for any breakthrough of analytes, back elution time from the RAM column to the analytical column, wash time to ensure no carryover, and equilibration time and the parameters for each of these steps can be viewed in Figure 7.1.

For each analyte monitored in these studies, a calibration curve was constructed and the R^2, linear range monitored, LOD, and LOQ for each compound was determined (Table 7.2). It was found for these experiments that the retinol and cholesterol compounds were not within linear dynamic range. For these experiments

1 of each type of egg yolk (14 total) were pooled and used as the matrix. Although these experiments returned a non-linear result for retinol when pooled, when each egg was individually tested all returned linear results, except egg number 10 (cage-free) and 12 (pasture raised) that were higher than the linear dynamic range.

7.4.3 LC-MS/MS Application to Samples

An example chromatogram for the second to lowest concentration tested of the target analytes can be seen in solvent (Figure 7.2-7.3) and in matrix (Figure 7.4-7.5). A scan (100-1000 *m/z*) was performed for a sample in the egg matrix and can be seen in Figure 7S2 of the supplementary information and displays how complex the egg matrix is. In solvent, the majority of the standards have good peak shape as shown in Figure 7.2, with the exception of some of the female hormones shown in Figure 7.3 (zoomed in chromatogram of Figure 7.2 to see lower intensity analytes). Upon matrix matching, a majority of the analytes displayed good peak shape (Figure 7.4). In a zoomed in version of Figure 7.4 the lower intensity compounds can be seen (Figure 7.5). Derivatization could possibly improve the peak shape of these compounds, but was not applicable for these experiments due to the multi-class compound analysis.

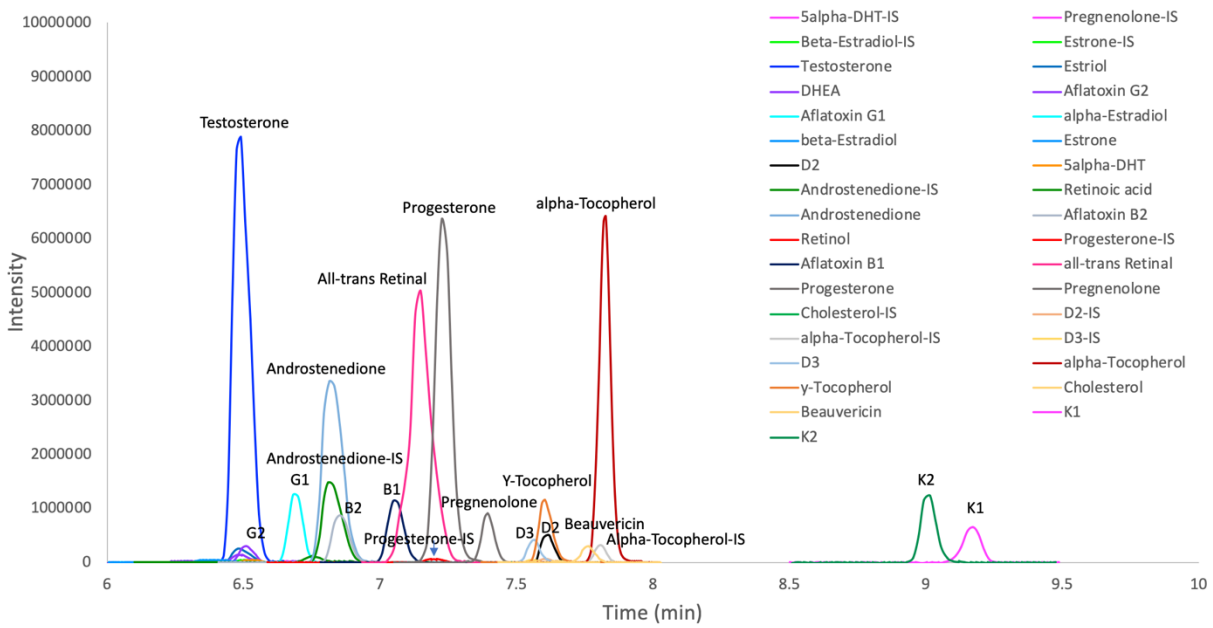

Figure 7.2. Labeled chromatogram for second lowest concentration analyzed in solvent.

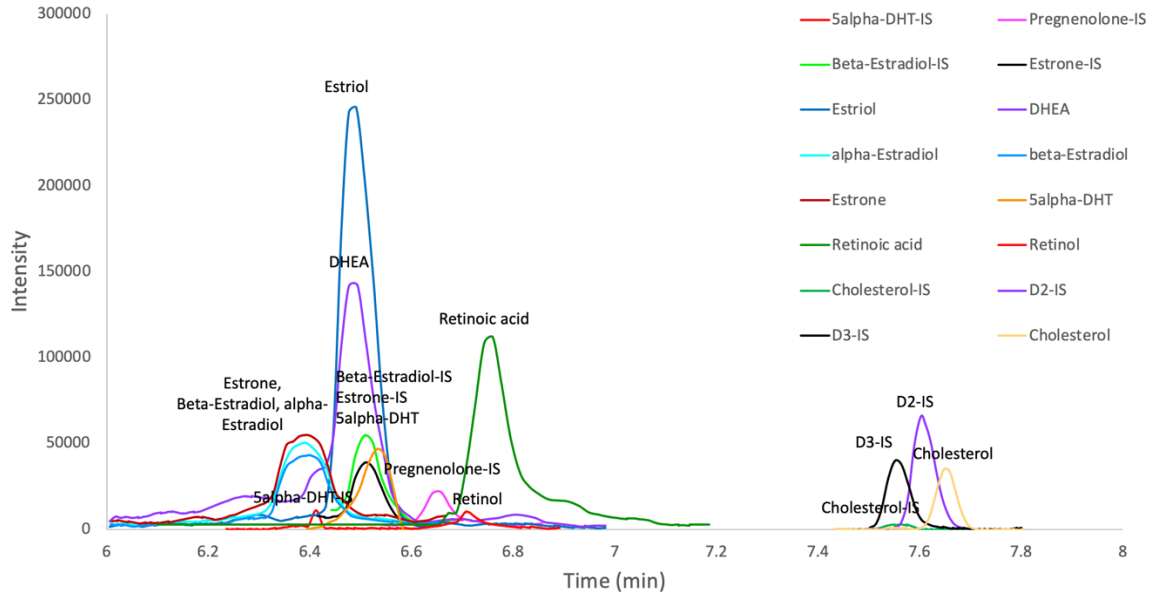

Figure 7.3. Labeled chromatogram for second lowest concentration analyzed in solvent zoomed in to visualize low intensity compounds.

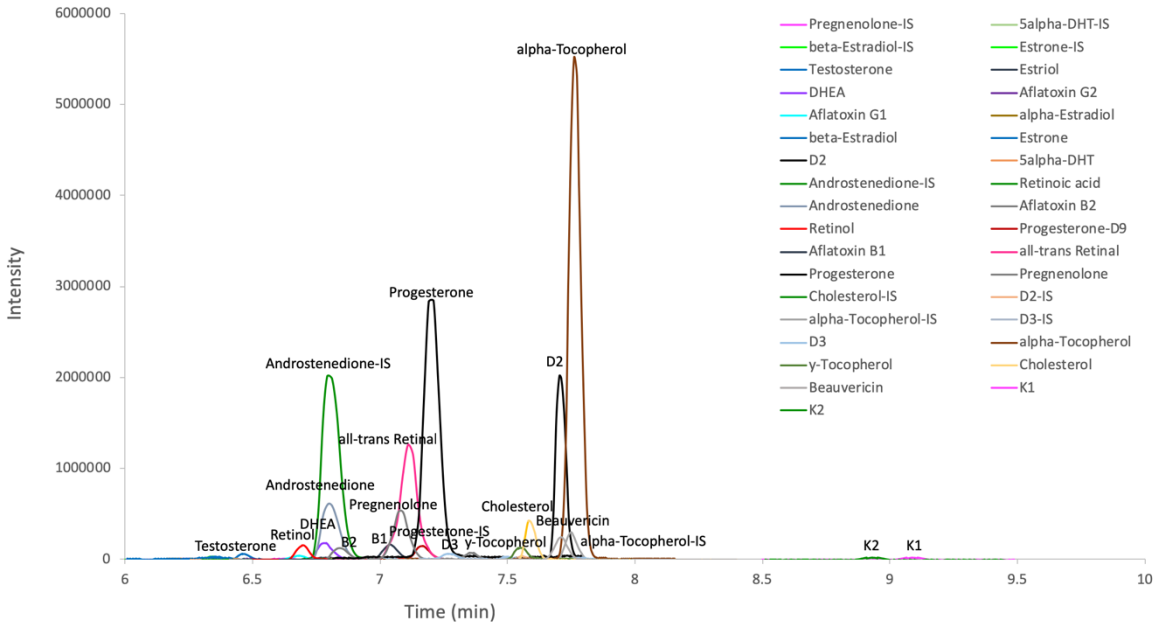

Figure 7.4. Labeled chromatogram for second lowest concentration in egg matrix.

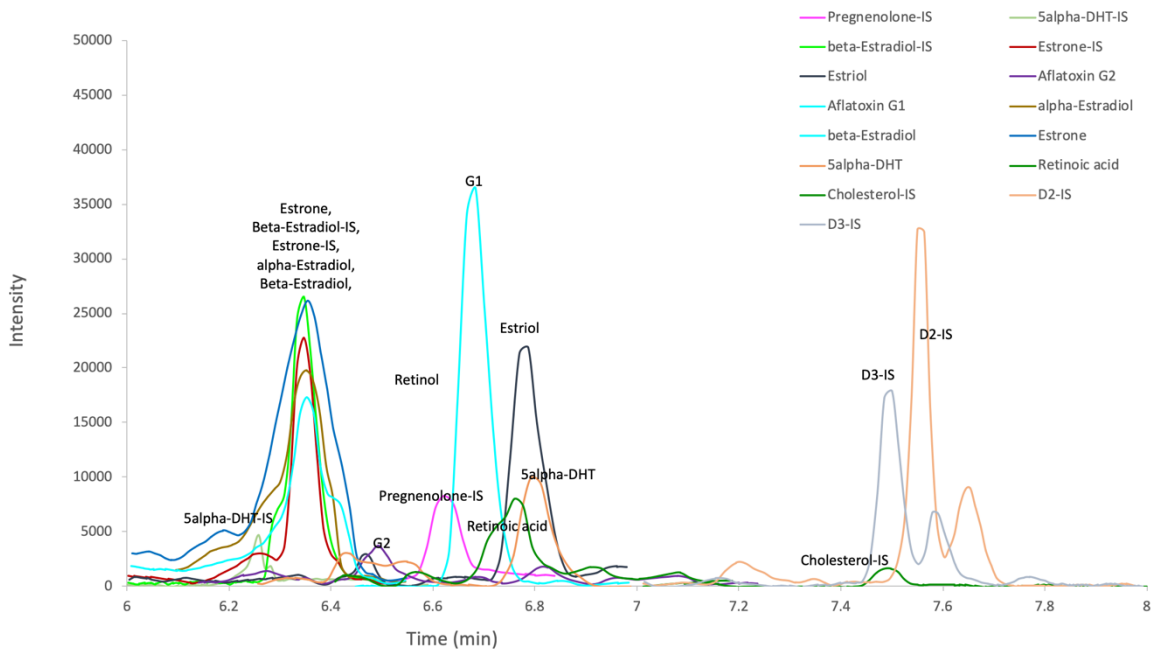

Figure 7.5. Labeled chromatogram for second lowest concentration in egg matrix zoomed in to visualize low intensity compounds.

Previous research was surveyed and a list compiled of the previously reported concentration of each target analyte determined in eggs (Table 7.6). These values were then compared to the concentration that was detected in these experiments. Three different forms of Vitamin A were monitored, including retinol, retinoic acid, and retinal. The results can be seen in Figure 7.6A. Retinol was the most abundant form of Vitamin A found in all eggs ranging from 212.09 ± 48.09 to 845.28 ± 144.24 μg/g, but was so highly concentrated for samples 10 (cage-free) and 12 (pasture raised) that it was outside the linear dynamic range and could not be quantified. Retinoic acid had comparable concentrations for samples tested ranging from 17 ± 6 to 66 ± 13 ng/g. Retinal did have variable concentrations with lower values for two of the three eggs tested for pasture-raised (40 ± 7 and 22.2 ± 0.6 ng/g), all the cage free (47.3 ± 6.3, 32.5 ± 3.2, 7.3 ± 0.7, 20 ± 2 ng/g), and one of the two home raised eggs tested (63.7 ± 5.5 ng/g). All other eggs were between 240 ± 50 to 430 ± 20 ng/g for retinal.

The main component of Vitamin A found in eggs is retinol, and in a previous study, when hens were fed 120 μg retinol/g of feed, the eggs returned a retinol increase from 3.99 ng/g for unfortified to 85.11 ng/g.[17] It has also been shown that feed enhanced with retinyl acetate will also increase the retinol content of the eggs.[17] Overall the Vitamin A variability in the eggs tested in these experiments is likely dependent on diet rather than living conditions as shown in previous findings.[17]

Other analytes monitored included Vitamins D, E, and K. All eggs tested had detectable amounts of both forms of Vitamin D ranging from 5.5 ± 1.7 to 59.4 ± 16.8 ng/g of Vitamin D2 and 1.9 ± 8.1 to 110.6 ± 27.3 ng/g of Vitamin D3 (Figure 7.6B).

Mattila et. al reported that hens that received feed enhanced with vitamin D3 at concentrations of 6,000 or 15,000 IU of D3/kg of feed measured a D3 concentration of 9.1-13.6 or 25.3-33.7 μg/100g of egg yolk but when fed the same concentrations of food enriched with D2, the egg yolk concentration of D2 was measured between 4.7-7.0 and 13.3-21.0 μg/100 g of yolk.[18] A review on vitamins in eggs by Ward summarizes the correlation of D3 enhanced feed fed to hens to their vitamin D3 content in egg yolk.[17] Experiments ranged from 1,064- 10,000 IU of D3/kg of feed and the concentrations measured in eggs for D3 ranged from 56- 2,060 IU/100 g yolk.[17] Vitamin D3 is overall more effected by the contents of the feed than Vitamin D2, but both can be enhanced by fortification of hen's food.

As for Vitamin E, all eggs tested had higher concentrations of α-tocopherol than γ-tocopherol. The values for γ-tocopherol ranged from 0.75 ± 0.04 to 7.5 ± 0.9 ng/g and 2.7 ± 0.2 to 96 ± 15 ng/g for α-tocopherol (Figure 7.6C). Vitamin E is another vitamin that is heavily dependent on hen's diet. In experiments where dietary Vitamin E was enhanced in hens feed, the produced eggs contained up to 18 times more α-tocopherol than the control eggs.[17]

Vitamin K content had strong correlations to the hen's living and feeding conditions and the results for Vitamin K2 and K1 content can be seen in Figure 7.6D. Vitamin K2, which is produced by most animals, was present in all eggs and ranged from 197 ± 47 to 322 ± 11 ng/g. Vitamin K1 originates from plants, specifically leafy greens, and was only present in detectable levels in 5 of the 14 eggs tested. The eggs that contained the Vitamin K1 included eggs from free-range, pasture-raised, and home raised chickens. These values ranged from 4.8 ± 1.5 to 48 ± 12 ng/g. This

result can be explained by the animals' living conditions, as hens that were not allowed access to outdoor conditions had no production of Vitamin K1 in their eggs.

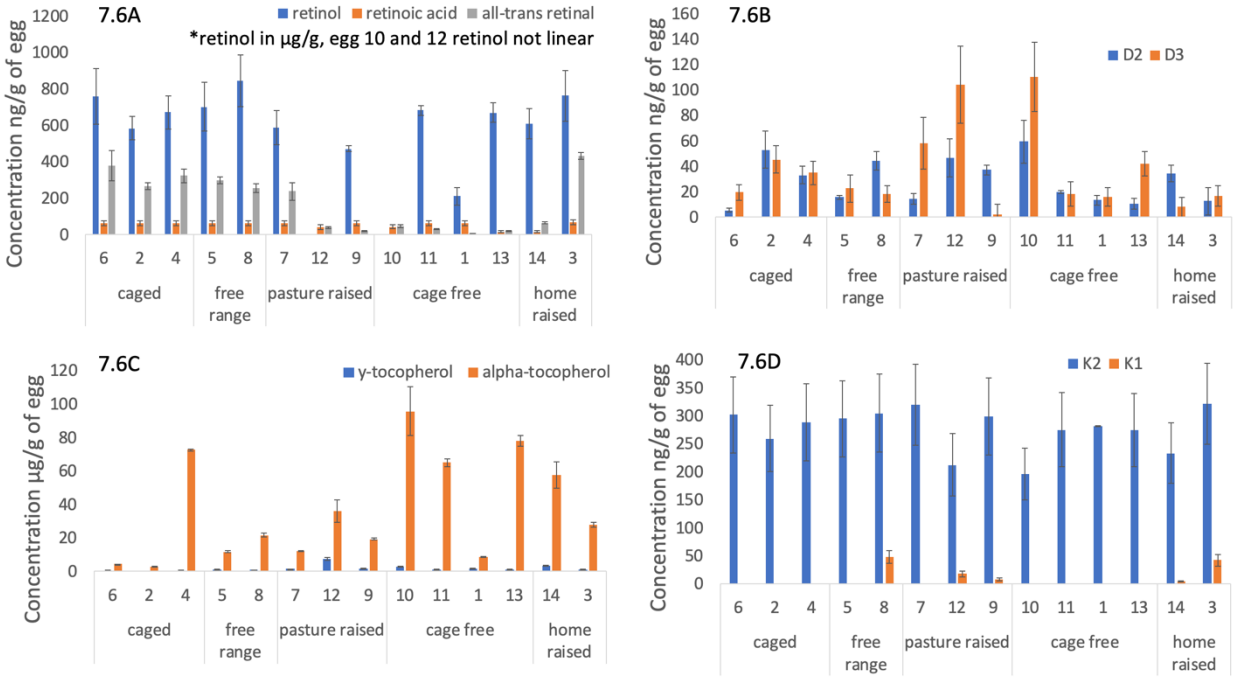

Figure 7.6. Vitamins detected in egg yolk. A) Vitamin A, B) Vitamin D, C) Vitamin E, D) Vitamin K.

Table 7.6. Comparison of previously reported values to values found in these experiments.

Compound class	Analyte	Range Reported in Egg	Concentration Detected
Fat-Soluble Vitamins	Retinol	1.62- 1620 µg/g[3,19,26]	212.09- 845.28 µg/g
	Retinal	none reported	7.33- 378.96 ng/g
	Retinoic acid	none reported	16.93- 66.27 ng/g
	D3	20- 56 ng/g[3,18,20,21]	1.91- 110.58 ng/g
	D2	0.47- 2.1 ng/g[18]	5.45- 52.94 ng/g
	y-Tocopherol	5 µg/g[3]	0.45- 7.5 µg/g
	alpha-Tocopherol	10.6- 477 µg/g[3,19,26]	2.74- 95.8 µg/g
	K1	nd- 198 ng/g[3,22,23]	4.83- 42.74 ng/g
	K2	1.55- 19.2 ng/g[22,23]	196.53- 321.59 ng/g
Mycotoxins	Beauvericin	nd- 2 ng/g[8]	nd- 10.19 ng/g
	G1	nd- 1 ng/g[8,24]	nd- 15.2 ng/g
	G2	nd- 2 ng/g[8,24]	nd
	B1	nd- 5 ng/g[8,24]	nd
	B2	nd- 1 ng/g[8,24]	nd
Hormones/ Steroids	Pregnenolone	19- 116.03 ng/g[5,25]	0.45- 833.53 ng/g
	Progesterone	9- 89.8 ng/g[4,5,25]	113.43- 470.1 ng/g
	Testosterone	0.04- 0.5 ng/g[5,25]	3.31- 14.41 ng/g
	Estrone	0.05- 21 ng/g[5,7,20]	15.59- 95.84 ng/g
	Androstenedione	1.83- 9.3 ng/g[5,20]	8.13- 182.46 ng/g
	alpha-Estradiol	nd- 1.72 ng/g[23]	26.3- 115.41 ng/g
	beta-Estradiol	nd- 0.22 ng/g[7,25]	59.62- 140.07 ng/g

A summary of the fat-soluble vitamin content detected in egg yolk can be seen in Table 7.6 along with previously reported values from literature with all units converted to be synonymous.[3-7,17-26] The values of the previously reported concentrations for the fat-soluble vitamins are mostly in agreement with the concentrations detected in these experiments but some of the values reflected in the table were the results of testing the full egg (albumen + yolk) instead of just the egg yolk, and could account for some deviation.

As seen previously with the fat-soluble vitamins, diet can have a great effect on contents of the egg yolk and the same is true for mycotoxin content. Mycotoxins, a secondary metabolite of fungus, have been studied due to their carcinogenic effects. They are of particular interest in these studies due to the likelihood that the chicken's feed could be contaminated with mycotoxins and pass them to the eggs. Five different mycotoxins were monitored: aflatoxin B1; aflatoxin B2; aflatoxin G1; aflatoxin G2; and beauvericin. Action levels set by the United States Food and Drug Administration (FDA) for aflatoxins in food for human consumption are set at 20 ppb.[27] Beauvericin was also monitored due to its high occurrence in feed, but according to the Food and Safety Authority in the European Union, acute exposure is not a concern for human health but chronic exposure is still inconclusive.[28] Two of the five mycotoxins screened were detected in some of the egg yolks (Figure 7.7A). Beauvericin was present in all but one of the eggs at levels ranging from 3.2 ± 0.7 to 18.9 ± 1.1 ng/g and aflatoxin G1 was present in two of the eggs at concentrations of 14.5 ± 3.8 and 15.2 ± 4.0 ng/g. Frenich et. al reported finding aflatoxin G2, G1, B1, and B2 as well as beauvericin in various samples of eggs but in lower concentrations than were detected in these experiments.[8] Previously reported values for mycotoxin content can be seen in Table 7.6 in comparison with this study's findings.[8,24] The previously reported values for beauvericin and aflatoxin G1 range from nd- 2 ng/g and nd-1 ng/g, respectively, while the ranged from nd-10.19 ng/g and nd- 15.2 ng/g, respectively. Both of these methods use the whole egg, instead of just the yolk where the mycotoxins are more likely to be contained since mycotoxins are hydrophobic. It has been suggested that because of the lipophilic

properties of beauvericin, it may bioaccumulate in the egg yolk by transportation via lipoproteins.[29] Mycotoxins are relatively chemically and thermally stable therefore cooking temperatures up to 100 °C may have little effect on concentration but higher temperatures could cause a reduction of mycotoxins in the eggs.[30] Future work could investigate the fate of the mycotoxin contaminates in cooked eggs to determine the exposure of these compounds upon consumption.

To investigate the findings of mycotoxins in the eggs further and to try to hone in on the source, chicken feed and scratch samples were collected from the local home raised chicken owners whose eggs were analyzed in these experiments to determine if their food source had detectable levels of mycotoxins. Chicken food samples were analyzed (Figure 7.7B) and were qualitatively determined to contain some levels of beauvericin, while aflatoxin B1 was also found in the scratch fed to hens from egg sample number 14 (Figure 7.7BIII). In a previous study by the European Food Safety Authority 81 feed samples were tested and 98% returned positive result for the beauvericin mycotoxin.[29] These results show that our findings of beauvericin in the feed and scratch samples is not unique and the fungi that produces the beauvericin mycotoxin is a common occurrence.

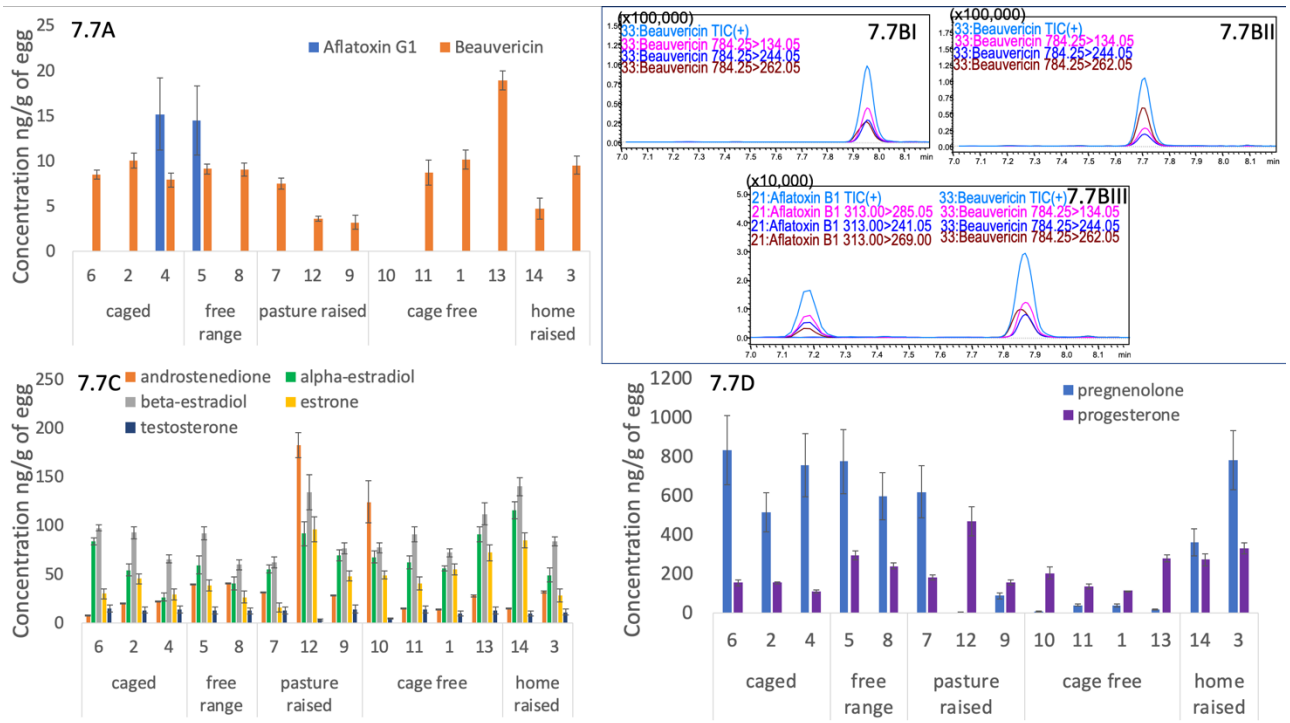

Figure 7.7. A) Mycotoxin content detected in eggs. Beauvericin detected in B1) Feed fed to chickens belonging to egg sample 14, BII) Feed fed to chickens belonging to egg sample 3, BIII) scratch fed to chickens belonging to egg sample 14.

Naturally occurring hormones and steroids were also monitored in these experiments. Androstenedione (8.1 ± 0.3 to 182.5 ± 12.9 ng/g), α-estradiol (26.3 ± 3.9 to 115.4 ± 8.9 ng/g), β-estradiol (62.4 ± 5.5 to 140.1 ± 8.9 ng/g), estrone (15.59 ± 4.74 to 95.84 ± 13.03 ng/g), and testosterone (3.31 ± 1.08 to 14.41 ± 3.61 ng/g) were all detected in each of the eggs (Figure 7.7C). No strong correlations were found for these naturally occurring hormones and the living/feeding conditions of the chickens. However, two additional naturally occurring hormones, pregnenolone and progesterone, did produce some trends. Pregnenolone was found in relatively low concentrations in all of the cage-free hen eggs tested and two of the three pasture-raised eggs. The cage-free eggs measured 8.7 ± 3.2 to 41 ± 7 ng/g for pregnenolone and the two low level pasture-raised eggs contained 0.5 ± 5 and 88.3

± 15.9 ng/g, while all other eggs measured from the range of 361 ± 70 to 833.5 ± 178.1 ng/g of egg (Figure 7.7D). Pregnenolone is the precursor for most steroid hormones and is a neurosteroid, meaning it decreases with age[25], which indicates the varying levels of pregnenolone could correspond to the maturity of the hen. Progesterone, a female sex hormone, had levels between 113.4 ± 7.7 to 470.1 ± 73.6 ng/g (Figure 7.4D), with some of the cage-free and caged hens having overall lower levels than the free-range, pasture-raised, and home raised counterparts. Natural hormone contents in eggs has also been an extensively researched topic. In 1998, Hartmann et. al reported pregnenolone, dehydroepiandrosterone (DHEA), androstenedione, progesterone, testosterone, and estrone found in eggs at levels of 83.3-143 µg/kg, 0.06-1.76 µg/kg, 1.83-9.27 µg/kg, 12.5-43.6 µg/kg, 0.04- 0.49 µg/kg, nd-0.22 µg/kg, and nd- 0.89 µg/kg, respectively.[25] In another article, sex hormones were detected in egg samples including estrone, α-estradiol, and β-estradiol ranging from 0.05 -1.72 µg.kg, 0- 0.13 µg/kg, and 0- 0.16 µg/kg, respectively.[6] A summary of previously reported values and the concentrations found herein can be viewed in Table 7.6.[3-7,17-26] The majority of the hormone analytes were detected at higher concentrations than previously reported. This could be due to only analyzing the egg yolk, instead of the entire egg, or the previous methods losing some compound during sample preparation.

7.4.4 Practical Challenges with This Study

There were many challenges during the development and implementation of these experiments. Seven-point solvent and matrix matched calibration curves were constructed and most of the analytes produced strong linearity with an R^2 range of

greater than 0.99 in most cases. In the overall analysis, there were two problematic compounds, which needed special attention. Retinol was in such high concentration for two of the eggs that it fell out of the linear dynamic range and could not be quantified by standard addition (egg samples 10 and 12). Cholesterol was another problematic compound due to its high concentration in each sample. To overcome this, that naturally occurring carbon 13 isotope of cholesterol was monitored $[M+2]^+$ to allow the observation of the high concentration of cholesterol within a range that was still linear, as shown in previous research,[31] but unfortunately, the levels of cholesterol were still too high to be within the linear dynamic range, even using the low-abundance natural isotope. To overcome this, further dilution could be performed in future experiments. This was not performed in these experiments because it would hinder the detection of lower trace analytes.

Recovery experiments were performed for all analytes at low, medium, and high level concentrations that were expected to be seen in the native egg. Acceptable percent recoveries are within the range of 80-120% and can be seen highlighted in green in Table 7.3. Most of the early and mid-eluting compounds are within the acceptable range but some have %RSD higher than 15% which shows a large deviation between the triplicate measurements. The later eluting compounds had more complications starting with Vitamin D2 and had values for percent recovery in the low (<50%) and high (<120%) range highlighted in red and dark red in Table 7.3, respectively. To try to mitigate poor recoveries for these analytes, further experiments were performed that involved diluting the egg by either 2 or 5 times with water before precipitating the proteins. The results of these experiments can be

seen in Table 7.4. These experiments did not yield improved results, and resulted in analytes that were previously in the acceptable recovery range to fall below or above the optimal range. Overall, it was discovered that dilution, which has been reported to be a method for improving recoveries when dealing with biological fluid samples,[32] did not provide any improvement in this study.

7.5 Conclusions

The method developed here for multi-class analysis on LC-MS/MS for the determination of mycotoxins, hormone, and fat-soluble vitamin content in egg yolk could serve as a valuable tool in evaluating the variability in different types of eggs. These are not the first reports of detection of fat-soluble vitamins, naturally occurring hormones, or mycotoxin content in eggs, but to the author's knowledge this is the first time that a multi-class compound analysis has been performed for these analytes with a simplified dilute, precipitate, and shoot on-line sample preparation for eggs. Standard addition using internal standards was imperative to overcome matrix effects and obtain accurate quantitation. Levels of fat-soluble vitamins and mycotoxins in the eggs are most likely related to the feed the hens eat more so than their living conditions, though the detection of Vitamin K1 can give some insight into living conditions. Future work could include the monitoring of these compounds in egg whites, to determine what the benefits or drawbacks are for people who don't consume the yolk. Monitoring these compounds in cooked egg could also provide valuable information in determining the concentration of these compounds one is likely to come into contact with upon consumption.

Acknowledgments

Support for this research was provided by Restek Corporation.

7.6 References

1. Complete guidelines for cage and cage free housing. Animal husbandry guidelines for US egg-laying flocks. United egg producers. 2017 https://uepcertified.com/wp-content/uploads/2015/08/UEP-Animal-Welfare-Guidelines-20141.pdf
2. “Free range” and “pasture raised” officially defined by HFAC for certified human label. Certified humane. 2014. https://certifiedhumane.org/free-range-and-pasture-raised-officially-defined-by-hfac-for-certified-humane-label/
3. Larsen, D. S. Encyclopedia of Food Chemistry: The Structure and Properties of Eggs; Elsevier: Amsterdam, 2018.
4. Yang, Y. et al. Analysis of eight free progestogens in eggs by matrix solid-phase dispersion extraction and very high pressure liquid chromatography with tandem mass spectrometry. J. Chrom. B. 2008, 870, 241-246.
5. Mi. X. et al. Quantitative determination of 26 steroids in eggs from various species using liquid chromatography-triple quadrupole-mass spectrometry. J. Chromatogr.. A. 2014, 1356, 54-63.
6. Wang, Q. Zhang, A., Chen, L. Simultaneous determination of sex hormones in egg products by ZnCl2 depositing lipid, solid-phase extraction and ultra-performance liquid chromatography/electrospray ionization tandem mass spectrometry. Analytica Chimica Acta, 678 (2010), 108-116.
7. Zeng, Z. et al. Determination of Seven Free Anabolic Steroid Residues in Eggs by High-Performance Liquid Chromatography-Tandem Mass Spectrometry. J. Chromatogr. Sci. 2013, 51, 229-236.
8. Frenich, A. G. et al. Multi-mycotoxin analysis in eggs using a QuEChERS-based extraction procedure and ultra-high-pressure liquid chromatography coupled to triple quadrupole mass spectrometry. J. Chrom. A. 2011, 1218, 4349-4356.
9. Pinherio-Sant’Ana, H. M.; Guinazi, M.; Olivera, D.; Lucia, C.; Reis, B.; Brandao, S. Method for simultaneous analysis of either vitamin E isomers in various foods by high performance liquid chromatography and fluorescence detection. J. Chrom. A. 2011, 1218, 8496-8502.
10. Yang, S. H.; Fan. H.; Classon, R. J.; Schug, K. A. Restricted access media as a streamlined approach toward on-line sample preparation: Recent advancements and applications. J. Sep. Sci. 2013, 36, 2922-2938.
11. Faria, H. Abrao, L. Santos, M. Barbosa, A. Figueiredo, E. New advances in restricted access materials for sample preparation: A review. Anal. Chim. Acta. 2017, 959, 43-65.
12. Meuer, H., Egbers, C. Changes in density and viscosity of chicken egg albumen and yolk during incubation. Journal of experimental zoology 255 (1990), 16-21.
13. United States Department of Agriculture. Egg-Grading Manual. Agricultural Handbook Number 75.

14. Yang, S.H.; Morgan, A.A.; Nguyen, H.P.; Moore, H.; Figard, B.J.; Schug, K.A.* Quantitative Determination of Bisphenol A from Human Saliva using Bulk Derivatization and Trap-and-Elute HPLC-Electrospray Ionization – Mass Spectrometry. Environ. Toxicol. Chem. 2011, 30, 1243-1251.
15. Baghdady, Y.Z.; Schug, K.A.* Evaluation of Efficiency and Trapping Capacity of Restricted Access Media Trap Columns for Online Trapping of Small Molecules. J. Sep. Sci. 2016, 39, 4183-4191.
16. Papouskova, B.; Fan, H.; Lemr, K.; Schug, K.A.* Aspects of Trapping Efficiency And Matrix Effects in Development of a Restricted Access Media-Based Trap-and-Elute Liquid Chromatography-Mass Spectrometry Method. J. Sep. Sci. 2014, 37, 2192-2199.
17. Ward, E. N. (2017). Vitamins in eggs. Egg Innovations and Strategies for Improvements. 207-217. DOI: 10.1016/B978-0-12-800879-9.00020-2.
18. Mattila, P., Valaja, J., Rossow, L., Venalainen, E., & Tupasela, T.(2004) Effect of Vitamin D_2- and D_3- Enriched Diets on Egg Vitamin D Content, Production, and Bird Condition During and Entire Production Period. *Poultry Science*, 83, 433-440.
19. Jiang, Y. H. alpha-Tocopherol, B-Carotene, and Retinol Enrichment of Chicken Eggs. Poult. Sci. 1994, 73, 1137-1143.
20. Mattila, P. et al. Determination of Vitamin D3 in Egg Yolk by High-Performance Liquid Chromatography with Diode Array Detection. J. Food Compos. Anal. 1992
21. Schmid, A.; Walther, B. Natural Vitamin D Content in Animal Products. Adv. Nutr. 2013, 4, 453-462.
22. Suzuki, Y.; Okamoto, M. Production of Hen's Eggs Rich in Vitamin K. Nutr. Res. 1997, 17, 1607-1615.
23. Elder, S. J. et al. Vitamin K Contents of Meat, Dairy, and Fast Food in the U.S. Diet. J. Agric. Food Chem. 2006, 54, 463-467
24. Zhu, R. A simple sample pretreatment method for multi-mycotoxin determination in eggs by liquid chromatography tandem mass spectrometry. J. Chromatogr. A. 2015, 1417, 1-7.
25. Hartmann, S.; Lacorn, M.; Steinhart, H. Natural occurrence of steroid hormones in food. Food Chem. 1998, 62, 7-20.
26. Mori, A. V. et al. Supplementing Hen Diets with Vitamins A and E Affects Egg Yolk Retinol and alpha-Tocopherol Levels. J. Appl. Poult. Res. 2003, 12, 106-114.
27. FDA mycotoxin regulatory guidance. A guide for grain elevators, feed manufacturers, grain processors and exporters. National Grain and Feed Association. August 2011.
28. Mallebrera, B.; Prosperini, A. Font, G.; Ruiz, M. In vitro mechanisms of Beauvericin toxicology. Food Chem. Toxicol. 2018, 111, 537-545.
29. Scientific Opinion the risks to human and animal health related to the presence of beauvericin and enniatins in food and feed. European Food Safety Authority. EFSA Journal 2014, 12, 3802.
30. Karlovsky, P.; Suman, M.; Berthiller, F.; De Meester, J.; Eisenbrand, G.; Perrin, I.; Oswald, I. P.; Speijers, G.; Chiodini, A.; Recker, T.; Dussort, P. Impact of food

processing and detoxification treatments on mycotoxin contamination. Mycotoxin Res. 2016, 32, 179-205.
31. Liu, H.; Lam, L.; Yan, L.; Chi, B.; Dasgupta, P. K. Expanding the linear dynamic range for quantitative liquid chromatography-high resolution mass spectrometry utilizing natural isotopologue signals. Anal. Chimica Acta. 2014, 850, 65-70.
32. Beinhauer, J.; Liangqiao, B.; Fan, H.; Sebela, M.; Kukula, M.; Barrera, J.A.; Schug, K.A.* Bulk derivatization and cation exchange restricted access media-based trap-and-elute liquid chromatography-mass spectrometry method for determination of trace estrogens in serum. Anal. Chim. Acta 2015, 858, 74-81.

7.7 SUPPLIMENTARY INFORMATION

Jamie L. York,[1] Robert H. Magnuson II,[1] Kevin A. Schug[1*]

[1]Department of Chemistry and Biochemistry, The University of Texas at Arlington, Arlington, TX, USA

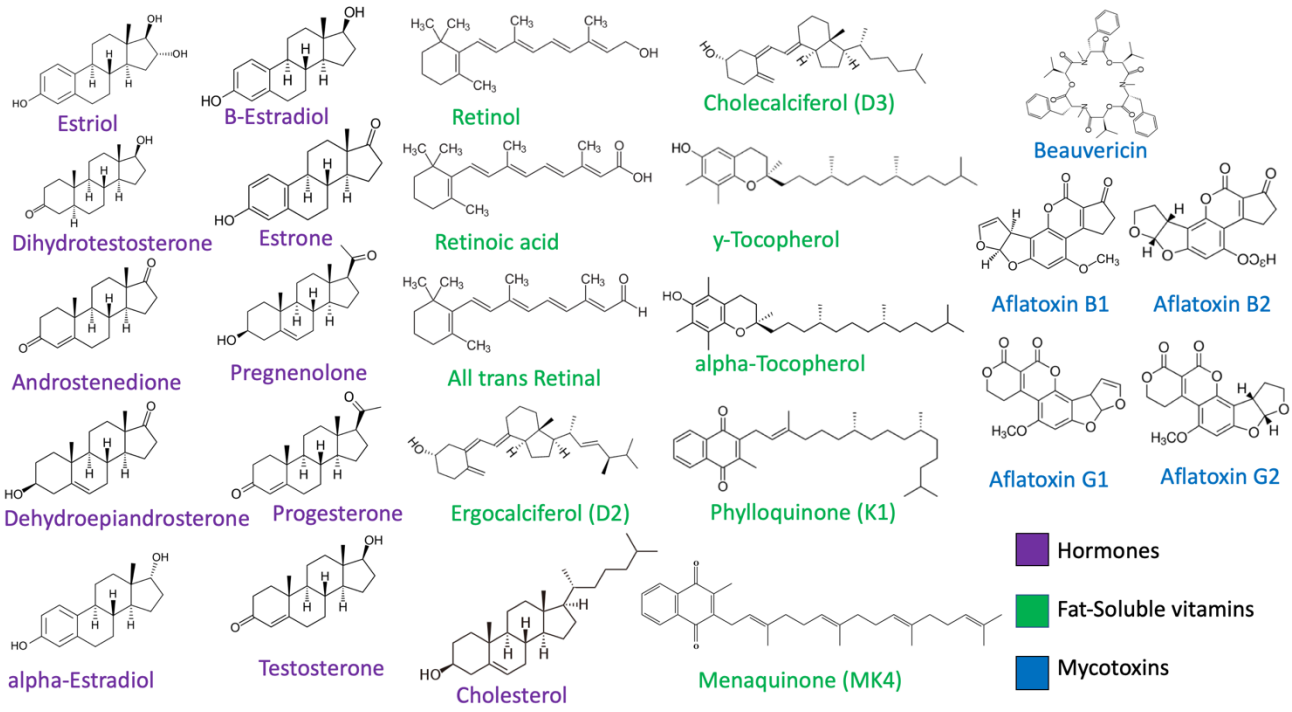

Figure 7S1. Structures for target analytes. Compounds included from hormone, fat-soluble vitamin, and mycotoxin classes.

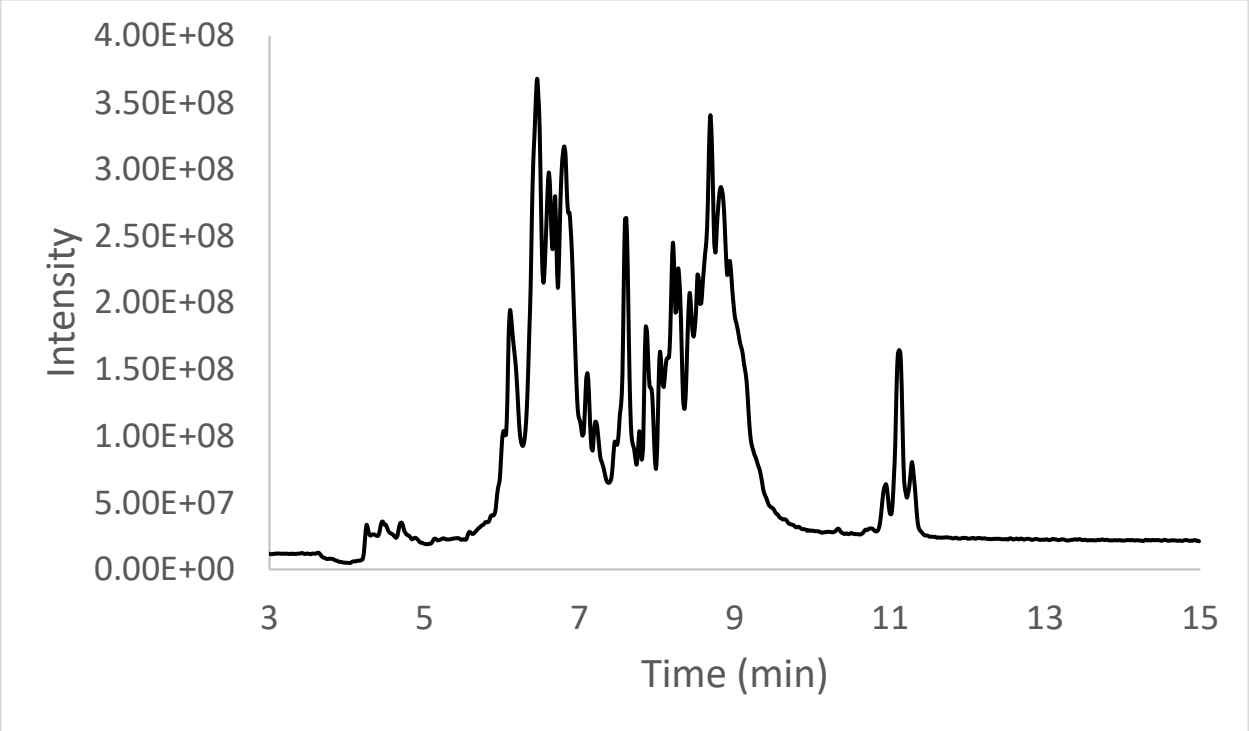

Figure 7S2. Q3 scan from 100- 1000 *m/z* for matrix matched sample.

Table 7S1. Slopes calculated for standards in solvent, matrix matched, dispersive solid-phase extraction treated, and dextrose-treated samples. Each method was tested by analyzing 7 different concentrations, constructing a calibration curve, and extrapolating the slope. Matrix effects were calculated by dividing the slope by the slope in solvent and expressed as a percentage.

	Slope				Matrix Effects		
name	**Solvent**	**Matrix Matched**	**dSPE-treated**	**Dextrin-treated**	**Matrix Matched**	**dSPE-treated**	**Dextrin-treated**
Estriol	0.0739	0.0090	0.0074	0.0081	12	10	11
5alpha-DHT	0.0845	0.0146	0.0130	0.5706	17	15	675
Androstenedione	2.2777	1.4531	1.0927	0.8357	64	48	37
DHEA	0.0503	0.0044	0.0036	0.0132	9	7	26
alpha-Estradiol	0.0199	0.0038	0.0095	6.0492	19	48	30436
beta-Estradiol	0.0091	0.0030	0.0067	4.5942	32	73	50340
Estrone	0.0247	0.0044	0.0126	8.4426	18	51	34194
Pregnenolone	0.0941	0.0863	0.0593	36.1298	92	63	38377
Retinol	0.0944	0.2829	0.1966	0.0010	300	208	1
Retinoic acid	0.3250	0.5925	0.8163	0.0105	182	251	3
Progesterone	2.2026	1.7128	1.8359	193.3830	78	83	8780
Testosterone	1.6417	0.1776	0.6628	0.1513	11	40	9
G2	87.1234	5.6521	62.7349	0.0612	6	72	0
all trans Retinal	13.5376	22.8486	24.8380	549.9800	169	183	4063
G1	181.4880	113.8850	292.6210	0.4866	63	161	0
B2	175.1430	114.3940	283.7420	31.4273	65	162	18
B1	246.2460	260.3530	592.1690	64.8150	106	240	26
D2	0.8287	0.7319	0.6448	0.9237	88	78	111
D3	0.5746	0.5977	0.6269	1.2310	104	109	214
Beauvericin	22.7256	98.4716	115.9340	188.3290	433	510	829
y-Tocopherol	0.3790	0.2106	0.6000	0.0910	56	158	24
alpha-Tocopherol	0.8982	0.7443	1.0228	0.9127	83	114	102
Cholesterol	0.0001077	not linear	0.0002153	0.0000205	not linear	200	19
K2	0.2868	0.1339	0.0512	0.0658	47	18	23
K1	1.0074	0.2307	0.5283	0.3377	23	52	34

CHAPTER EIGHT: SUMMARY AND FUTURE WORK

In this dissertation, different food and environmental samples were used to develop and apply analytical techniques for analysis of target analytes. For each sample set, a new method had to be produced to assess and mitigate matrix effects. The DMN project was able to use the VUV's capabilities of deconvolution to deconvolve coeluting isomers of the DMNs into their respective concentrations. It was found that the ratio of the two coeluting isomers could be deconvoluted up to a ratio of concentration of 99:1 accurately. Spectral filters were applied post-run to complex samples of diesel and jet fuel to determine naphthalene content since deconvolutions could not be performed. This work can be extended by including the application of spectral filters to detect DMNs in other complex environmental samples, where deconvolutions cannot be performed. In the case of carbohydrates, after derivatization, the GC-VUV was also used to deconvolute any isomers that coeluted, but not as efficiently as seen with the DMNs due to the extreme similarity in spectra for the carbohydrates. In addition, carbohydrates in pharmaceutical samples were able to be detected by this method. The next step for carbohydrate analysis would include the use of a chiral derivatizing agent or chiral stationary phase column to resolve enantiomeric compounds.

Next, hydraulic fracturing additives were investigated including proppants and friction reducers. Polyurethane and phenol-formaldehyde resin-coated proppants were tested for their ability to leach formaldehyde at downhole conditions over time. It was found that the phenol-formaldehyde resin coated proppant leached more

formaldehyde than its polyurethane counterpart. When the most complex and closely related to downhole conditions matrix was tested (produced water with added shale core) the lowest amount of formaldehyde was detected. This indicated that some competing reactions were possibly taking place. In the future, further investigation of the competing reactions would need to be done to determine the fate of the formaldehyde. Friction reducers were also tested under lab-simulated downhole conditions to understand their behavior once injected below the surface. Two different ethoxylated alcohols were detected in the friction reducers by MALDI-TOF-MS with carbon chain lengths of 12 and 14 and varying degrees of ethoxylation. In future work, other polymers in friction reducers could be investigated, such as polyacrylamide and its fate at downhole conditions.

Finally, eggs were investigated for their fat soluble vitamin, hormone, and mycotoxin content. These were prepared with minimal clean-up, only needing protein precipitation. The LC-MS/MS equipped with a RAM column was used to clean-up the large biomolecules that were not removed during precipitation and subsequent analysis performed. It was found that eggs originating from hens that were allowed outdoors such as free-range, pasture-raised, and home raised had Vitamins K1 detected in their eggs which originates from leafy greens. Mycotoxins were detected in thirteen of the fourteen tested eggs, which likely originates from moldy feed/food. Three chicken feed samples were collected from local chicken raisers to test for mycotoxins and all three of the samples contained some amount of mycotoxin. To follow up on this study, a method for detecting mycotoxins in chicken feed could be developed for hen feed samples collected from chicken farms to

further investigate the mycotoxin contamination in eggs. Egg whites could also be tested for these target compounds to determine if there is an advantage/disadvantage for those who only eat egg whites. Cooked eggs could also be tested to determine the actual concentration of these analytes in the eggs that are consumed upon eating.

In all, for each method careful consideration had to go into possible matrix effects such as salinity, high protein content, coeluting compounds, competing reactions, and solubility and these matrix effects had to be overcome by sample preparation techniques, on-line sample clean-up, and instrument capabilities.

Biographical Information

Jamie York was born in the United States and received a bachelor of science in chemistry in 2016. She graduates with her Ph.D. in chemistry in 2019 and wants to start a career in industry.

Publication Rights

Copyright Authorization

JOHN WILEY AND SONS LICENSE TERMS AND CONDITIONS

Jul 17, 2019

This Agreement between The University of Texas at Arlington -- Jamie York ("You") and John Wiley and Sons ("John Wiley and Sons") consists of your license details and the terms and conditions provided by John Wiley and Sons and Copyright Clearance Center.

License Number	4631380335404
License date	Jul 17, 2019
Licensed Content Publisher	John Wiley and Sons
Licensed Content Publication	Rapid Communications in Mass Spectrometry
Licensed Content Title	Characterization of ethoxylated alcohols in friction reducers using matrix-assisted laser desorption/ionization time-of-flight mass spectrometry
Licensed Content Author	Jamie L. York, Robert H. Magnuson, Dino Camdzic, et al
Licensed Content Date	Jul 2, 2019
Licensed Content Volume	33
Licensed Content Issue	15
Licensed Content Pages	7
Type of use	Dissertation/Thesis
Requestor type	Author of this Wiley article
Format	Print and electronic
Portion	Full article
Will you be translating?	No
Title of your thesis / dissertation	Analytical methods for solving complex problems in food and environmental science

Expected completion date	Aug 2019
Expected size (number of pages)	200
Requestor Location	The University of Texas at Arlington 700 Planetarium Place ARLINGTON, TX 76019 United States Attn: Jamie York
Publisher Tax ID	EU826007151
Total	0.00 USD

Royal Society of Chemistry: Permission is granted for you to use the material requested for your thesis/dissertation subject to the usual acknowledgements (author, title of material, title of book/journal, ourselves as publisher) and on the understanding that you will reapply for permission if you wish to distribute or publish your thesis/dissertation commercially.

You should also duplicate the copyright notice that appears in the Wiley publication in your use of the Material. Permission is granted solely for use in conjunction with the thesis, and the material may not be posted online separately.

Any third-party material is expressly excluded from this permission. If any material appears within the article with credit to another source, authorisation from that source must be obtained.